



THE HONG KONG  
POLYTECHNIC UNIVERSITY

香港理工大學

Pao Yue-kong Library

包玉剛圖書館

---

## Copyright Undertaking

This thesis is protected by copyright, with all rights reserved.

**By reading and using the thesis, the reader understands and agrees to the following terms:**

1. The reader will abide by the rules and legal ordinances governing copyright regarding the use of the thesis.
2. The reader will use the thesis for the purpose of research or private study only and not for distribution or further reproduction or any other purpose.
3. The reader agrees to indemnify and hold the University harmless from and against any loss, damage, cost, liability or expenses arising from copyright infringement or unauthorized usage.

### IMPORTANT

If you have reasons to believe that any materials in this thesis are deemed not suitable to be distributed in this form, or a copyright owner having difficulty with the material being included in our database, please contact [lbsys@polyu.edu.hk](mailto:lbsys@polyu.edu.hk) providing details. The Library will look into your claim and consider taking remedial action upon receipt of the written requests.

**A STUDY OF AUXETIC PLIED YARNS AND THEIR  
RESULTANT AUXETIC FABRICS**

NG WING SUM

M.Phil

THE HONG KONG POLYTECHNIC UNIVERSITY

2018

**THE HONG KONG POLYTECHNIC UNIVERSITY**  
**INSTITUTE OF TEXTILES AND CLOTHING**

**A STUDY OF AUXETIC PLYED YARNS AND THEIR  
RESULTANT AUXETIC FABRICS**

**NG WING SUM**

A Thesis Submitted in Partial Fulfillment of the Requirements for the Degree of  
Master of Philosophy

August 2017

# CERTIFICATE OF ORIGINALITY

I hereby declare that this thesis is my own work and that, to the best of my knowledge and belief, it reproduces no material previously published or written, nor material that has been accepted for the award of any other degree or diploma, except where due acknowledgement has been made in the text.

\_\_\_\_\_ (Signed)

Ng Wing Sum \_\_\_\_\_ (Name of Student)

## ABSTRACT

Poisson's ratio in tensile deformation is one of the fundamental properties of textile materials. Over the past few decades, science and technology have been crossed to alter the positive Poisson's ratio behavior in conventional materials. Innovative auxetic textiles have been developed utilizing the auxetic behavior to create unique mechanical properties for various kinds of specific applications. Recently, auxetic plied yarn structure has been proposed and fabricated. Arranging two groups of yarns with different thickness and stretching properties in a specific configuration, different types of auxetic plied yarn structure can be developed to exhibit negative Poisson's ratio (NPR) behavior. This is a very interesting field of research but remains largely unexplored. Therefore, this project is conducted with the aim to study this novel kind of auxetic plied yarn structure and their resultant auxetic fabrics.

A range of 4-ply auxetic yarn samples that vary in material properties and geometry were fabricated and subjected to tensile test to evaluate the effects of different design parameters on the tensile properties and auxetic behavior of the 4-ply auxetic yarn structure. Additional double helix yarn and 6-ply auxetic yarn samples were made for a comparative purpose to investigate the effect of helical structure under monotonic and cyclic tensile loading. The study shows that under proper diameter ratio, 4-ply

auxetic yarns exhibit a NPR during extension, and the magnitude is greater with a smaller soft yarn diameter, a larger stiff yarn diameter, a higher tensile modulus of stiff yarn and a lower twist level. By comparing the auxetic behavior of the three helical auxetic yarns (HAYs), the results reveal that 4-ply auxetic yarns have the advantages to produce immediate auxetic effect upon stretching. Under cyclic loading, three HAYs demonstrate a similar elastic recovery behavior regardless of their helical structures and extension levels.

Apart from the tensile test, changes in the internal structure of auxetic plied yarns upon stretching were investigated through microscopic examination. The study shows that auxetic behaviors inside the 4-ply and 6-ply structures are generated by the interplay between the soft yarns and the stiff yarns. Stiff yarns with higher tensile modulus clearly demonstrate a higher migration intensity inside the 4-ply auxetic yarn structure.

Finally, 4-ply auxetic yarns were further incorporated into a series of woven fabric to evaluate the effect of auxetic plied yarn arrangement, weft type, 4-ply auxetic yarn properties and weave structure on the auxetic behavior and percent open area of the resultant fabrics. Additional DHY and 6-ply auxetic yarn fabric samples were made to compare with the fabric sample made of 4-ply auxetic yarn. The results show that different kinds of auxetic plied yarn arrangement produce similar auxetic effect, while

higher stiff yarn modulus results in a higher auxetic behavior but finer soft yarn does not necessarily generate a higher NPR. Weft yarns with low modulus and short float are favorable to produce high auxetic effect. On the other hand, weft cover factor has a great influence on the percent open area of the auxetic fabrics made of 4-ply auxetic yarns. Open pore properties of the fabric samples made of various HAYs are vastly different. However, such differences are not correlated to their auxetic performances.

# LIST OF PUBLICATIONS

## **Journals**

W.S. Ng and H. Hu, Tensile and Deformation Behavior of Auxetic Plied Yarns.

Physica Status Solidi (b): p. 1600790-n/a

W.S. Ng and H. Hu, Woven Fabric Made of Auxetic Plied Yarns. Polymers 2018.

10(2), 226: p.1-19

## **Conference Presentations**

W.S. Ng, Hong Hu, Negative Poisson's Ratio Behavior and Pore Characteristics of

Woven Fabric made of Auxetic Plied Yarn under Tension, The Fiber Society 2017

Spring Conference, 17-19 May 2017, Aachen, Germany



## ACKNOWLEDGEMENTS

I would like to show my deepest gratitude to my supervisor, Prof. Hong Hu, for providing the opportunity to undertake this research project, and for his wise guidance, invaluable advice and continuous encouragement during my years at The Hong Kong Polytechnic University. He always listened to me to understand what I had issues with and continuously gave me new ideas to carry out my research work.

My sincere appreciation is also given to Dr. Zhaoyang Ge for her insightful suggestions and guidance when I first began my study. Many special thanks go to my research group members, especially Ms. Lin Zhou, for sharing their experiences with me.

My cordial thanks are extended to Ms. Mownin Sun for her kind assistance and valuable advice in the physical testing laboratory.

Finally, special thanks are given to my beloved family and friends for supporting and encouraging me to go through all the difficulties during my study.

# CONTENTS

	Page
<b>ABSTRACT</b> .....	i
<b>LIST OF PUBLICATIONS</b> .....	iv
<b>ACKNOWLEDGEMENTS</b> .....	v
<b>CONTENTS</b> .....	vi
<b>LIST OF FIGURES</b> .....	x
<b>LIST OF TABLES</b> .....	xiv
<b>CHAPTER 1 INTRODUCTION</b>	
1.1 Background.....	1
1.2 Research Objectives .....	4
1.3 Methodology .....	5
1.4 Significance of the Study .....	6
1.5 Outline of the Study .....	7
<b>CHAPTER 2 LITERATURE REVIEW</b>	
2.1 Introduction.....	9
2.2 Auxetic Materials .....	9
2.2.1 Properties of Auxetic Materials .....	10
2.2.2 Applications of Auxetic Materials .....	13
2.3 Variety of Auxetic Textiles.....	14
2.3.1 Auxetic Polymers and Fibers .....	14
2.3.2 Auxetic Yarns.....	15

2.3.3 Auxetic Fabrics .....	16
2.3.3.1 Retrospect of Conventional Textile Fabrics.....	16
2.3.3.2 The Approach to the Manufacturing of Auxetic Textiles .....	17
2.3.3.3 Auxetic Weft Knitted and Warp Knitted Fabrics.....	18
2.3.3.4 Auxetic Woven Fabrics.....	19
2.3.3.5 Other Auxetic Textiles .....	20
2.3.4 Auxetic Composites .....	20
2.4 Different Helical Structures and Their Respective Deformation Mechanism .....	21
2.4.1 Double Helix Yarn .....	23
2.4.2 Auxetic Plied Yarn.....	25
2.5 Auxetic Textiles Fabricated from Helical Auxetic Yarn .....	27
2.6 Methods for Investigation of Yarn Structure .....	29
2.6.1 Introduction.....	29
2.6.2 Image Processing Technique.....	30
2.6.3 Photoelectric Technique.....	31
2.6.4 Tracer Fiber Technique .....	32
2.6.5 Cross-sectional Microscopic Examination.....	33
2.6.6 Micro-computed Tomography (Micro-CT) .....	35
2.7 Summary.....	36

### **CHAPTER 3 FABRICATION OF AUXETIC PLIED YARN**

3.1 Introduction.....	39
3.2 Spinning Process .....	39
3.3 Samples Preparation.....	41

## **CHAPTER 4 TENSILE PROPERTIES AND AUXETICITY OF THE AUXETIC PLYED YARN**

4.1 Introduction .....	45
4.2 Experimental Details .....	46
4.2.1 Sample Preparation .....	46
4.2.2 Experimental Design .....	47
4.2.3 Measurement Method.....	49
4.3 Results and Discussion.....	52
4.3.1 Typical Tensile and Deformation Behavior .....	52
4.3.2 Effect of Soft Yarn Diameter .....	55
4.3.3 Effect of Stiff Yarn Diameter.....	59
4.3.4 Effect of Tensile Modulus of Stiff Yarn .....	61
4.3.5 Effect of Twist Level .....	64
4.3.6 Effect of Helical Structure .....	66
4.4 Conclusion.....	73

## **CHAPTER 5 ANALYSIS OF CROSS-SECTIONAL DEFORMATION OF THE AUXETIC PLYED YARNS**

5.1 Introduction.....	75
5.2 Cross-sectional Sample Preparation.....	76
5.3 Microscopic Examination .....	79
5.4 Results and Discussion.....	80
5.4.1 Cross-sectional Deformation Behavior of 4-ply Auxetic Yarns .....	80
5.4.2 Cross-sectional Deformation Behavior of 6-ply Auxetic Yarn.....	84
5.4.3 Poisson's Ratio and Cross-sectional Parameters .....	87
5.5 Conclusion.....	91

## **CHAPTER 6 DEVELOPMENT OF TEXTILE FABRICS MADE OF AUXETIC PLIED YARN**

6.1 Introduction.....	93
6.2 Design Consideration of Fabrics made of Auxetic Plied Yarn .....	94
6.3 Experimental Details.....	98
6.3.1 Experimental Design.....	98
6.3.2 Fabric Sample Preparation .....	100
6.3.3 Testing Method .....	104
6.4 Results and Discussions .....	106
6.4.1 Typical Mechanical Properties of the Woven Fabrics made of 4-ply Auxetic Yarn.....	106
6.4.2 Effect of 4-ply Auxetic Yarn Arrangement .....	110
6.4.3 Effect of Weft Type .....	113
6.4.4 Effect of 4-ply Auxetic Yarn Components .....	116
6.4.5 Effect of Weave Structure.....	120
6.4.6 Effect of Helical Structure .....	123
6.4.7 The Hexagonal Mesh Net Based on 4-ply Auxetic Structure.....	125
6.5 Conclusions.....	126

## **CHAPTER 7 CONCLUSIONS AND FUTURE WORK**

7.1 Conclusions .....	128
7.2 Future Work.....	130

<b>REFERENCES.....</b>	<b>131</b>
------------------------	------------

# LIST OF FIGURES

	Page
Figure 2-1 Indentation resistance of (a) non-auxetic and (b) auxetic materials [32].	11
Figure 2-2 Response of the non-auxetic and auxetic fibres under tensile load [35].	12
Figure 2-3 (a) Synclastic curvature (auxetic); (b) Anticlastic curvature (conventional) [39].....	13
Figure 2-4 Schematic of smart bandage concept [97].....	22
Figure 2-5 (a) DHY at zero strain; (b) DHY under tension .....	23
Figure 2-6 (a) 4-ply auxetic yarn (a) at rest; (b) under tension .....	26
Figure 2-7 Poisson’s ratio as a function of axial strain [23]. .....	27
Figure 2-8 6-ply auxetic yarn: (a) side view; (b) cross-section view at different states .....	37
Figure 2-9 4-ply auxetic yarn in x-y-z coordinate system .....	37
Figure 3-1 Schematic diagram of the helical auxetic yarn spinning device .....	40
Figure 3-2 Helical auxetic yarn samples .....	43
Figure 4-1 A schematic diagram and photograph of the tensile testing system.....	51
Figure 4-2 Conversion of the captured colour image (a) Original image (b) Greyscale image (c) Binary image.....	51
Figure 4-3 Binary images of the 4-ply auxetic yarns at different strains.....	52
Figure 4-4 (a) Typical tensile stress-strain curves of 4-ply auxetic yarn sample A-4 and its constituent single yarns. ....	54
Figure 4-4(b) Correlated Poisson’s ratio-axial strain curve.....	55
Figure 4-5 Tensile stress-strain curves: (a) samples A-1, B-1, C-1 and D-1 .....	56
Figure 4-5 Tensile stress-strain curves: (b) samples A-4, B-4, C-4 and D-4.....	57
Figure 4-6 Poisson’s ratio-tensile strain curves: (a) samples A-1, B-1, C-1 and D-1	58

Figure 4-6 Poisson's ratio-tensile strain curves: (b) samples A-4, B-4, C-4 and D-4	59
Figure 4-7 Photograph of sample D-1 at zero strain .....	59
Figure 4-8(a) Tensile stress-strain curves: samples A-5, A-6, A-7 and A-8.....	60
Figure 4-8(b) Poisson's ratio-tensile strain curves: samples A-5, A-6, A-7 and A-8..	61
Figure 4-9 Tensile stress-strain curves: (a) samples A-1, A-2, A-3 and A-4; (b) samples C-1, C-2, C-3 and C-4 .....	63
Figure 4-10 Poisson's ratio- tensile strain curves: (a) samples A-1, A-2, A-3 and A-4; (b) samples C-1, C-2, C-3 and C-4. ....	64
Figure 4-11 Comparisons among samples A-1-L, A-1-M, A-1 and A-1-H: (a) tensile stress-strain curves; (b) Poisson's ratio-tensile strain curves.....	66
Figure 4-12 Poisson's ratio behavior of auxetic yarns made with different helical structures.....	68
Figure 4-13 Tensile stress-strain behavior under cyclic loading: (a) sample A-1-D; (b) sample A-1; (c) sample A-1-T .....	70
Figure 4-14 Variation of Poisson's ratio under cyclic loading up to (a) 5% in strain; (b) 10% in strain; (c) 15% in strain.....	72
Figure 4-15 Photograph of 6-ply auxetic yarn sample at the end of the first cycle. ..	72
Figure 5-1 Schematic diagram and photograph of the cross-sectional sample preparation device .....	77
Figure 5-2 Schematic drawing for preparing the cross-sectional sample .....	78
Figure 5-3 Cross-sectional sample .....	79
Figure 5-4 Auxetic plied yarn measurements .....	80
Figure 5-5 Cross-sectional images of sample A-1 (a) at zero strain; (b) at strain of 0.02; (c) at strain of 0.04; (d) at strain of 0.06; (e) at strain of 0.08; (f) at strain of 0.10 (g) at strain of 0.11; (h) at strain of 0.13; (i) at strain of 0.15 .....	82

Figure 5-6 Cross-sectional images of yarn A-4: (a) at zero strain; (b) at strain of 0.02; (c) at strain of 0.04; (d) at strain of 0.06; (e) at strain of 0.08; (f) at strain of 0.10; (g) at strain of 0.11 .....	84
Figure 5-7 Cross-sectional images of yarn A-1-T (a) at zero strain; (b) at strain of 0.02 (c) at strain of 0.04; (d) at strain of 0.06; (e) at strain of 0.08; (f) at strain of 0.10; (g) at strain of 0.11 .....	87
Figure 5-8(a) Poisson's ratios of sample A-1 obtained with different methods .....	88
Figure 5-8(b) Poisson's ratios of sample A-4 obtained with different methods .....	88
Figure 5-8(c) Poisson's ratios of sample A-1-T obtained with different methods ....	89
Figure 5-9(a) Cross-sectional area of soft yarns and stiff yarns as a function of axial strain for sample A-1 .....	90
Figure 5-9(b) Cross-sectional area of soft yarns and stiff yarns as a function of axial strain for sample A-4.....	91
Figure 5-9(c) Cross-sectional area of soft yarns and stiff yarns as a function of axial strain for sample A-1-T.....	91
Figure 6-1 Single jersey fabric with the laying-in auxetic plied yarns.....	95
Figure 6-2 Woven fabric design with crimp-free auxetic plied yarns.....	96
Figure 6-3(a) Hexagonal mesh net with 4-ply auxetic structure; (b) typical hexagonal mesh net pattern.....	97
Figure 6-4 Arrangement of DHYs in previous literature [56].....	100
Figure 6-5 Photograph of the hexagonal mesh net sample.....	104
Figure 6-6 Schematic diagram and photograph of the fabric tensile testing system	105
Figure 6-7 Conversion of the cropped image: (a) original image; (b) threshold color; (c) binary image.....	106
Figure 6-8 Tensile behavior of a typical auxetic woven fabric and its constituent auxetic yarn: (a) load-strain curves (the inset shows the enlargement at	



small load); (b) transverse-tensile strain curves; (c) PR-tensile strain curves.....	110
Figure 6-9 Poisson’s ratio-tensile strain curves for samples F1 and F2.....	111
Figure 6-10 Alignment of 4-ply auxetic yarns in the fabric sample.....	112
Figure 6-11 Percent open area in relation to tensile strain for samples F1 and F2...	113
Figure 6-12 Poisson’s ratio-tensile strain curves for samples F1 and F3.....	114
Figure 6-13 Tensile stress-strain curves of the weft yarns used.....	114
Figure 6-14 Percent open area in relation to tensile strain for samples F1 and F3...	116
Figure 6-15 PR-tensile strain curves of fabrics F3, F4, F5 and their respective 4-ply auxetic yarns.....	118
Figure 6-16 Percent open area in relation to tensile strain for samples F3, F4 and F5 .....	118
Figure 6-17 Poisson’s ratio-tensile strain curves for samples F3, F6 and F7 and their respective 4-ply auxetic yarns.....	119
Figure 6-18 Percent open area in relation to tensile strain for samples F3, F6 and F7.....	120
Figure 6-19 Poisson’s ratio-tensile strain curves for samples F1, F8, F9 and F10...	122
Figure 6-20 Percent open area in relation to tensile strain for samples F1, F8, F9 and F10.....	122
Figure 6-21 Poisson’s ratio-tensile strain curves for samples F11, F3 and F12.....	124
Figure 6-22 Sample F12 at strain of 0.4.....	124
Figure 6-23 Percent open area in relation to tensile strain for samples F11, F3 and F12.....	125
Figure 6-24(a) Poisson’s ratio-tensile strain curve for sample F13; (b) Percent open area in relation to tensile strain for sample F13.....	126

## LIST OF TABLES

	Page
Table 3-1 Specifications of the single yarns .....	42
Table 3-2 Construction characteristics of the helical auxetic yarn samples .....	44
Table 4-1 Specifications of the experimental design .....	48
Table 6-1 Constructional characteristics of woven fabrics investigated.....	102
Table 6-2 Photographs of the woven fabric samples .....	103
Table 6-3 Pictures and Poisson's ratio values of sample F3 at different extension levels .....	110

## CHAPTER 1 INTRODUCTION

### 1.1 Background

We may not realize it, but we are all familiar with Poisson's ratio in reality. Take rubber band as an example, it becomes narrower when stretched. Poisson's ratio is defined as the negative ratio of transverse strain to the extension strain.

Almost all common materials exhibit a positive Poisson's ratio, which means they laterally contract when stretched and vice versa when compressed. However, it is still possible to find materials which have a NPR in nature, and they are known as auxetic materials. The first example of natural auxetic material was given by Love in 1944 [1]. Since then, various naturally existing auxetics have been discovered, such as the  $\alpha$ -cristobalite, single crystals arsenic, cancellous bones, cow teat, cat skin and salamander skin [2-6].

In 1987, Lakes developed the first NPR material, which was a polyurethane foam with re-entrant structure made by triaxial compression and heat treatment [7]. Ever since, a variety of man-made auxetic materials have been manufactured and synthesized, including but not limited to microporous polymers[8, 9], honeycomb structures [10, 11], polymeric and metallic foams [12-15], ceramics [16, 17], auxetic composites [18]

and molecular auxetic materials [19, 20]. Synthesized auxetic materials are of interest as the auxeticity in material may enhance mechanical properties such as fracture toughness, shear modulus, indentation resistance, pullout resistance, synclastic curvature and sound absorption capacity [21].

Over in the textiles sector, a wide range of auxetic textiles have been made and have shown great potential application in many areas. Years of research works have shown that auxetic effect can be introduced at different stages of the textile manufacturing process. If the auxetic effect can be obtained at an early stage, the auxetic materials can be used directly or they can serve as inputs to fabricate some other kinds of auxetic textile in the next stage. For example, individual auxetic fibers can be used in fiber reinforced composites, and on the other hand, they can be used as raw materials to fabricate knitted and woven textiles with NPR effect.

Creating auxetic effect at the yarn stage is a new and interesting area of research, because unlike auxetic fibers which are manufactured under complicated processing conditions, helical auxetic yarn (HAY) can be made simply by winding or twisting different conventional filaments together with existing spinning machinery and standard manufacturing techniques. Therefore, development of HAY has been

attracting considerable attention from the academic community.

It has been proven that stretching the HAY can result in a net increase in the effective diameter of the yarn and hence to generate a NPR. Many studies were carried out to investigate the basic structure and mechanics of the HAYs. However, these studies have been limited almost exclusively to double helix yarn (DHY), which is a yarn comprised of two conventional filaments in which a high stiffness filament is wrapped around a relatively thicker and softer filament in a helical manner [22]. Until recently, 4-ply auxetic yarn has been developed and an alternative route to produce HAY finally existed [23].

It should be pointed out that development and investigation on this kind of auxetic plied yarn are still in its early stages, and the potential to fabricate auxetic fabrics with auxetic plied yarn remains largely unexplored. It is expected that investigation on auxetic plied yarn and auxetic fabrics made therefrom could provide some useful information for the technologists to tailor the mechanical properties of the yarn and the corresponding textiles for specific applications.

## 1.2 Research Objectives

The main purpose of this project is to develop an understanding on the newly proposed auxetic plied yarns, in particular, to identify design parameters influencing the mechanical properties of the auxetic plied yarn, and to investigate the potential and constraints for these yarns to fabricate textiles with NPR. Specifically, the principle objectives of this project are listed as follows:

- (1) To study the tensile properties and auxetic behaviour of the auxetic plied yarns under monotonic and cyclic loading, and to evaluate the effect of different design parameters that generate a NPR in the 4-ply auxetic yarn structure.
- (2) To study the cross-sectional deformation mechanism leading to auxetic behaviour in the auxetic plied yarns, and to evaluate the variation brought by different yarn components and helical structures.
- (3) To develop auxetic fabrics with auxetic plied yarns, and to investigate different yarn and fabric structural parameters on the auxetic effect and open pore behaviour of the fabric under tensile load.

### 1.3 Methodology

To achieve the objectives of the project, a systematic experimental investigation is carried out and the following research methodologies are employed:

- (1) A range of auxetic plied yarns that vary in material properties and geometry will be manufactured and then subjected to tensile test to evaluate their tensile properties and auxetic behavior by means of image processing technique. Influencing parameters that affect the performances of the 4-ply auxetic yarn will be characterized and discussed. In addition, HAYs with different helical structures will be subjected to monotonic and cyclic tensile loading to evaluate their variations in tensile properties and auxetic behavior.
- (2) A new approach will be developed to prepare the cross-sectional sample of 4-ply and 6-ply auxetic yarns under different strain levels. The cross-sectional samples will be viewed under optical microscope. Images will be captured to investigate the deformation mechanism of the auxetic plied yarns and variations brought by different stiff yarn components and helical structures.
- (3) A few 4-ply auxetic yarn samples will be chosen to produce various fabrics with different auxetic plied yarn arrangements, weft materials, auxetic plied yarn components and weave structures. For a comparative purpose, DHY and 6-ply

auxetic yarn will be used to make two different fabric samples as well. All of them will be subjected to tensile test, during which consecutive images will be captured at the same time to measure the Poisson's ratio value and percent open area of the fabrics under various extension levels. Influence of each design parameter will be discussed.

#### **1.4 Significance of the Study**

Poisson's ratio in tensile deformation is one of the fundamental properties of textile materials which can show the deformation behavior when subjected to force and use as an index to determine their applications. Over the past few decades, science and technology have developed to alter the fundamental positive Poisson's ratio behavior in conventional materials. Innovative auxetic textiles are proposed and developed with the utilization of auxetic behavior to result in many beneficial effects for various kinds of specific applications.

This thesis presents a detailed study of the newly developed auxetic plied yarn structure with a special configuration and deformation characteristic. The auxetic plied yarn is not only suitable to use exclusively, but also feasible to incorporate into fabric to obtain NPR behavior. It opens up the possibilities for alternatives other than those



currently present in the academic community. More importantly, it can serve as an indication to idealize suitable material and structure to produce auxetic effect in the auxetic plied yarn and their resultant fabrics.

### **1.5 Outline of the Study**

The thesis consists of seven chapters. In **Chapter 1**, the background of auxetics, the objectives, methodology as well as the significance of this research are introduced. Apart from them, an outline of this thesis is also included.

In **Chapter 2**, previous investigations on auxetic materials are studied, in particular of the research works related to the helical auxetic yarns and the fabrics made therefrom.

In **Chapter 3**, the helical auxetic yarn spinning device is described in detail with the operating procedure; construction characteristics of the auxetic plied yarn samples are introduced.

In **Chapter 4**, experiments are carried out to evaluate the tensile properties and auxetic behavior of the auxetic plied yarns upon extension. Design variables to generate a NPR in the 4-ply auxetic yarn structure are discussed. In addition, double helix yarn, 4-ply and 6-ply auxetic yarns will be subjected to monotonic and cyclic tensile loading. Variations in their tensile properties and auxetic behavior will be discussed.

In **Chapter 5**, cross-section analysis is conducted to study the deformation behavior of auxetic plied yarns, in particular of the migration behavior of soft yarns and stiff yarns, and their variation in size correspond to the Poisson's ratio calculated.

In **Chapter 6**, experiments are carried out to develop auxetic fabrics with 4-ply auxetic yarns. Design considerations are discussed, while project constraints are identified. Series of fabric samples are made and their respective auxetic behavior and percent open area are measured by means of image processing analysis. Effect of different design variables are evaluated.

In **Chapter 7**, a general conclusion of the present study is provided. Recommendations for future study based on the present work are also proposed.

## CHAPTER 2 LITERATURE REVIEW

### 2.1 Introduction

The literature review is presented in five parts. Firstly, Poisson's ratio is introduced, and background information of auxetic materials is presented in terms of properties and potential applications. Secondly, variety of auxetic textiles is reviewed, including auxetic fibers, auxetic yarns, auxetic fabrics and auxetic composites. Thirdly, previous works of helical auxetic yarns are reviewed, including literature on double helix yarn and auxetic plied yarn. Fourthly, auxetic textiles fabricated by auxetic yarns are studied. Lastly, different techniques to study the yarn from internal and external structures are reviewed.

### 2.2 Auxetic Materials

Poisson's ratio of an object is defined as the negative ratio of transverse strain to axial strain in a simple tension condition, i.e.,

$$\nu_{xy} = -\varepsilon_y / \varepsilon_x \quad (1)$$

where  $\nu_{xy}$  is the resulting Poisson's ratio in the XY plane,  $\varepsilon_x$  is the tensile strain in loading direction while  $\varepsilon_y$  is the contractile strain perpendicular to this. There is a minus sign in the above equation so that normal materials which get thinner as it is being stretched will have a positive ratio. Nearly all common materials have a positive

Poisson's ratio value ranging between 0.0 and 0.5 while auxetic materials are different from most conventional materials in that they exhibit NPR, i.e., they laterally expand when stretched and contract when compressed [24].

### **2.2.1 Properties of Auxetic Materials**

Fabrication of auxetic materials has been attracting considerable attention during the past three decades because the auxeticity in materials may enhance certain mechanical properties, including fracture toughness, shear stiffness, indentation resistance, pullout resistance, synclastic curvature, sound absorption capacity and variable permeability.

#### **Fracture toughness**

It has been suggested that auxetic materials have a higher ability to resist fracture in the presence of a crack. When the auxetic material is being pulled apart, it expands laterally and closes up the crack before further crack growth. In other words, auxetic materials deter crack propagation [25, 26].

#### **Shear stiffness**

It was demonstrated that shear stiffness of the auxetic materials is higher than that of the conventional materials with a positive Poisson's ratio. Since auxetic materials contract laterally upon compression, they become highly compressible and more

difficult to shear [27-29].

### Indentation resistance

It was found that auxetic materials are relatively more resistant to denting than the non-auxetic equivalents. As shown in Figure 2-1(a), when the surface of a common material is hit by an object and compressed, it flows away from the zone of impact in a lateral direction and causes a reduction in density. In contrast, when an auxetic material is subjected to impact loading, it contracts laterally into the vicinity of the impact, as shown in Figure 2-1(b). As a result, the material becomes denser at that point and results in an increased indentation resistance [30, 31].

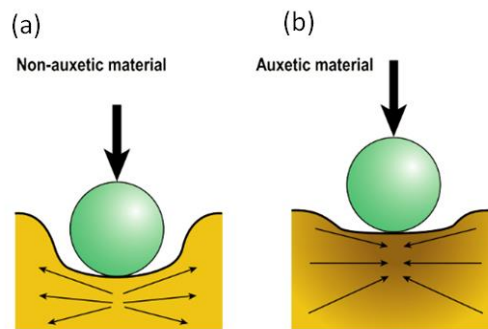


Figure 2-1 Indentation resistance of (a) non-auxetic and (b) auxetic materials [32]

### Pullout resistance

It has been proven that a better pullout resistance could be resulted if the conventional fibre used in the composite is replaced by auxetic fibre. The weakest part of a fibre

reinforced composite is the interface between the matrix and fibres [33]. As shown in Figure 2-2, when conventional fibre is used, it will be pulled out easily under tensile load due to lateral contraction. However, when an auxetic fibre is used, it will expand during pull-out and effectively lock into the matrix. Therefore, substituting the conventional fibre by the auxetic one could delay fiber pull-out process[34].

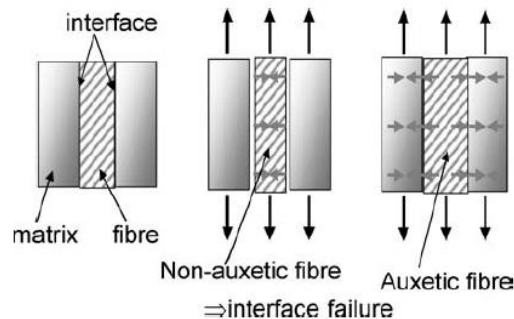


Figure 2-2 Response of the non-auxetic and auxetic fibres under tensile load [35]

### Synclastic curvature

Materials with synclastic curvature have better conformability for support and comfort [36]. Previous studies have demonstrated that auxetic materials exhibit synclastic curvature when they are subjected to a bending force. In other words, they can bend into doubly-curved spherical shell (Figure 2-3a) rather than anticlastic shell (Figure 2-3b) that is presented in the non-auxetic materials [37, 38].

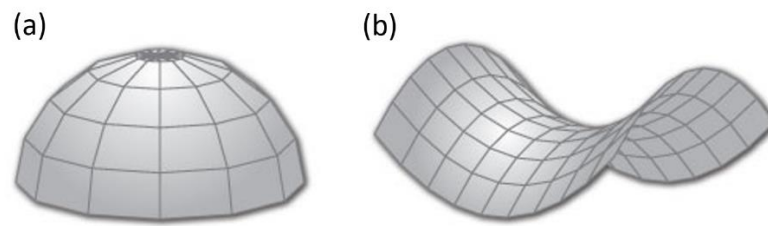


Figure 2-3 (a)Synclastic curvature (auxetic); (b)Anticlastic curvature (conventional) [39]

### **Sound absorption capacity**

Previous studies revealed that foams with NPR have a higher sound absorption capacity at all levels of frequencies. Besides, it was found that smaller pore-size NPR foams absorb sound more efficiently than those with larger pores at frequencies above 630 Hz [40, 41].

### **Variable permeability**

As pore size is increased when the auxetic materials are being stretched, auxetic materials display wide porosity variation under tensile load. This open-pore characteristic is highly desirable for certain applications, for instance, different substances can be stored in the pores of the auxetic material and released upon stretching [42, 43].

## **2.2.2 Applications of Auxetic Materials**

The enhanced mechanical properties derived from the auxetic materials over their non-

auxetic counterparts make them very attractive for a broad range of potential applications, including but not limited to personal and sports protective equipment [44]; composite reinforcements for aerospace and automotive applications [45, 46]; packaging [47]; fasteners [48]; seat cushion materials [49, 50]; smart filters [51, 52]; smart wound-healing bandages and vascular implants in biomedical industry [53-55]; blast mitigating curtains [56, 57]; adaptable garments such as maternity and kids clothes [58-60]; sound-proofing materials [61, 62]; and apparel with specific color changing effect [63].

### **2.3 Variety of Auxetic Textiles**

A wide range of auxetic textiles have been proposed and developed, including auxetic fibres, helical auxetic yarns, semi-auxetic yarns, auxetic fabrics and auxetic composites.

#### **2.3.1 Auxetic Polymers and Fibers**

Real interest in auxetic polymers fabrication begun when Caddock and Evans observed the auxetic effect in a microporous polymeric material due to its complex microstructure [64, 65]. Thereafter, different polymers were produced in such a manner to create auxetic effects, including ultrahigh molecular weight polyethylene [66], polypropylene [67] and nylon [68].



Although large auxetic effects have been reported, actual application of these auxetic microporous polymeric materials is considerably difficult. Therefore, Alderson et al. developed a novel processing route to produce the very first auxetic polymeric fibres using a modified melt spinning technique, and Poisson's ratio of the fibres was found to be around -0.6 [69]. Ravirala et al. fabricated some other auxetic polymeric fibres and films using a similar processing route to induce auxetic behavior into the fibers. Polypropylene films, polyester and nylon fibers were successfully produced and proved to exhibit a NPR. For instance, Poisson's ratio of the auxetic polyester fibers was measured to vary between -0.65 to -0.75 [70, 71].

### **2.3.2 Auxetic Yarns**

Hook produced a double helix yarn (DHY) by wrapping a high-stiffness filament over a low-stiffness filament to produce an auxetic effect and NPR as low as -5 was achieved [22]. At a later time, Zhang et al. coated the double helix yarn with silicone gel to fabricate a 3-component auxetic yarn. The resultant structure provided a good binding between the wrap and the core, and protected the high stiffness wrap yarn from breaking when it is stretched along the axial direction [72]. Lim fabricated a semi-auxetic yarn by stitching a thin inextensible cord into a thick elastic cord in a zigzag manner, and the maximum NPR value reported was similar to the double helix yarn

[73]. More recently, Ge et al. developed a novel kind of plied yarn structure by helically twisting two elastic filaments and two high modulus filaments together. Poisson's ratio of the helical auxetic yarns with this structure was found to be over -4 [23].

### **2.3.3 Auxetic Fabrics**

#### **2.3.3.1 Retrospect of Conventional Textile Fabrics**

Before the auxetic fabrics were developed, considerable studies have been undertaken to investigate the Poisson's ratio of various kinds of conventional fabrics. Shahabi et al. made a very detailed investigation on the effect of crimp to the contraction of worsted fabrics under tensile loading. It is stated that in the weaving production process, warp yarns are held in tension and the weft yarns are crossing over from above and below to produce a woven fabric. Crimp exists both in warp and weft direction, and they always interact with each other. When the fabric is extended in one direction, yarns in the direction of loading are straightened and their crimp reduces until it reaches zero. It conversely introduces more crimps to the yarn perpendicular to loading so that contraction is resulted in the transverse direction, which corresponds to a positive Poisson's ratio [74].

Hu carried out an experiment on the KES-F apparatus and revealed that Poisson's ratios of conventional woven fabrics in the two principal directions are very close to each other- that is, when a fabric is elongated lengthwise in one direction, widthwise contraction will be resulted in the other [75].

In the area of knitted fabric, Ajeli and Jeddi presented an experimental and theoretical study on the relationship between the warp-knitted structures and Poisson's ratio. It was found that the underlap length of loop fabric imposes the most significant effect on the Poisson's ratio of the warp-knitted fabric [76].

### **2.3.3.2 The Approach to the Manufacturing of Auxetic Textiles**

Although studies have shown that conventional fabrics possess a positive Poisson's ratio, it is still possible to alter this fundamental property in fabrics. In general, there are two approaches to fabricate auxetic textiles. The first approach is to use conventional fibres and yarns to create auxetic effect by knitting or weaving them in a special geometrical configuration. The second approach is to use auxetic fibers and yarns to fabricate auxetic textiles directly, such that auxetic effect can be created by simple weaving or knitting patterns. Previous studies have shown that both of the approaches could be adopted to produce fabrics with auxetic effect. A variety of weft-knitted and warp-knitted auxetic fabrics have been produced using the first approach;

however, their application has been rather limited by the three dimensional structure. Application of the second approach remains largely unexplored as there are limited auxetic fibers and yarns up to now [77].

### **2.3.3.3 Auxetic Weft Knitted and Warp Knitted Fabrics**

Since individual needle selection grants a high flexibility in pattern design, flat knitting technology has a great advantage in making fabrics with NPR. Liu et al. produced various weft-knitted auxetic fabrics on a flat-knitting machine. The auxetic fabrics were formed with a revised purl structure, in which the face loops and reverse loops were arranged in a zigzag pattern to create a 3-dimensional auxetic structure. A NPR as low as -0.5 was achieved when stretched [78]. Subsequently, Hu et al. manufactured a range of weft-knitted auxetic fabrics based on three different geometrical structures, including reentrant hexagons, rotating rectangles and foldable structures. The fabrics showed a good auxetic effect and the highest NPR achieved was about -0.5 [79]. Besides, Glazzard and Breedon reported variant auxetic weft-knitted fabrics based on a different knitting structure, by which relief stitches were adopted to create raised patterns while transferred stitches were used to distort the directions of the courses and wales such that a chevron shape could be achieved [58]. Exploration of auxetic fabrics is not limited to weft-knitting technique only; a series

of warp knitted auxetic fabrics were made during the last decade. Starbuck et al. held a patent valid for applying a triangular lattice shape in fabric to impart an auxetic effect [80]. Ugbolue et al. produced series of fillet warp knitted fabrics on a crochet knitting machine by using open lap loops to form the base structure and inlay yarns to effect compound repeating units. All of them were found to exhibit an auxetic effect with a maximum NPR of around -0.6 [47, 81]. Subsequently, the knitting pattern was modified by using a relatively stiff filament yarn to form a honeycomb structure and a highly elastic inlay yarn to change the disposition of the ribs in the net, and NPR value as low as -1.33 was achieved [82, 83]. On the other hand, Alderson et al. designed several warp knitted fabrics based on triangular and double arrowhead structure to impart an auxetic property to the fabric. The fabric samples were tested in different directions and the auxetic behavior was confirmed [84]. Most lately, Wang and Hu invented a novel kind of 3D auxetic warp-knitted spacer fabric by arranging two parallelograms in a V form to knit the two covering layers. Poisson's ratio of the spacer fabric produced under this method was found to be around -2.5 [85].

#### **2.3.3.4 Auxetic Woven Fabrics**

Although a wide range of auxetic textiles have been proposed and developed, most of them were focused on knitting and little attention has been paid to fabricate auxetic

woven fabrics. All of the auxetic woven fabrics developed so far are based on the use of DHY to generate auxetic effect, with a NPR value ranging from -0.1 to -0.3 [86, 87]. When the DHYs were converted into woven fabric composite, a maximum auxetic effect of -6.8 was achieved [88]. Related studies will be discussed in greater detail in section 2.5.

#### **2.3.3.5 Other Auxetic Textiles**

Studies of auxetic fabrics are not limited to woven and knitted textiles only. He et al. fabricated an entangled materials with a stainless steel continuous wire and a maximum NPR of -1.5 was achieved [89]. Quadrini et al. developed several auxetic epoxy foams by solid state foaming and found that foam plate with a re-entrant hexagonal pattern could generate an auxetic effect under different temperatures [90]. Most recently, Verma et al. applied a heat-compression protocol to the conventional needle-punched nonwoven fabrics and found that the heat-compressed nonwovens exhibited a large out-of-plane auxetic behavior. Lowest Poisson's ratio value for the auxetic non-woven fabrics was evaluated as -7.2 [91].

#### **2.3.4 Auxetic Composites**

Ge and Hu produced an auxetic three-dimensional fabric by combining the non-weaving and knitting techniques together, and the NPR was closed to -0.20 under

compression [92]. Most recently, Jiang et al. fabricated a different kind of auxetic three-dimensional composite by foaming a multilayer orthogonal auxetic structure and Poisson's ratio of the auxetic composite was around -0.10 under compression [93].

#### **2.4 Different Helical Structures and Their Respective Deformation Mechanism**

Fabrication of helical auxetic yarns is an exciting new area of research in the field of auxetics due to their wide range of potential applications. For example, they can be used as dental floss to remove food particles and plaque effectively. As the auxetic yarn expands when it is being stretched, it can fill in the gaps between teeth and make cleaning more effective. In addition, auxetic yarn can be used as a composite reinforcement in civil engineering industry [57]. Substituting conventional yarn by auxetic yarn could delay the pull-out process because auxetic yarn embedded in the composite will expand laterally and effectively lock into the matrix when tension load is applied [35].

It should be noted that auxetic yarns are not only suitable to use exclusively, but also feasible to fabricate woven and knitted fabrics with auxetic effect. Auxetic fabrics made of helical auxetic yarns display wide porosity variation under tensile load. Placing a substrate of a different color under the auxetic fabric layer, the open-pore

characteristic can generate a color changing effect for indicative or aesthetic purpose when stretched [86]. In addition, the open-pore characteristic can be utilized to control drug delivery for wound healing. For instance, anti-inflammatory agent can be stored in the smart compression bandage and released from the pores when the bandage extends due to wound swelling (Figure 2-4) [94]. Moreover, the open pore characteristic is favorable for filtration since particles of different sizes can be filtered out under different extension levels [95, 96].

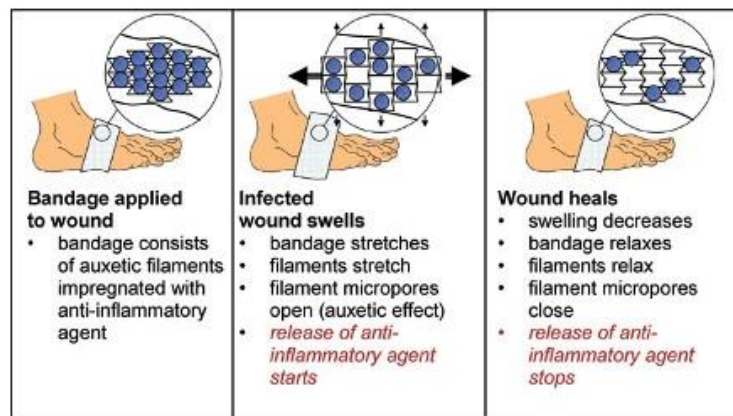


Figure 2-4 Schematic of smart bandage concept [97]

Auxetic fabrics made of helical auxetic yarns also demonstrated an excellent energy absorption property. Evans et al. made use of this property to produce a blast-proof curtain by interlacing the double helix yarns in a special alignment. During a bomb explosion, the blast-proof curtain can open up and disperse blast energies efficiently. Meanwhile, the expanded curtains can catch the debris and glass fragments effectively so that injuries caused by an explosion are mitigated [56, 98].



### 2.4.1 Double Helix Yarn

Two basic types of helical auxetic yarns (HAYs) can be defined according to the deformation mechanism that give rise to NPR, i.e. the double helix yarn (DHY) and the auxetic plied yarn. DHY is the first reported HAY in the field of auxetics which was proposed by Hook in 2003 [22]. As shown in Figure 2-5(a), DHY consists of two filaments in which a high stiffness filament is helically wrapped around a straight core filament with a larger diameter and lower stiffness. When DHY is being stretched longitudinally, two filaments gradually interchange their positions. As shown in Figure 2-5(b), the inextensible filament tends to straighten, thereby causing the low stiffness core filament to helically wrap around it and resulting in a net increase in the effective diameter of the yarn. When the load is removed, the low stiffness core filament serves as a return spring to resume its original configuration [99].

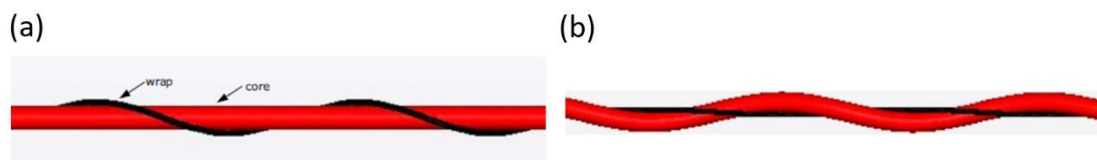


Figure 2-5 (a) DHY at zero strain; (b) DHY under tension

The basic structure and mechanics of the DHY have been widely studied. Wright, Sloan and Evans carried out a finite element analysis and an experimental study to

investigate the influence of structural and material parameters on the auxetic performance of the DHY. Both of the numerical and experimental results revealed that auxeticity of DHY is dominantly affected by diameter ratio, inherent Poisson's ratio of the constituent yarns and initial wrapping angle of the DHY [99, 100].

Du et al. conducted a theoretical analysis to predict the auxetic performance of the DHY for any given tensile strain. An experimental study was carried out afterward to verify the accuracy of the model. The studies demonstrated that it is possible to engineer the auxetic behavior of the DHY by means of appropriate selection of certain structural and material parameters, including diameter ratio, wrapping angle and tensile modulus of the stiff yarn [101, 102].

Sibal and Rawal proposed a DHY system to predict the auxetic behaviour of the DHY through energy minimization approach and the DHY system was validated with the experimental results obtained from previous research [103].

Bhattacharya et al. investigated the core-indentation effects on the auxetic behaviour of the DHY. Cross-sectional images of a series of strained DHYs were captured to examine deformation of the elastic core yarn by the high stiffness wrap yarn. It was found that NPR can be maximized if the core-wrap moduli ratio is just high enough to

generate an auxetic effect and low enough to prevent the stiff yarn from embedding into the soft yarn [104].

### **2.4.2 Auxetic Plied Yarn**

Studies of helical auxetic yarn were predominantly focused on DHY, until recently, Ge et al. have developed another new type of HAY, the auxetic plied yarn that exhibits NPR [23]. Figure 2-6(a) schematically illustrated the structure of the auxetic plied yarn. It can be seen that two soft yarns of a relatively large diameter are employed to form the base structure in the centre position while two stiff yarns are spiralling around them to form a 4-ply helix structure.

Deformation mechanism of the auxetic plied yarn is different from that of DHY in which the auxetic behaviour is caused by the migration of stiff yarns in the plied structure. As shown in Figure 2-6(b), when the auxetic plied yarn is stretched along its longitudinal axis, the stiff yarns will tend to migrate to the centre and push the soft yarns outward, resulting in a lateral expansion of the auxetic yarn's maximal width. Compared with the DHY which has a filament helically wrapping around a barely twisted filament and being unbalanced, the auxetic plied yarn is more stable so that twist regularity of the auxetic yarn can be improved.

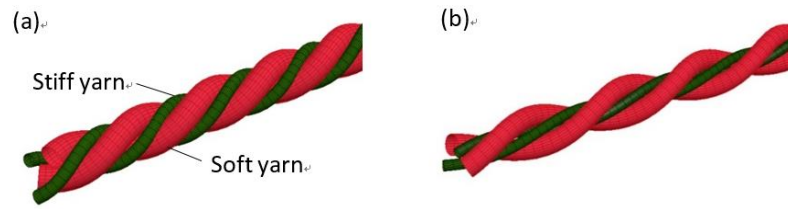


Figure 2-6 4-ply auxetic yarn (a) at rest; (b) under tension

The work of Ge et al. presented a geometric analysis to calculate the Poisson's ratio values of the auxetic plied yarn under tension theoretically. As shown in Figure 2-7, experimental study was carried out to verify the auxetic effect and to compare with the geometric analysis. The study revealed that the auxetic plied yarn samples possessed a NPR effect but the geometrical analysis was only capable to predict the Poisson's ratio at high strain region. In low strain range the predicted radial strain values are much higher than the actual values measured in the experiment. Correspondingly, the expected Poisson's ratio values are much higher than the actual one, leading to an opposite trend in the Poisson's ratio-axial strain curves [23].

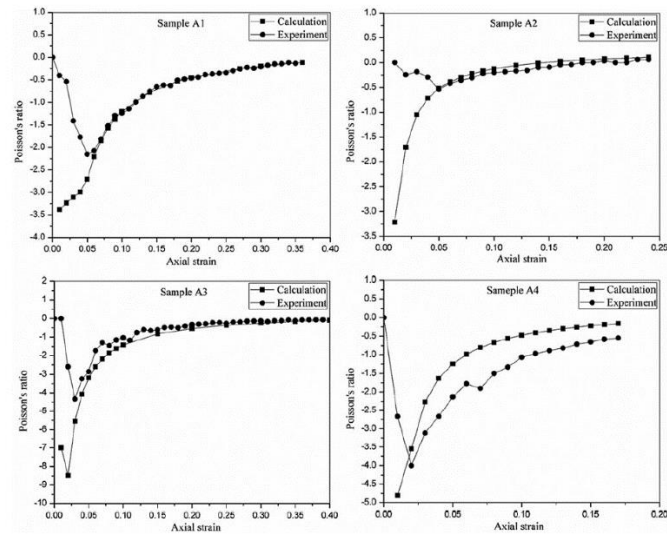


Figure 2-7 Poisson's ratio as a function of axial strain [23].

## 2.5 Auxetic Textiles Fabricated from Helical Auxetic Yarn

Apart from investigations on the structure and mechanics of the HAYs, previous research works also focused on employing DHY to produce fabrics with auxetic effect. Wright et al. fabricated two kinds of DHYs and used them separately to produce narrow plain weave fabrics. The DHYs were made of different cores and warps with the same wrap angle. To fabricate the woven fabrics, DHYs in both of S and Z directions were arranged alternatively in the warp to weave with different weft yarns. The result showed that only one of the fabrics exhibited an auxetic effect at a particular strain range, with a maximum negative value of -0.1. It implied that selection of weft material and weaving pattern are significant to generate in-plane and out-of-plane NPR. In addition to the Poisson's ratio measurement, the study demonstrated the possibility for the auxetic fabric to generate open pore effect for different applications [86].

Lee et al. held a patent for the production of a porous sheet by arranging pairs of S- and Z- twisted moisture-sensitive auxetic filaments in a parallel manner to generate auxetic effect. The auxetic filament consists of two components in which a moisture-sensitive shrinkable filament is helically wrapped around an elastomeric material resting in the core. By means of an aqueous solution, a pseudo tensile force is generated in the shrinking filament. It tends to straighten out, thereby causing the two components to interchange their positions with each other. As a result, auxetic effect can be produced even if no external force is applied. At the same time, pores are created because the elastic components undergo opposite displacement under specific alignment [105].

Vysanska and Vintrova used conventional multifilament yarn for the warp and double helix yarn for the weft to produce three woven fabrics with various weaving structures. It was found that the 2/2 twill weave could yield a highest NPR which was nearly -0.3, followed by plain and 3/5 satin weaves [87].

Miller et al. fabricated two kinds of auxetic composites which exhibited a NPR close to -0.1 when stretched. A twisted ultra-high molecular weight polyethylene fibre was used to wrap around a polyurethane core with an approximate wrap angle of 70° to

produce the DHY. Subsequently, two woven textiles were made using plain weave, with the weft being the DHYs and the warp being a meta-aramid fibre. The textile structures were then finished with silicone rubber gel to fabricate one single layer composite and one double layer composite. It was found that a minimum of two layers are required to generate in-plane NPR; stretching the single layer composite caused the DHYs to overlap each other and resulted in the loss of in-plane auxetic effect [106].

At a later time, Miller et al. have proposed another type of auxetic composite and a Poisson's ratio as low as -6.8 was achieved. A low tow count carbon fibre was used to wrap around a monofilament nylon fibre with different wrap angles to fabricate the DHY samples. The auxetic composite was then produced by adhering two layers of DHYs uniaxially with polyester resin. The study demonstrated that the auxetic composite samples not only possessed reasonable high stiffness, but also capable to produce NPR effect upon axial lengthening [88].

## **2.6 Methods for Investigation of Yarn Structure**

### **2.6.1 Introduction**

Over the past few decades, a wide range of devices and methods have been proposed and developed to study the yarn from the internal and external structures. In the

following section, different techniques are reviewed, including the image processing technique, photoelectric technique, tracer fiber technique, cross-sectional microscopic examination and micro-computed tomography.

### **2.6.2 Image Processing Technique**

Image processing techniques have been widely used in textile research to study the external structure of the yarn, by which images of yarn from the longitudinal view are captured and processed for evaluation.

Ge et al. applied an image processing technique to verify the auxetic effect of the auxetic plied yarns. The yarn samples were subjected to a tensile test and a digital camera was used to capture the longitudinal view of the yarns at a time interval of 3 seconds. The images captured were then used to measure the maximal thickness of the yarn, and to calculate the transverse strain and Poisson's ratio correspondingly [23].

Cybulska presented a computer image processing system to estimate yarn thickness, hairiness and twist from the greyscale images of yarn before and after breakage [107].

Watanabe et al. used a similar technique to evaluate the blend irregularity in blended yarns, by which a CCD camera was used to capture the image, and the standard images were converted into trivalued images. Number of pixels were counted afterward to



calculate the yarn diameter, blend ratio and the size of a cluster of fibers [108]. A modified system was then developed to evaluate blend irregularity from the original images directly, which was done by measuring series of intensity values around the center line along the yarn axis [109]. Behtaj et al. proposed an image analysis-based technique to characterize air-jet textured yarn structure. Two images were captured at right angles to examine the yarn in the same section and a Canny algorithm was applied to determine core diameter, average loop size, loop frequency and extent of hidden loops [110].

### **2.6.3 Photoelectric Technique**

Photoelectric method has long been used to measure diameter of yarns by researchers. A photoelectric sensor consists of an emitter for emitting light and a receiver for receiving light. According to the silhouette principle, as the irradiance reflected on the receiver varies by varying yarn diameter, resistance of the receiver is recorded and converted into a voltage. After the relationship between the yarn diameter and output voltage of the sensor device is derived, yarn diameter can be calculated accordingly [111].

Miao measured the diameter of carbon nanotube yarns by mounting the yarn on a

tensile testing machine accompanied with a laser diffraction system [112, 113]. Huh et al. developed a system to deliver the yarn between the transmitter and receiver to measure the thickness variations in ring spun yarns with the aid of the laser slit beam [114]. Yoshiki et al. studied the structural changes of carbon nanotube yarn with the use of photoelectric device during tensile testing, for which fiber diameter, transversal strain and Poisson's ratio of the yarn were determined by separating the intensity minima from the diffraction pattern [115]. Tsai and Chu designed a new method to measure diameter of yarns with an elliptical cross-section using the photoelectric technology. Considering that certain yarns have an elliptical cross-section, a sensor device was employed to emit two incident beams of light perpendicular to each other to measure diameter of the yarns [111, 116].

#### **2.6.4 Tracer Fiber Technique**

Tracer fiber technique has been frequently used to investigate the structure of yarns. To apply this technique, a small proportion of colored fibers is mixed with the uncolored fibers during the spinning process. The yarns produced are then immersed in a liquid of the same refractive index as the fibers so that the uncolored fibers in yarn become almost transparent, and the colored fibers can be seen easily.

Feng et al. studied the internal structure of the yarns based on this technique. Yarn samples were made with tracer fibers and a CCD camera was used to capture yarn images from two perpendicular planes. The images captured were then processed to re-construct the whole trajectory of a tracer fiber inside the yarn and analysis was carried out in a three-dimensional way [117]. Kumar et al. also applied this technique to characterize and visualize the configuration of fibers in ring spun yarn during progressive yarn extension [118]. Ishtiaque et al. applied the multi-colored tracer fiber technique to study the configuration of fibers in yarn during extension. An optical microscope equipped with a Microcontroller-based 3D yarn structure analyzer was used to capture images of extended yarn in two orthogonal planes, and a specially designed software was used to identify the position of colored tracer fibers and yarn boundary [119].

### **2.6.5 Cross-sectional Microscopic Examination**

Considerable research has been carried out to study the internal structure of the yarn by cross-sectional microtomy. In conventional cross-section analysis, yarn samples are embedded into resin, cut into slices and observed under microscope, so that internal structure of the yarns can be observed from the cross-sectional images.

Salehi and Johari studied the fiber packing density of lyocell ring-spun yarns based on this method. Yarn cross-sectional images were used as input data to calculate the fiber packing density [120]. Zhong and Jin studied the cross section structural parameters of blended yarns by cross-sectional microtomy. The software ImageJ was used to convert the cross-sectional slice images into grey scale and then binary images. Particle analysis was further conducted to measure the blending ratio, spatial distribution and geometric size of fibers in the blended yarns [121]. Zheng et al. used a similar approach to investigate the fiber distribution pattern in yarn cross section for vortex-spun yarn. The software Photoshop was used to calculate fiber packing density by counting the pixel of the fibers and the yarn cross section [122]. Najar et al. used a similar technique to investigate the fiber-blending irregularities and fiber migration of the blended yarns. Images were captured and processed by a software called YICP from which yarn diameter, index of blend irregularities, sizes of fiber clusters and preferential fiber migration were measured by applying a mathematical technique on bitmap data [123]. Ishtiaque also used this technique to measure the packing density and radial packing density of engineered carpet yarns [124].

Chiu and Liaw proposed a new image processing method to recognize the fiber patterns from the cross-sectional image of PET/Rayon composite yarn based on the

voting concept of the Hough transform. Gray level segmentation method was used to cluster the original image, a binary and an edge image were then obtained. The binary image was used to implement the connected component voting technique to locate the position of the fiber while the edge image was used to detect the circular shape of the fiber through circle parameter voting method. Finally, the results of fiber location and circle detection were combined to recognize the fiber [125].

In the work of Herath et al., yarn samples were wrapped around an aluminum frame, embedded into epoxy resin and then ground to half of the height of the aluminum frame such that filament distribution of the hybrid yarns could be viewed under microscope and cross-sectional images could be captured for analysis [126].

#### **2.6.6 Micro-computed Tomography (Micro-CT)**

Micro-CT is a non-destructive technique which allows three-dimensional observation of the internal structure of an object as small as a few micrometers in size [127].

Pazmino et al. carried out an X-ray micro-CT analysis to investigate the internal deformed geometry of a composite reinforcement. Samples were scanned and the radiographic images were processed to study the damage mechanism and to observe the internal geometry of the samples during shear deformation [128].

## 2.7 Summary

In summary, two kinds of HAYs have been proposed and developed so far. Previous studies have predominantly focused on DHY while available literature on the auxetic plied yarn is limited. A geometric analysis has been presented to calculate the Poisson's ratio values of the 4-ply auxetic yarn at different strains. However, the experimental study revealed that the geometrical model was only capable to predict the Poisson's ratio in high strains. Factors affecting the tensile properties and auxetic behaviour of the auxetic plied yarn are not well understood and characterized.

In addition, it should be noted that this kind of auxetic plied yarn includes, but not limited to a 4-ply structure. For instance, as shown in Figure 2-8, auxetic plied yarn can be produced in a 6-ply structure by arranging three soft yarns and three stiff yarns alternatively to create auxetic effect with the same mechanism. Investigations can be carried out to compare the tensile and auxetic behaviour of different types of helical auxetic yarns under monotonic and cyclic tensile loading.

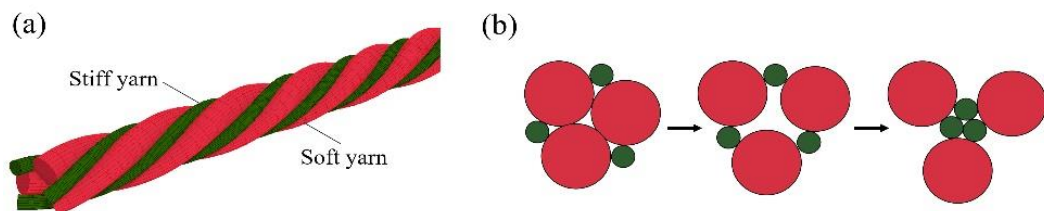


Figure 2-8 6-ply auxetic yarn: (a) side view; (b) cross-section view at different states

Different methods for the investigation of yarn structures have been reviewed. In the previous research, image processing technique was applied to assess the auxetic performance of auxetic plied yarn in the XY plane (Figure 2-9), which is referred to the plane of elongation. This two-dimensional assessment is capable to measure the growth of yarn along the X direction when stretched along the Y axis, but not able to provide a deep understanding on the deformation mechanism of the auxetic plied yarn under axial tension load. Internal structure of the auxetic plied yarn in XZ plane should be examined as various information can be obtained from a series of cross-sectional image of auxetic plied yarn under different extension levels, such as migration of stiff yarns and soft yarns; variation in shape and size of the cross sections of the constituent yarns; and changes in diameter of the auxetic plied yarn. The research findings should be able to validate the mechanism of the auxetic plied yarn to produce NPR effect experimentally by removing assumptions and replacing them with actual data.

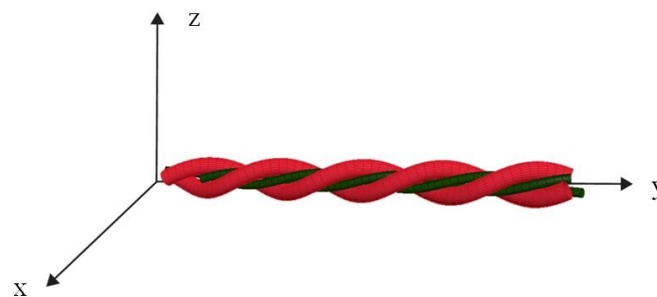


Figure 2-9 4-ply auxetic yarn in x-y-z coordinate system

Based on the literature review on the auxetic textiles as given above, auxetic yarns can be used to generate NPR effect in fabrics. However, this approach remains largely unexplored as only a few auxetic woven fabrics and composites were proposed and made using DHYs and no attention has been paid to fabricate auxetic fabrics from auxetic plied yarns. NPRs and strain-dependent mechanical properties of textiles made of auxetic plied yarns are unknown. Experiment can be carried to fabricate textiles with different auxetic plied yarns and fabric structures, and to evaluate their variations brought by different design parameters.



## **CHAPTER 3 FABRICATION OF AUXETIC PLIED YARN**

### **3.1 Introduction**

Auxetic plied yarn samples were prepared for the cross-sectional examination, factorial analysis and fabrication of the auxetic fabrics. In order to keep a constant yarn quality in spinning, a helical auxetic yarn spinner is built to fabricate lab-scale lengths of auxetic plied yarns.

### **3.2 Spinning Process**

The schematic diagram of the auxetic yarn spinning device is shown in Figure 3-1. Auxetic yarns with different helical structures can be made by feeding different amount of single yarn to the spinning device. To produce a 4-ply auxetic yarn, two strands of soft yarns and two strands of stiff yarns are alternately arranged and fed through the yarn guiding board which is fixed at one end of the spinning device. Ends of the constituent yarns are wrapped with adhesive tape in which the stiff yarns are separated by the soft yarns while the soft yarns are adhered to one another. The wrapped yarns are then held in the clamp which is fixed on a movable board connected with a rotating handle.

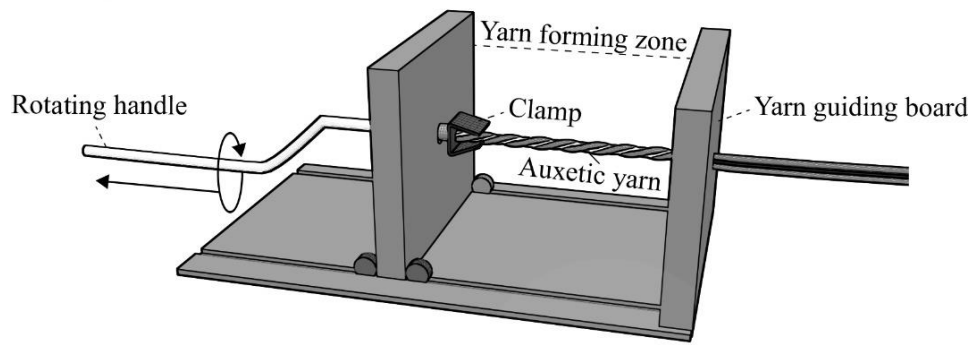


Figure 3-1 Schematic diagram of the helical auxetic yarn spinning device

In making ply yarns from spun strands, the movable board is initially positioned in front of the yarn guiding board. The handle is manually rotated and moved backward simultaneously to draw free ends of constituent yarns to the yarn forming zone, such that the constituent yarns are combined into 4-ply helix yarn after it passed through the yarn guiding board. Consistent rotation speed is kept to avoid irregularity in the 4-ply auxetic yarn structure. A very long length of auxetic plied yarn can be produced at once as the spinning process can be repeated infinitely by removing the yarn sample from the clamp, drawing it forward, and retighten the clamp to clear the finished ply yarn in the yarn forming zone.

The auxetic plied yarn can be spun in two different directions to create either an S- or a Z-twist. In addition, different twist level can be obtained by varying the spinning parameters. The amount of twist inserted is determined by the length of the yarn fed

through the yarn guiding board and by the number of twists imparted over that length. Therefore, the twist can be modified by keeping either parameter constant and varying the other. To increase the twist level, rotational speed can be kept constant while decreasing the yarn drawing speed; or the yarn drawing speed can be kept constant while increasing the rotational speed. The same result will be obtained in either case.

### **3.3 Samples Preparation**

To quantitatively evaluate the effect of different parameters on the mechanical properties of the 4-ply auxetic yarn, twelve kinds of single yarns were procured to fabricate the yarn samples and their specifications are shown in Table 3-1. Firstly, to make clear the effect of soft yarn diameter, four different polyester covered rubber cords were used as soft yarns, with a diameter of 2.18 mm, 1.56mm, 1.14 mm and 1.02mm respectively. Secondly, to investigate the effect of tensile modulus of stiff yarn, four different single yarns of similar diameter were selected as stiff yarns, with an elastic modulus of 630MPa, 489MPa, 985MPa and 1307MPa respectively. Thirdly, to further investigate the effect of diameter ratio, four nylon monofilaments were selected, with diameters of 0.3mm, 0.4mm, 0.45mm and 0.5mm respectively. Relatively coarser filaments were chosen to fabricate the yarn samples due to the fact that they can be recognized more accurately thus a better profile could be obtained for further analysis.

Table 3-1 Specifications of the single yarns

Single Yarn	Material	Diameter (mm)	Elastic modulus (MPa)	Elongation at break (%)
A	Polyester covered rubber cord	2.18	13	189
B	Polyester covered rubber cord	1.56	14	150
C	Polyester covered rubber cord	1.14	8	222
D	Polyester covered rubber cord	1.02	9	247
1	Polyester covered monofilament cord	0.87	630	20
2	Polyester braided cord	0.87	489	28
3	3 ply polyester thread	0.80	985	14
4	Waxed polyester cord	0.77	1307	10
5	Nylon monofilament	0.30	2214	19
6	Nylon monofilament	0.40	2197	17
7	Nylon monofilament	0.45	2061	14
8	Nylon monofilament	0.50	2427	16

Different soft yarns and stiff yarns were combined together to fabricate 21 kinds of yarn samples and their construction characteristics are listed in Table 3-2. In this study, my focus remained here on the auxetic plied yarn in 4-ply structure; 4-ply auxetic yarn samples were made at a twist level of 51 turns/m. Additional twist levels of 35 turns/m, 43 turns/m and 58 turns/m were employed for sample A-1 to evaluate the effect of twist level, such that a total of 19 different 4-ply auxetic yarn samples were produced.

For comparative purposes, yarn A and yarn 1 were selected to fabricate additional DHY and 6-ply auxetic yarn samples (named A-1-D and A-1-T) with a twist of 51 turns/m to investigate the effect of helical structures on the auxetic behavior of the HAY. To ensure consistent quality, these yarn samples were produced with a length of two meters each time and cut into sections for further sampling. Photograph of the yarn samples is shown in Figure 3-2.

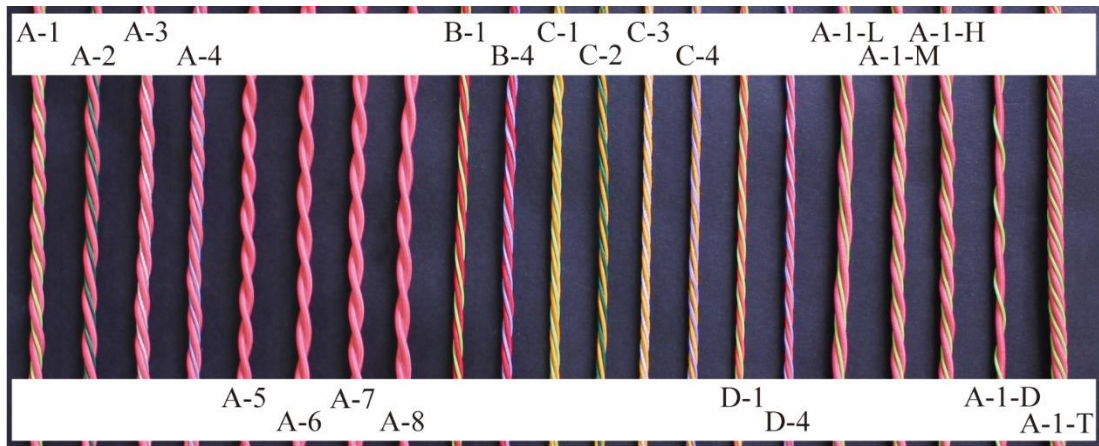


Figure 3-2 Helical auxetic yarn samples

Table 3-2 Construction characteristics of the helical auxetic yarn samples

Sample Code	Yarn type	Yarn composition		Yarn twist (turns/m)	Diameter (mm)
		Soft yarn	Stiff yarn		
A-1	4-ply	A	1	51	4.06
A-2	4-ply	A	2	51	4.06
A-3	4-ply	A	3	51	4.07
A-4	4-ply	A	4	51	4.16
A-5	4-ply	A	5	51	3.95
A-6	4-ply	A	6	51	4.03
A-7	4-ply	A	7	51	4.09
A-8	4-ply	A	8	51	4.09
B-1	4-ply	B	1	51	3.05
B-4	4-ply	B	4	51	2.98
C-1	4-ply	C	1	51	2.88
C-2	4-ply	C	2	51	2.68
C-3	4-ply	C	3	51	2.55
C-4	4-ply	C	4	51	2.68
D-1	4-ply	D	1	51	2.59
D-4	4-ply	D	4	51	2.76
A-1-L	4-ply	A	1	35	4.09
A-1-M	4-ply	A	1	43	4.09
A-1-H	4-ply	A	1	58	4.06
A-1-D	Double helix	A	1	51	3.33
A-1-T	6-ply	A	1	51	4.51

## **CHAPTER 4 TENSILE PROPERTIES AND AUXETICITY OF THE AUXETIC PLIED YARN**

### **4.1 Introduction**

As important as tension, transverse compression, torsion and bending, Poisson's ratio in tensile deformation is one of the fundamental characteristics of yarn. Relationships between physical properties and contraction of yarns have long been concerned before 'Poisson's ratio' is realized. Barella studied the effect of twist on yarn diameter under different tensile loads [129]. Onions et al. evaluated the effect of twist and fibre crimp on thickness of a range of worsted-spun yarns [130]. Hearle and Merchant investigated the effect of tension on diameter of spun nylon yarns [131]. Regarding the research works related to auxetic yarn, it has been suggested that helical auxetic yarns would only exhibit a NPR under certain conditions. Many studies have been carried out to investigate the influence of different structural parameters on the auxetic behavior of double helix yarns. However, such studies for the 4-ply auxetic yarns were absent.

Therefore, a quantitative study on the auxetic plied yarns is carried out to evaluate their tensile properties and auxetic behavior under different extension levels. Three main purposes are accomplished by conducting such a study. Firstly, the experimental study is carried out to discuss design variables that generate a NPR in the 4-ply auxetic yarns, in terms of diameter of soft yarn and stiff yarn, tensile modulus of the stiff yarn and

twist level. Secondly, comparisons are made to evaluate the effect of helical structures on the auxetic behavior of the HAYs under monotonic and cyclic tensile loading. Thirdly, auxetic behavior of the 4-ply auxetic samples will be reviewed and some of the samples will be chosen to make auxetic fabrics in later chapters.

Various methods can be used to measure diameter change of HAYs upon extension including photoelectric technique, tracer fiber technique and image processing technique. Photoelectric devices can be used to measure the thickness variation of HAY during tensile test, but it is expensive for device acquisition. About the tracer fiber technique, it is not applicable for the HAY analysis because all of the constituent yarns provide important information on the production of the NPR. Therefore, although application of image processing technique is time consuming, it is the best method to measure the continuous change of diameter under different extension levels, since digital camera and tensile testing machine are readily available for the experiment. In addition, mechanical data of the yarn can be obtained simultaneously.

## **4.2 Experimental Details**

### **4.2.1 Sample Preparation**

Refer back to Table 3-2 in Chapter 3, all types of the HAY samples were tested. All of



the samples were conditioned at  $20 \pm 2^\circ\text{C}$  and  $65 \pm 2\%$  relative humidity for 24 hours prior to testing.

#### **4.2.2 Experimental Design**

Experiments were carried out to evaluate the tensile properties and auxeticity of the HAY samples and the specifications of the experimental design are listed in Table 4-1. Comparisons were made on different groups of yarn samples to study the effect of each design parameter on the mechanical properties of the 4-ply auxetic yarn, and the effect of helical structures on the mechanical properties of the HAYs under monotonic and cyclic loading.

Table 4-1 Specifications of the experimental design

Group	Comparison	Parameters	Factor	Tensile Testing Condition
1	A-1, B-1, C-1, D-1	Soft yarn diameter:	Diameter of soft yarn	Monotonic to failure
2	A-4, B-4, C-4, D-4	2.18mm, 1.56mm, 1.14mm, 1.02mm		
3	A-5, A-6, A-7, A-8	Stiff yarn diameter: 0.30mm, 0.40mm, 0.45mm, 0.50mm	Diameter of stiff yarn	Monotonic to failure
4	A-1, A-2, A-3, A-4	Stiff yarn tensile modulus:	Tensile modulus of stiff yarn	Monotonic to failure
5	C-1, C-2, C-3, C-4	630 MPa, 489 MPa, 985 MPa, 1307MPa		
6	A-1-L, A-1-M, A-1, A-1-H	Yarn twist: 35 turns/m, 43 turns/m, 51 turns/m, 58 turns/m	Twist level	Monotonic to failure
7	A-1-D, A-1, A-1-T	Yarn type: double helix, 4-ply, 6-ply	Helical structure	Monotonic to failure
8	A-1-D, A-1, A-1-T	Yarn type: double helix, 4-ply, 6-ply	Helical structure	Cyclic loading (10 cycles)

### 4.2.3 Measurement Method

Single yarns (Yarn A, B, C, D, 1, 2, 3, 4, 5, 6, 7, 8) were prepared for mechanical testing according to ASTM D2256 – tensile properties of yarns by the single-strand method. Tensile measurements were conducted on INSTRON 4411 mechanical testing machine using a 500N load cell. Individual soft yarns of 150mm length were stretched at a rate of 500mm/min while individual stiff yarns of 250mm length were stretched at a rate of 50mm/min until rupture. Three tests were conducted for each sample to obtain the average tensile properties. Load and elongation were measured during the test and converted to tensile stress and strain to make comparison between different yarns possible.

To measure the tensile properties of samples from all groups, tensile tests were conducted on the same machine at a gauge length of 250mm and a crosshead speed of 50mm/min until breakage. Considering that the auxetic yarns may be repeatedly stretched and relaxed in real-world applications, a second batch of HAY samples made with different helical structures (samples A-1-D, A-1 and A-1-T) was prepared and subjected to repeated cycles of loading and unloading to evaluate whether there is loss of mechanical properties during repeated tensile test. Preliminary tests showed that the maximum extension achievable is equal to 29 percent for A-1-D, 23 percent for A-1

and 25 percent for A-1-T. Therefore, three extensions levels were chosen to assess the HAYs. These levels were 5, 10 and 15 percent. Yarn samples were loaded for ten cycles at the same gauge length and rate of extension. In each cycle, the specimen was loaded to the specific extension level; then unloaded to zero force with the same speed and held for 10 seconds for strain relaxation.

All of the specimens were tested with a pre-tension of 0.5N. One side of yarn end is secured in the upper clamp, and the other side is applied with pre-tension before closing the lower clamp to ensure that all the slack or kinks from the specimens are removed without appreciable stretching. Three tests were conducted for each sample to obtain average tensile properties, including axial strain, tensile strength, and elongation at break. To make comparison between different yarns possible, the load and elongation data gathered during the test were converted to tensile stress and strain, where the stress was calculated based on the initial cross-sectional area of the yarn measured in the cross-sectional image.

In order to measure the auxetic behavior of the HAY samples during different period of elongation, a high-resolution CMOS camera was attached to the tripod and placed in front of the tensile testing machine at a distance of 40cm to the specimen (Figure 4-

1). Consecutive images of the tested sample were captured at 2-second intervals during the experiments, which corresponded to a 0.7% interval of the tensile strain  $\epsilon_x$ . The raw images were saved in the computer and converted to greyscale, and then binary image (Figure 4-2).

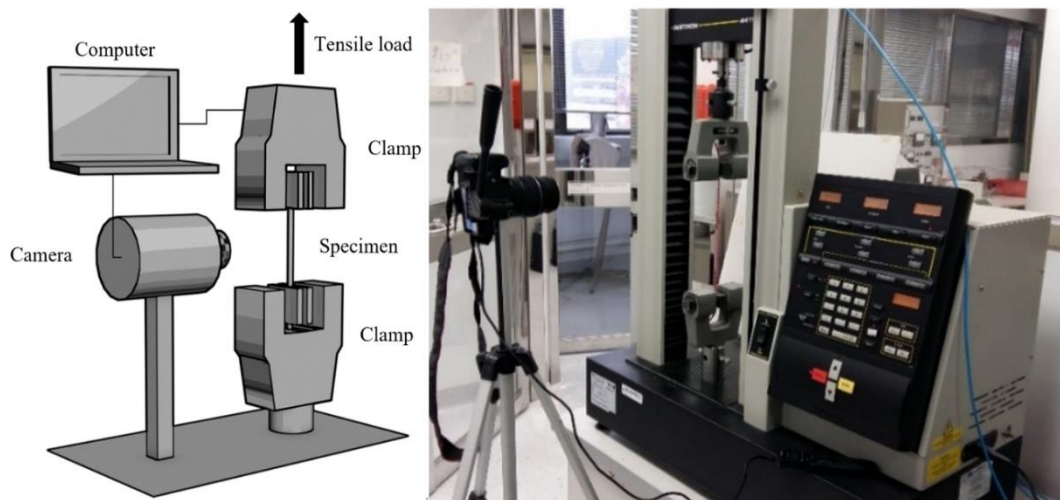


Figure 4-1 A schematic diagram and photograph of the tensile testing system

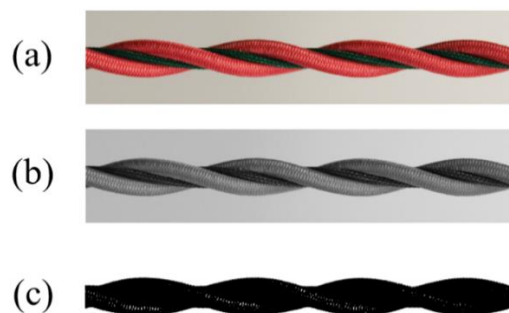


Figure 4-2 Conversion of the captured colour image  
(a) Original image (b) Greyscale image (c) Binary image

As shown in Figure 4-3, the binary images provided the maximal thickness of the yarn sample at the initial state  $D_0$  without tension and that at the stretched state  $D$ . Once the

values of  $D_0$  and  $D$  were obtained by counting the number of pixels in the images, transverse strain  $\varepsilon_y$  could be calculated from equation (1)

$$\varepsilon_y = \frac{D - D_0}{D_0} \quad (1)$$

As the tensile strain  $\varepsilon_x$  was directly provided by the tensile testing machine, Poisson's ratio of the HAY  $\nu$  could be calculated from equation (2).

$$\nu = -\varepsilon_y / \varepsilon_x \quad (2)$$

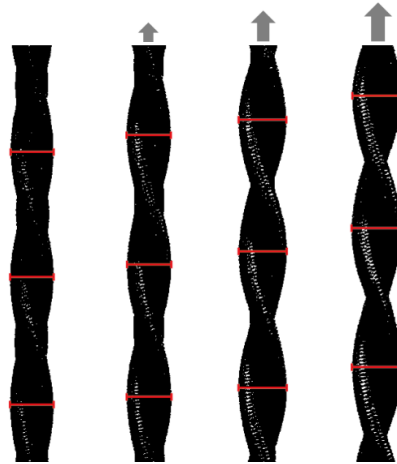


Figure 4-3 Binary images of the 4-ply auxetic yarns at different strains

### 4.3 Results and Discussion

#### 4.3.1 Typical Tensile and Deformation Behavior

Auxetic yarn sample A-4 is selected here as an example to discuss the typical tensile and deformation behavior of the 4-ply auxetic yarn structure. Its tensile stress-strain curve and those of its component single yarns are depicted in Figure 4-4(a). In order to get a better view of those curves at low level of stress, an inset is also shown in this

figure. It can be seen that stiff yarn 4 has a much higher stiffness and a much lower degree of elongation than soft yarn A. Combining two strands of soft yarns and two strands of stiff yarns in a 4-ply helix structure, sample A-4 shows a higher elongation at break than single stiff yarn, due to the obliquity effect in the 4-ply structure and variability in breaking extension brought by the soft yarns.

Figure 4-4(a) also shows that the typical tensile stress-strain curve of the 4-ply auxetic yarn structure can be divided into two stages. In the first stage, there is a relatively large increase in tensile strain for a very small increase in tensile stress. In other words, the auxetic yarn exhibits an initially low stiffness until it takes about 5 percent of the yarn's breaking strength. It is mainly governed by the tensile property of soft yarns, owing to the fact that the low modulus soft yarns located in the core region bear the load and the high modulus stiff yarns tend to move towards the yarn center to avoid being strained. As the specimens were pre-tensioned prior to testing, this eliminated the possibility that the effect is induced by yarn slack and inaccurate test length. In the second stage, the tensile stress-strain curve exhibits an increased slope. This can be explained by the fact that the two stiff yarns start to take more loads when they migrate to the yarn core and jam together; thereby, the tensile behavior of the 4-ply auxetic yarn is mainly dependent on that of stiff yarns at this stage.

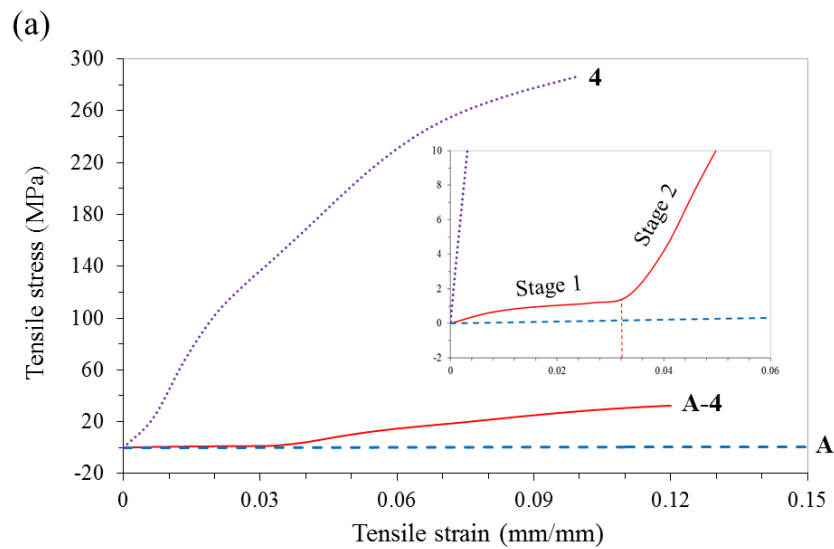


Figure 4-4 (a) Typical tensile stress-strain curves of 4-ply auxetic yarn sample A-4 and its constituent single yarns. The inset shows the enlargement at small stress

Correlated Poisson's ratio versus tensile strain for the 4-ply auxetic yarn sample A-4 is shown in Figure 4-4(b). It is observed that the NPR value first increased and then gradually decreased with increasing the tensile strain until the yarn was broken. Coupled with the tensile stress-strain curve, the increase in NPR once again supported that the resulting graph represents well the actual extension of the 4-ply auxetic yarn; since taking up the slack of the yarn, if any, should result in a positive Poisson's ratio.

Maximum NPR behavior is obtained at a strain of around 0.033, where stage 2 just starts. This can be attributed to the migration effect of stiff yarns in the auxetic plied yarn structure. When the two stiff yarns have an attempt to slide over the surface of the two soft yarns resting in the yarn core, a force is required to start the stiff yarn



moving. The force that resists the movement of stiff yarn is the frictional force. Once migration is initiated, the force required to keep it moving is lower than the original starting force. As a result, transversal strain of the auxetic yarn increases rapidly, leading to an increased NPR. Under high axial extension, yarn core starts to jam with stiff yarns. In this case, although the transversal strain decreases due to the cross-sectional contraction of the constituent yarns, the plied yarn is still auxetic as its instantaneous width is still bigger than its starting width before breakage.

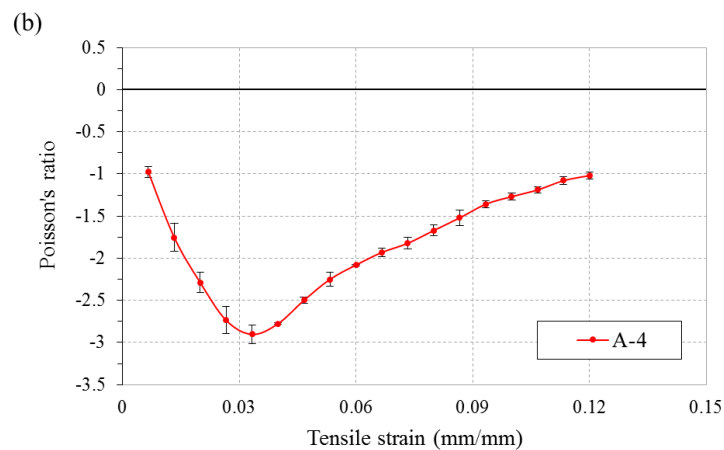


Figure 4-4(b) Correlated Poisson's ratio-axial strain curve

### 4.3.2 Effect of Soft Yarn Diameter

To investigate the influence of the diameter of soft yarn on the tensile and deformation behavior of the 4-ply auxetic yarn structure, comparisons were conducted between different auxetic yarn samples made with the same stiff yarn but soft yarns of different diameters (2.18mm, 1.56mm, 1.14mm and 1.02mm respectively). Two groups of

samples A-1/B-1/C-1/D-1 and A-4/B-4/C-4/D-4 were used for evaluation and the respective tensile stress-strain curves are depicted in Figures 4-5(a) and 4-5(b), respectively. It can be seen that samples which have a finer soft yarn in their respective group demonstrate an earlier onset of stage 2 during the tensile process, accompanying with a higher ultimate tensile strength. For samples C-1 and D-1, divisions of the two stages even become indistinguishable. It is most likely that the strength of auxetic plied yarn depends largely on the magnitude of the radial pressure exerted by the stiff yarn. Given that stiff yarns separated by a finer soft yarn can move to the yarn core shortly, once migration is completely restricted, the strength of the stiff yarns will impose a greater contribution to the strength of the auxetic plied yarn.

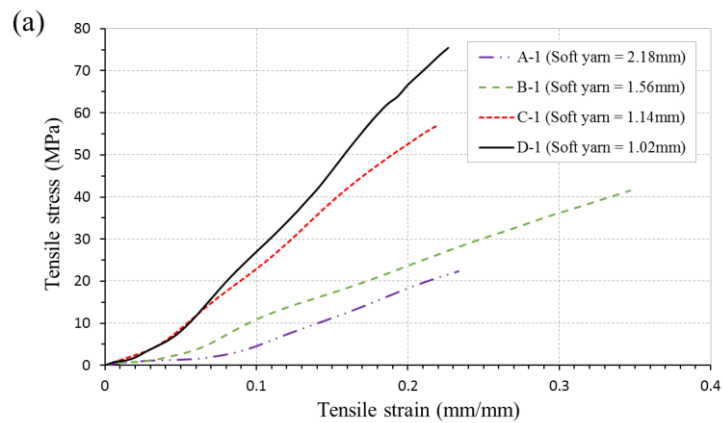


Figure 4-5 Tensile stress-strain curves: (a) samples A-1, B-1, C-1 and D-1

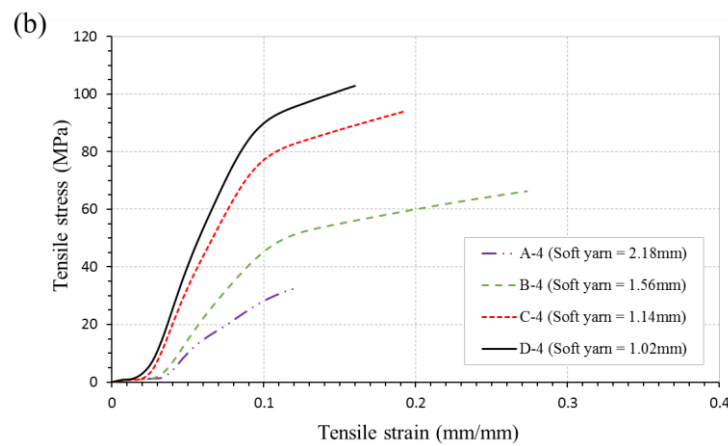


Figure 4-5 Tensile stress-strain curves: (b) samples A-4, B-4, C-4 and D-4

The Poisson's ratio-tensile strain curves of these samples are shown in Figures 4-6(a) and 4-6(b). For those yarn samples with a soft yarn diameter of 1.14mm and above, the reduction in soft yarn diameter results in a sharp increase in NPR at low strains, maximum NPR is achieved earlier and the deviation begins to decrease with increasing the tensile strain. It is believed that these differences occurred because relative position of the stiff yarns is dependent on the thickness of the soft yarns. Under the zero strain, the two stiff yarns are separated by the two soft yarns to form a 4-ply auxetic yarn structure. When a finer soft yarn is selected in a 4-ply auxetic yarn structure, the distance from the center of the stiff yarns to the center of the plied yarn becomes shorter. Accordingly, the stiff yarns can reach the yarn core shortly, thereby the migration of stiff yarn is expedited and a higher maximum NPR is achieved.

It is interesting to note, however, that the above holds true only if a proper ratio between the diameter of soft yarn and stiff yarn is maintained. Even though samples D-1 and D-4 have the finest soft yarn in their respective group, they did not follow the same trend with the other three samples and yield the highest auxetic behavior. Even worse, they are the only sample in their respective group which possessed a positive Poisson's ratio in the initial stage of tensile loading. Sample D-1 was selected for explanation and its photograph at zero strain is shown in Figure 4-7. It is observed that when soft yarn diameter is as small as 1.02mm, effective diameter of the auxetic yarn is determined by the helix radii of the stiff yarns instead of soft yarns. When the auxetic plied yarn is being stretched, the stiff yarns will be straightened, thereby causing a decrease in the helix radii and offset the auxetic effect.

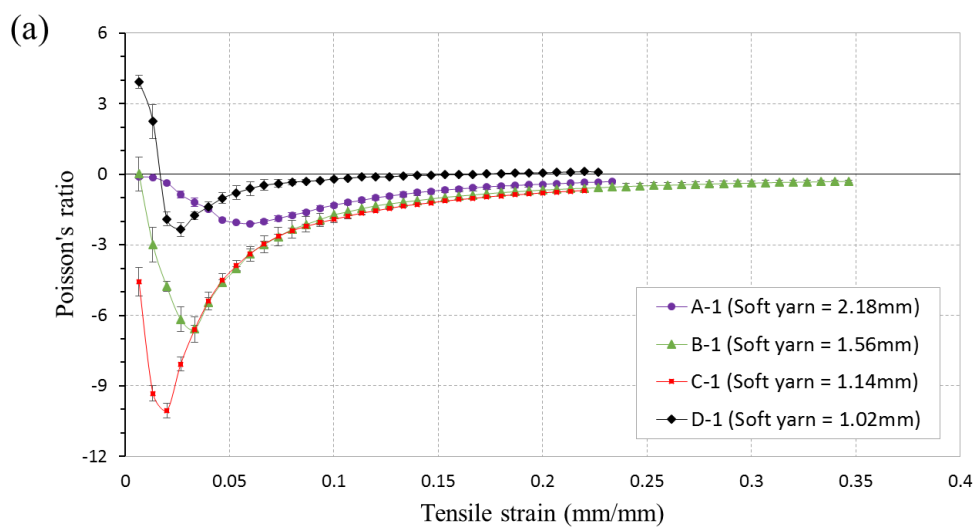


Figure 4-6 Poisson's ratio-tensile strain curves: (a) samples A-1, B-1, C-1 and D-1

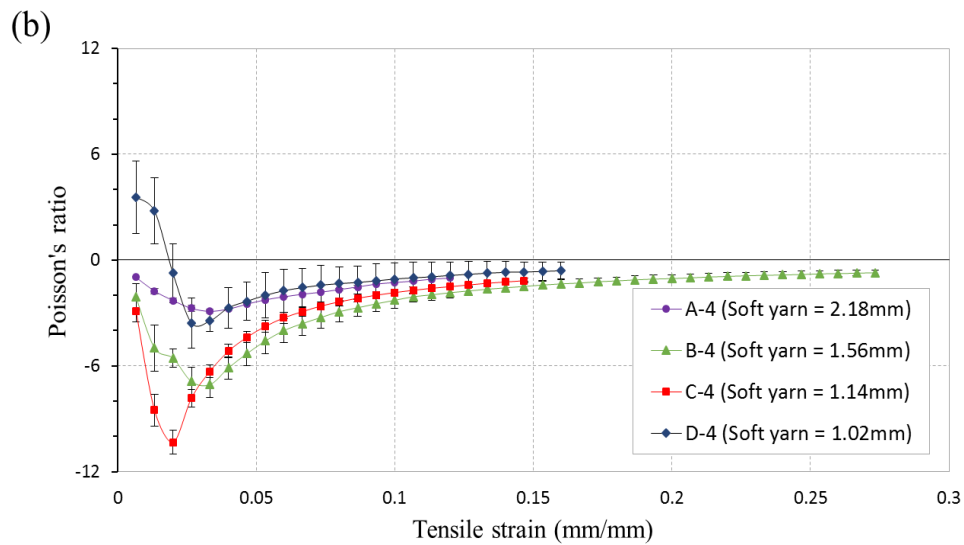


Figure 4-6 Poisson's ratio-tensile strain curves: (b) samples A-4, B-4, C-4 and D-4



Figure 4-7 Photograph of sample D-1 at zero strain

### 4.3.3 Effect of Stiff Yarn Diameter

Investigation was further extended to study the effect of stiff yarn diameter on the tensile properties and auxetic behavior of the 4-ply auxetic yarn. Considering that each type of yarn has different properties and characteristics that influence the final effect of stiff yarn, monofilaments of different thicknesses were used to evaluate the effect of stiff yarn diameter and their respective tensile stress-strain curves are depicted in Figure 4-8(a). It can be observed that initial modulus for each auxetic plied yarn was similar. At strain of about 0.3, the curves demonstrate an increased slope, and the amplitude increases with increasing stiff yarn diameter, accompanying with a higher

ultimate tensile strength.

The Poisson's ratio-tensile strain curves of these samples are shown in Figure 4-8(b).

It can be seen that auxetic plied yarn with a thicker stiff yarn yielded a higher auxetic effect at the initial stage. NPRs of all samples increased with increasing tensile strain, and achieved their maximum values at similar extension level. After that, Poisson's ratios returned towards zero, and their deviations decreased with increasing strain.

Variation in auxetic behavior may be attributed to the fact that stiff yarn in a larger diameter can push the soft yarn to a more outward radial position. As a result, maximal diameter of auxetic plied yarn can be expanded to a greater extent and a higher auxetic effect is resulted.

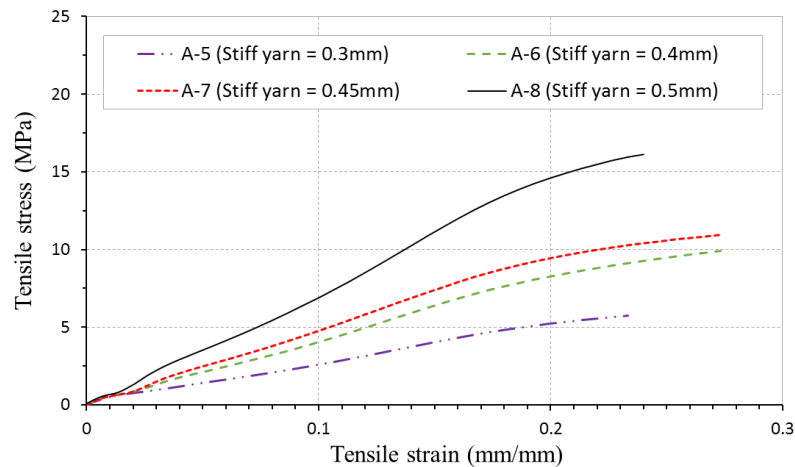


Figure 4-8 (a) Tensile stress-strain curves: samples A-5, A-6, A-7 and A-8

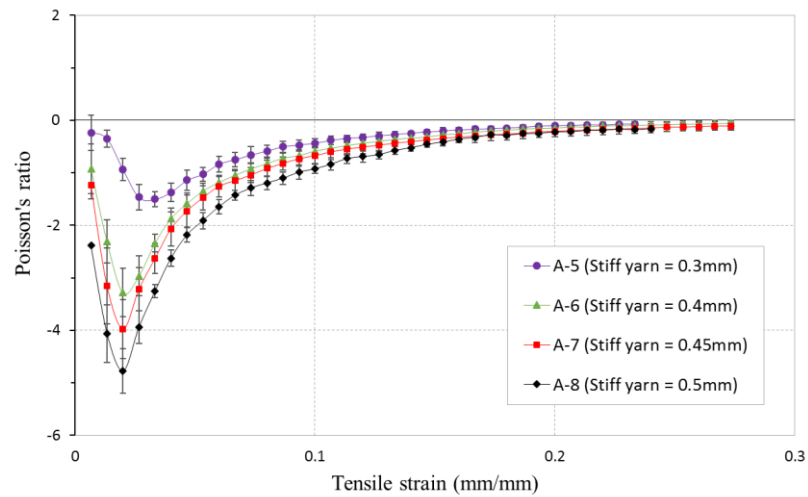


Figure 4-8(b) Poisson's ratio-tensile strain curves: samples A-5, A-6, A-7 and A-8

#### 4.3.4 Effect of Tensile Modulus of Stiff Yarn

To investigate the influence of tensile modulus of stiff yarn on the tensile and auxetic behavior of the 4-ply auxetic yarn structure, comparisons were carried out using auxetic yarn samples made with the same soft yarn but stiff yarns of different moduli (630, 489, 985 and 1307 MPa respectively). Two groups of samples A-1/A-2/A-3/A-4 and C-1/C-2/C-3/C-4 were used for evaluation and the respective tensile stress-strain curves are shown in Figures 4-9(a) and 4-9(b). The results show that samples which have a higher tensile modulus of stiff yarn in their respective group demonstrate an earlier onset of stage 2 during the tensile process. In addition, they have a steeper slope in stage 2 than samples which have a lower tensile modulus of stiff yarn, resulting in a higher ultimate tensile strength and lower extensibility.

The Poisson's ratio-tensile strain curves of these samples are shown in Figures 4-10(a) and 4-10(b). Using yarn A to combine with different stiff yarns, 4-ply auxetic yarn samples which have a higher tensile modulus stiff yarn exhibit a higher NPR at low strains (Figure 4-10a). However, when the soft yarn is replaced by yarn B, no obvious differences can be found among different samples as shown in Figure 4-10(b).

Indeed, except the tensile modulus of yarn, mechanical and deformation properties of the 4-ply auxetic yarn may be influenced to some extent by the frictional behavior between the soft yarn and different stiff yarn as well. However, quantitative measurement of the magnitude of effects of friction is likely to be difficult. Definite evidence indicates that tensile modulus of stiff yarn affects the tensile properties of the 4-ply auxetic yarn structure, which may be attributed to their difference in migration intensity. When the 4-ply auxetic yarn is being stretched, components with a higher tensile modulus tend to induce an inward migration. If the difference in tensile modulus between the soft yarns and stiff yarns becomes larger, a greater hoop tension will be generated in the helices of the stiff yarns and a higher migration intensity will be resulted. In other words, when the four different types of stiff yarn were separately used to fabricate 4-ply auxetic yarns, it would be easier for yarn 4 to push the soft yarns to the outside, thereby stage 2 in tensile tests is expedited. However, the effect



of tensile modulus of stiff yarn on the auxetic behavior of the 4-ply auxetic yarns has not shown a clear correlation with the variation in tensile properties between these samples. It is implicated that the diameter of soft yarn imposes a significant contribution to the auxetic behavior of the yarn, so that the effect of tensile modulus of stiff yarn to the auxetic performance of the 4-ply auxetic yarn structure becomes less significant.

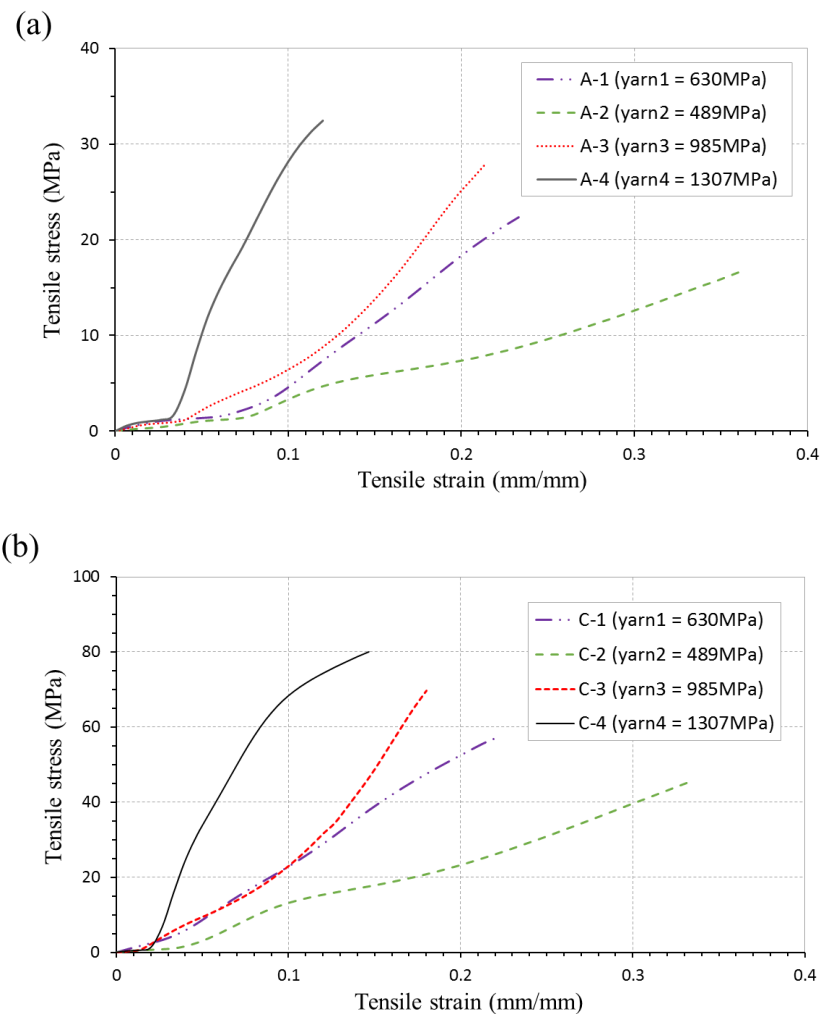


Figure 4-9 Tensile stress-strain curves: (a) samples A-1, A-2, A-3 and A-4; (b) samples C-1, C-2, C-3 and C-4

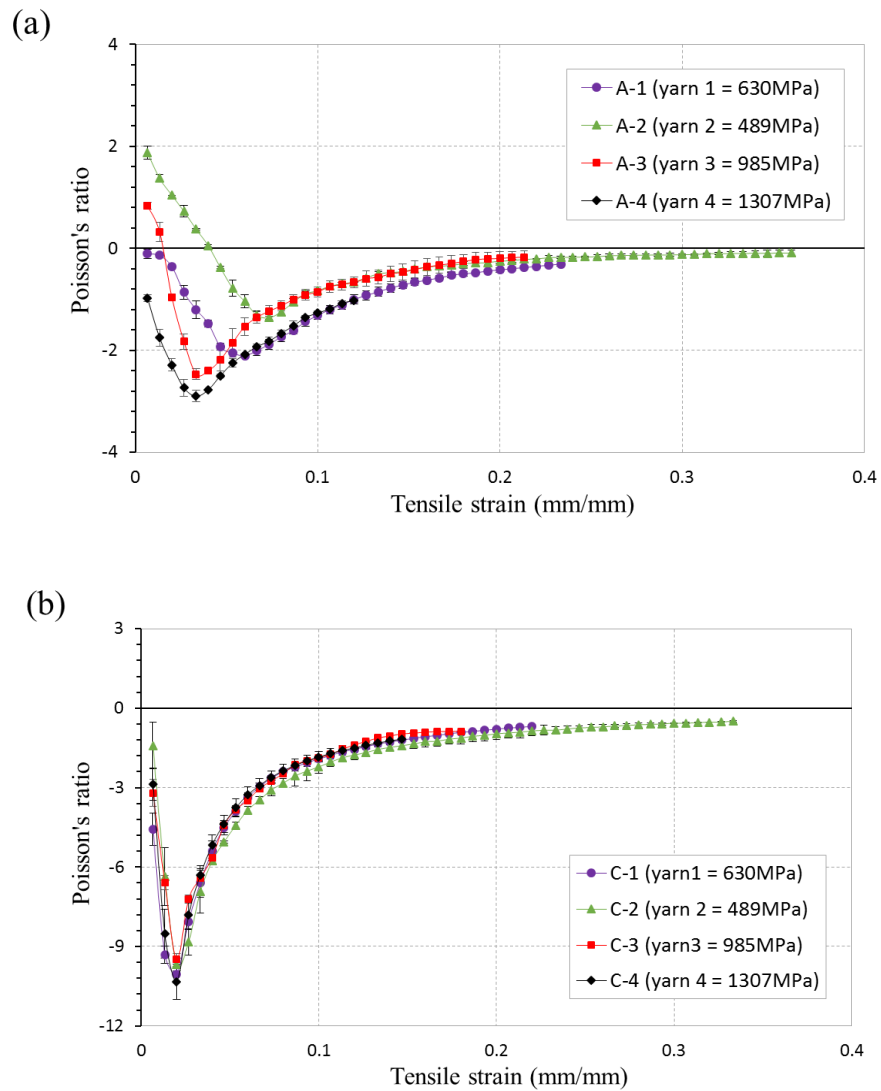


Figure 4-10 Poisson's ratio- tensile strain curves: (a) samples A-1, A-2, A-3 and A-4; (b) samples C-1, C-2, C-3 and C-4.

### 4.3.5 Effect of Twist Level

To investigate the influence of twist level on the tensile and deformation behavior of the 4-ply auxetic yarn structure, four twist levels (35, 43, 51 and 58 turns/m) were employed to fabricate different 4-ply auxetic yarn samples (A-1-L, A-1-M, A-1 and A-1-H) and their respective tensile stress-strain curves are shown in Figure 4-11a. The

results show that samples with different twist levels have a similar initial modulus; the initial stage of the curves are approximately the same but the length of this region varies. It is observed that an increase in twist level retards the onset of stage 2, accompanying with an increase in extensibility. Since lateral cohesion increases with twist level, it is likely that a greater internal force is generated in the highly twisted auxetic plied yarn. During tensile loading, large frictional forces among the constituent yarns increase the contribution of soft yarn modulus in the initial part of the tensile stress-strain curve. Therefore, elongation at break increases not only due to the increase in yarn contracted length, but also because the cohesive force prevents the stiff yarn to break earlier.

The Poisson's ratios-tensile strain curves of these samples are shown in Figure 4-11(b). The results show that the degree of auxeticity is reduced with an increase in twist level at low strains. NPR behavior of the auxetic plied yarn is consistent with the observed stress-strain behavior. These phenomena can be explained by the fact that when the twist level is increased, the 4-ply auxetic yarn structure becomes more compact because of the binding effect of the twist. Therefore, the migration of stiff yarns is hindered and a poorer auxetic performance is resulted.

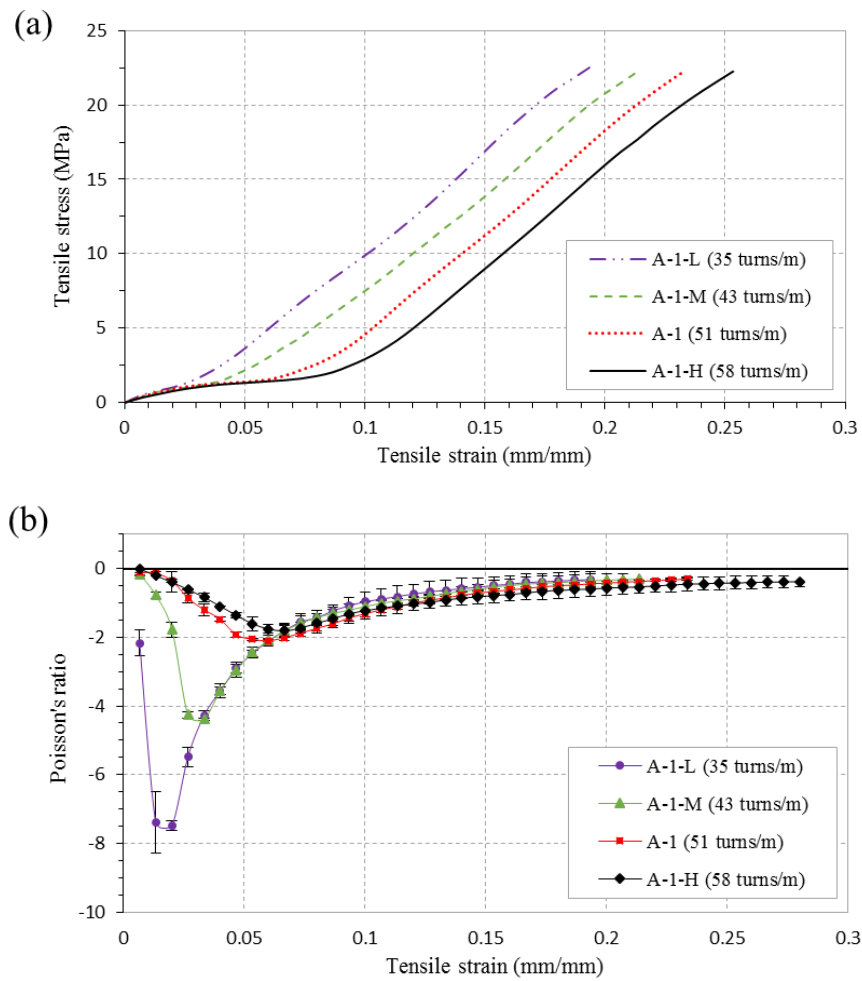


Figure 4-11 Comparisons among samples A-1-L, A-1-M, A-1 and A-1-H: (a) tensile stress-strain curves; (b) Poisson's ratio-tensile strain curves

### 4.3.6 Effect of Helical Structure

As explained before, three different auxetic yarn structures, i.e., DHY (sample A-1-D), 4-ply auxetic yarn (sample A-1) and 6-ply auxetic yarn (sample A-1-T) were fabricated to investigate the effect of helical structures on the deformation behavior of auxetic yarns. The Poisson's ratio-strain curves of these yarn structures under monotonic tensile loading are shown in Figure 4-12. It can be seen that DHY, 4-ply and 6-ply

auxetic yarns have a significant variation in auxetic behavior under stretching. DHY A-1-D has the same kind of Poisson's ratio-strain curve and similar auxetic characteristics consistent with the references [99, 101, 102], i.e., the Poisson's ratio is positive and increases with increasing tensile strain at the beginning of stretch, then decreases till its maximum negative value and finally increases toward zero until the yarn is broken. It is interesting to note that due to the core-wrap structure of the DHY, the initial elongation is inevitably accompanied with a positive Poisson's ratio. At the zero strain, the effective diameter of the DHY is determined by the helix radius of the stiff yarn. When the yarn is being stretched, the stiff yarn starts to straighten, thereby causing a decrease in its own helix radius. Since the initial increase in soft yarn helix radius is too small to alter the effective diameter of the auxetic yarn, a net decrease in effective diameter is resulted, which is correspondent to a positive Poisson's ratio.

Looking at the Poisson's ratio-tensile strain curve of the 4-ply auxetic yarn, sample A-1 exhibits a NPR behavior throughout the entire tensile process. It is due to the fact that diameter of the auxetic yarn in a ply structure is determined by the helix radii of the soft yarns under zero tensile extension. Upon stretching, the migration of stiff yarns pushes the two soft yarns away from the center of the plied yarn, thereby causing an increase in soft yarns helix radii. As a result, the maximal diameter of the 4-ply auxetic

yarn is increased with an achievement of NPR.

For another auxetic plied yarn sample A-1-T made with 6 plies, Poisson's ratio value fluctuated but remained positive at low strains, accompanied by a high standard deviation. It may be attributed to the fact that the three stiff yarns rarely migrate to the yarn core at the same extent, so that diameter of the 6-ply auxetic yarn is unpredictable at low strains. Auxetic behavior is achieved lately at strain of 0.09, after a sudden sharp increase in yarn diameter. A belated activation of auxetic behavior is resulted due to the fact that the auxetic plied yarn is more compact in a 6-ply structure so that the migration of stiff yarns is hindered.

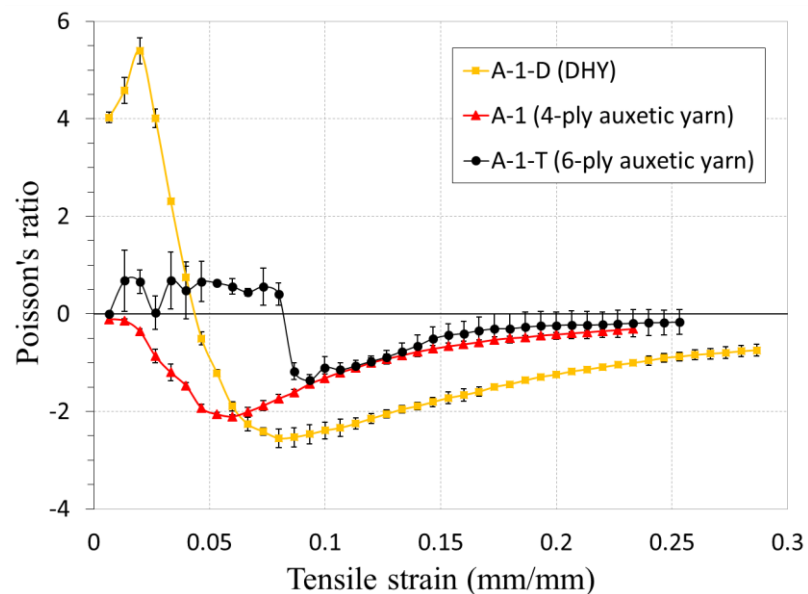
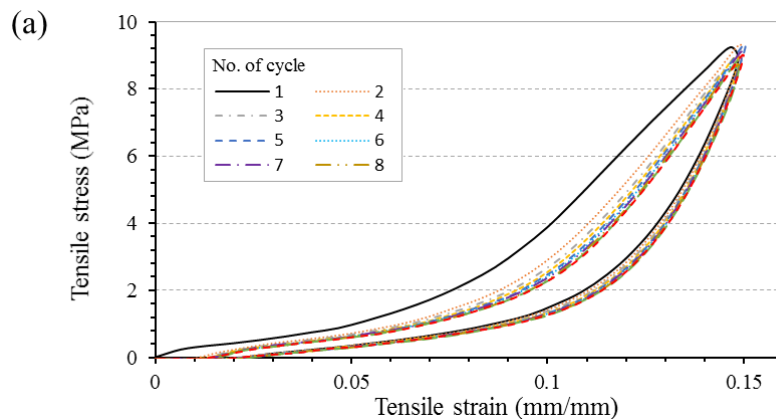


Figure 4-12 Poisson's ratio behavior of auxetic yarns made with different helical structures

Considering that the auxetic yarns may be repeatedly stretched and relaxed in real-

world applications, HAYs of different helical structures were tested under repeated solicitations at three levels of extension (5%, 10% and 15%). Similar elastic recovery behavior was observed regardless of the level of extension.

Tensile stress-strain curves of the HAYs under cyclic loading up to 15% in strain are shown in Figure 4-13. In the first loading cycle, a marked hysteresis loop between loading and unloading is observed, which indicates energy dissipation. A large residual strain is shown after the stress is totally unloaded to zero. Additional recovery occurred with time after unloading but tensile stress of the yarns still declined sharply during the second cycle, indicating decreased elasticity due to an irreversible elongation of the HAYs. However, the size of the hysteresis loop and the residual strain is significantly smaller in the subsequent loading-unloading cycles, and the tensile behavior tends to be stabilized.



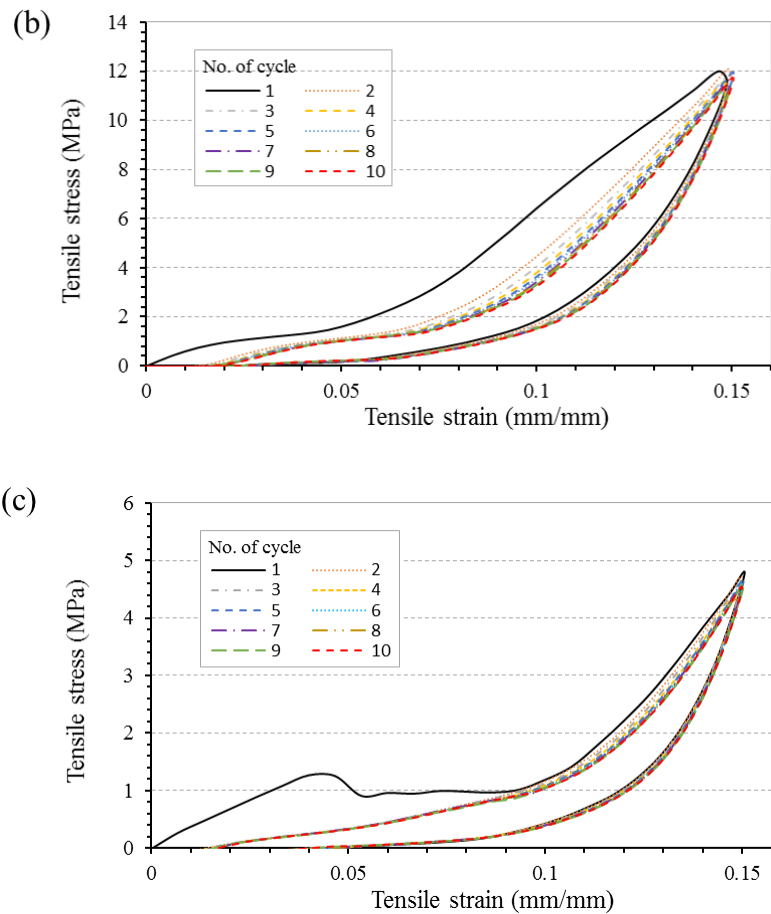


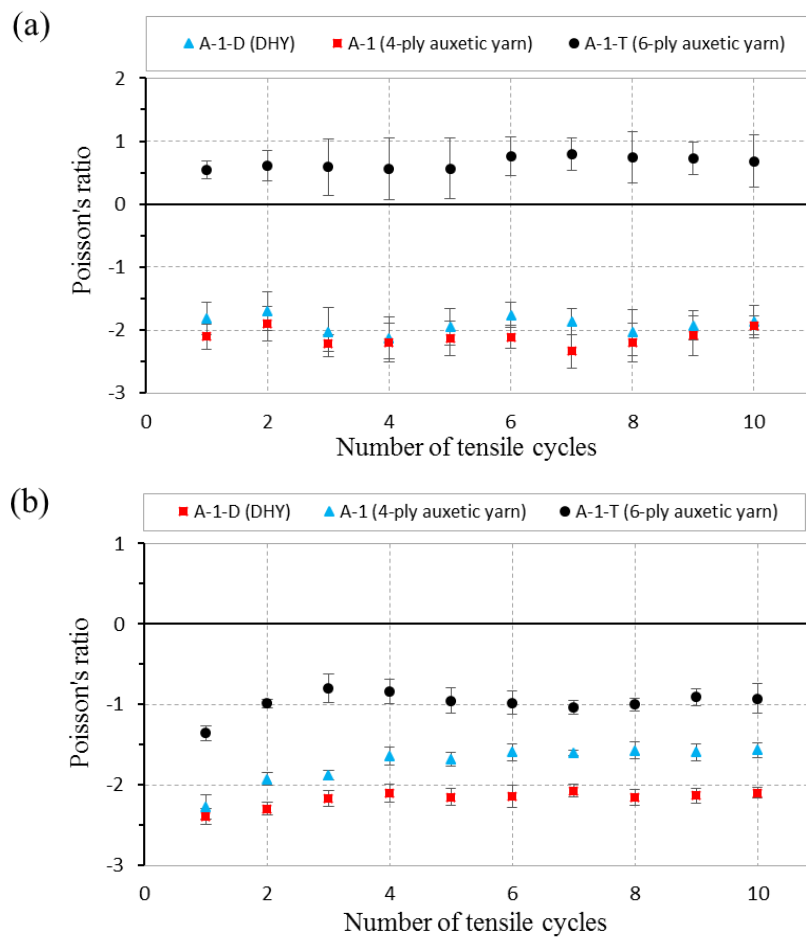
Figure 4-13 Tensile stress-strain behavior under cyclic loading: (a) sample A-1-D; (b) sample A-1; (c) sample A-1-T

In regard to the change in auxetic behavior, Figure 4-14 shows the Poisson's ratio variation of each kind of HAY samples under repeated cycles of loading and unloading at different extension levels. When the HAY samples were elongated repeatedly to a strain of 5%, it can be seen that Poisson's ratio values of each HAY do not remarkably differ from the first to the tenth cycle. NPR of the three HAY samples attained their highest value at a strain of 0.05, by which maximum stresses were obtained. Under cyclic tensile loading, each of the HAY samples obtained a similar maximum stress



value repeatedly. This may explain why NPR effect is unaffected under low extension.

Increasing the extension level to 10% and above, decrease in NPR is observed, followed by a more or less steady auxetic behavior around the third cycle. This trend can be explained by the tensile behavior of the HAYs under cyclic loading. At high strain level, NPR is maximized at some point before the peak stress; therefore, due to the retarded elastic effect, decrease in auxetic behavior is resulted.



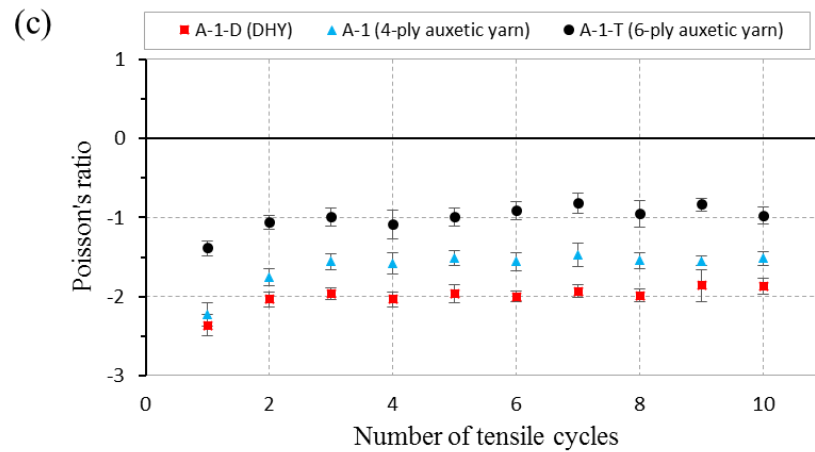


Figure 4-14 Variation of Poisson's ratio under cyclic loading up to (a) 5% in strain; (b) 10% in strain; (c) 15% in strain.

Apart from the change in auxetic behavior, it is important to know whether the HAYs can retain their original crimp shape under cyclic loading. From the digital images taken during the experiment, it is observed that helical auxetic yarn samples recovered well during repeated loading events, except the 6-ply auxetic yarn sample when stretched to a strain of 15%. See inserted picture of sample A-1-T at the end of the first cycle in Figure 4-15, three stiff yarns were loosen and slipped away from the two adjacent soft yarns. Thus, the 6-ply auxetic yarn became uneven and produced irregular auxetic effect under stretching.



Figure 4-15 Photograph of 6-ply auxetic yarn sample at the end of the first cycle.

#### 4.4 Conclusion

Tensile and deformation behavior of auxetic plied yarns were experimentally studied in this chapter. A series of 4-ply auxetic yarns were fabricated and tested, effects of various design parameters including diameter of soft yarn, diameter of stiff yarn, tensile modulus of stiff yarn and twist level of the 4-ply auxetic yarn were analyzed. On the other hand, double helix yarn and 6-ply auxetic yarn samples were fabricated and subjected to monotonic and cyclic tensile loading; effect of helical structure was investigated. The main conclusions to be drawn from this study are:

- (1) NPR of 4-ply auxetic yarn structure is more significant with a smaller soft yarn diameter, a larger stiff yarn diameter, a higher tensile modulus of stiff yarn and a lower twist level.
- (2) A proper diameter ratio is significant to produce a NPR behavior. When soft yarn diameter decreases to an extent in which the effective diameter of the auxetic plied yarn is determined by the helix radii of the stiff yarns, initial extension of the yarn will induce a net decrease in the effective diameter of the auxetic plied yarn, which is correspondent to a positive Poisson's ratio.

(3) Helical structure has a significant effect on the auxetic behavior of auxetic yarns.

Among the three HAY samples, 4-ply auxetic yarn is the only one exhibiting a NPR behavior throughout the entire tensile process, indicating that auxetic plied yarns with a 4-ply structure are favorable for applications which require an auxetic performance at low strains or a fast response to produce auxetic effect upon stretching.

(4) Under cyclic tensile loading, similar elastic recovery behavior was observed in the

helical auxetic yarns regardless of their helical structure and extension level. Tensile stress of yarn decreased sharply after the first cycle, and then tended to stabilize in the subsequent loading-unloading cycle. Regarding to the auxetic behavior under cyclic loading, Poisson's ratio values of each helical auxetic yarn do not have significant different under 5% extension throughout the 10 loading cycles. However, a decreased auxeticity was observed when extension level increased to 10% and 15%. Moreover, a loosen structure in the 6-ply auxetic yarn structure was identified under cyclic loading up to 15% strain.

## **CHAPTER 5 ANALYSIS OF CROSS-SECTIONAL DEFORMATION OF THE AUXETIC PLIED YARNS**

### **5.1 Introduction**

Assessing the auxetic yarn through longitudinal view is functional to verify the auxetic behavior and it is used for yarn diameter evaluation in previous experiment. This method, however, is not capable to provide a deep understanding on the deformation mechanism of the auxetic yarn to produce auxetic effect under axial tensile load. Auxetic properties of the 4-ply and 6-ply auxetic yarns are largely dependent on the original configuration of soft yarns and stiff yarns, and their migration behavior under tensile load. Therefore, investigation of auxetic plied yarn's internal structure under different extension levels is of great importance and thus forms the subject of this chapter.

There are two practical methods to evaluate the internal structure of the yarn, including micro-CT technique and cross-sectional microscopic examination. Micro-CT is a very promising tool to acquire cross-sectional images but high cost is involved to scan the auxetic plied yarn samples at different strains. In contrast, microscopic examination is readily available, inexpensive and fairly reliable to capture cross-sectional images for analysis, even though the cross-sectional sample preparation procedure is quite

laborious and time-consuming. Therefore, microscopic examination has been chosen for the cross-sectional analysis. Procedures involved in the preparation of cross-sectional sample and application of image analysis techniques are provided in the following sections.

## **5.2 Cross-sectional Sample Preparation**

In this study, samples A-1 and A-1-T were chosen to investigate the cross-sectional deformation behavior of the 4-ply and 6-ply auxetic yarn respectively. In addition, sample A-4 was selected to compare with sample A-1 in order to investigate the differences brought by the two stiff yarns with vastly different tensile moduli. This pair of 4-ply auxetic yarns was chosen because of their good optical properties, i.e. large diameter auxetic plied yarns can be observed easily, such that clear edge can be obtained and this could facilitate later analysis.

As it is not possible to obtain free-standing auxetic plied yarn for microscopic viewing, a specific cross-sectional specimen preparation method is developed to freeze the auxetic plied yarns into resin under different extension levels, such that yarn integrity could be maintained during cross-sectional observation. As shown in Figure 5-1, a device was made to prepare the cross-sectional samples, in which a plastic cylinder

round bottle was used as a mold and a hole was drilled through the center of the bottle to pass the yarn through.

The sampling procedure is illustrated in Figure 5-2. A 20 cm length of yarn sample was inserted vertically with the lower end secured by bottom screws and the other end straightened by upper screws without extension. The starting position of the instrument was adjusted to a distance of 105mm, from nip to nip of the cross dowels along the yarn axis. After the yarn was introduced, the bottom of the bottle was sealed to avoid resin-leaking. Following this, extension could be applied.

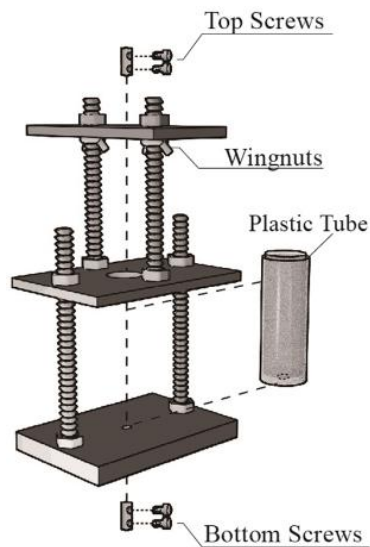


Figure 5-1 Schematic diagram and photograph of the cross-sectional sample preparation device

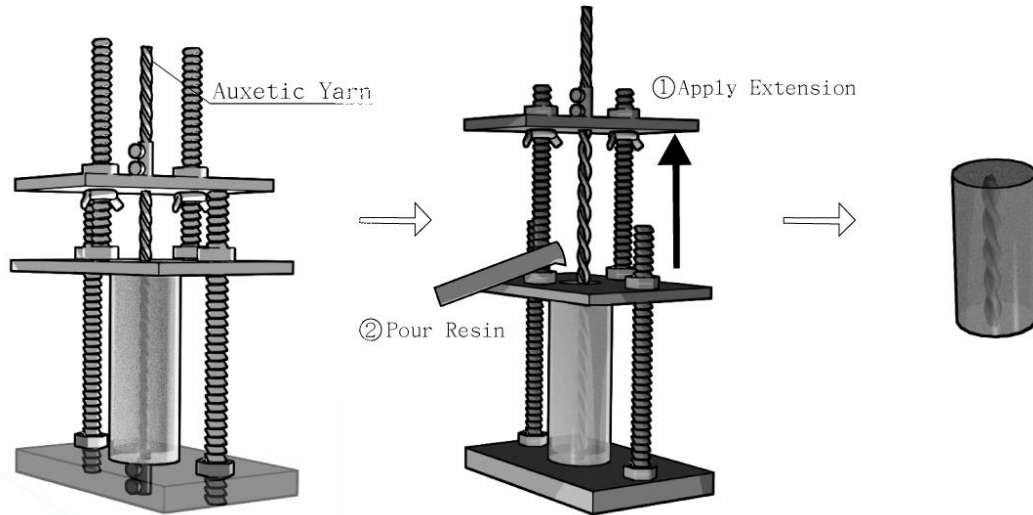


Figure 5-2 Schematic drawing for preparing the cross-sectional sample

Except the first cross-sectional sample which should be produced under zero strain, extension was applied in an increment of 2mm each by moving the cogs upward and retightened the wing nuts. For sample A-1, axial extension was applied in 8 increments until a final extension of 16mm, which corresponded to a strain from 0.00 to 0.15. For samples A-4 and A-1-T, higher load was required to stretch the yarn and the plastic bottle crushed easily at high strain due to overtightening. Therefore, axial extension was applied in 6 increments until a final extension of 12mm only, which corresponded to a strain from 0.00 to 0.11. During extension, care was taken to ensure that there was no yarn slippage. In order to freeze the auxetic yarn under specific strain, epoxy resin and hardener were mixed in a 10:1 ratio and poured into the bottle. To avoid interferences with transmission of light during microscopic examination, few drops of black ink were mixed in the solution as well. After several hours of consolidation under



room temperature, the cross sectional sample was pulled out from the bottle. Auxetic plied yarn under specific strain was then embedded and frozen in the resin so that the yarn was retained at that strain after removal of the load. Finally, the surface of the sample was ground progressively with sandpaper of 60 to 1000 grits. To reduce the depth of field and avoid confusion, a minimum polishing was done. Base on the method described above, cross-sectional samples (Figure 5-3) were prepared and examined under an optical microscope.



Figure 5-3 Cross-sectional sample

### **5.3 Microscopic Examination**

Three cross-sectional samples were prepared for each extension level, and these samples were viewed and captured under microscope with 20 times magnification. The cross-sectional images consist of 2048 x 1536 pixels and the length of one pixel is 3.289 $\mu$ m. Photoshop was used to convert the images to greyscale so that desired information could be represented in a condensed form for easy characterization. In addition, black and white adjustment was adopted to further improve the contrast of the images.

From the cross-sectional images, variation in position and shape of the constituent yarns under different strains were observed. In addition, the images were processed to measure the cross-sectional parameters with the software Adobe Illustrator. As shown in Figure 5-4, the circumference of each constituent yarn was outlined, cross-sectional area of soft yarn ( $A_s$ ) and stiff yarn ( $A_s$ ) were then calculated by counting the number of pixels within the outlined area. In addition, maximal diameter of the auxetic plied yarn ( $D_{max}$ ) was measured. Poisson's ratios for the three samples were then calculated and compared with those obtained through tensile test measurements.

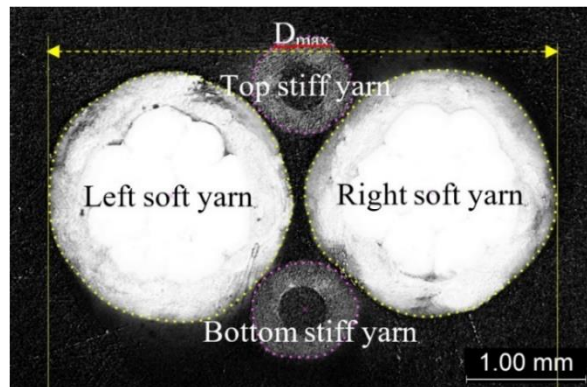


Figure 5-4 Auxetic plied yarn measurements

## 5.4 Results and Discussion

### 5.4.1 Cross-sectional Deformation Behavior of 4-ply Auxetic Yarns

Sample A-1 was first selected as an example to study the cross-sectional deformation behavior of the 4-ply auxetic yarn structure. Its cross-sectional images at strain of 0.00, 0.02, 0.04, 0.06, 0.08, 0.10, 0.11, 0.13 and 0.15 are shown in Figures 5-5 (a) to (i)

respectively. Considering that the axes of the constituent yarns are not perpendicular to the axis of the resultant plied auxetic yarn structure, a minor distortion of the yarn cross-section is resulted. It is observed that the cross-section of the two stiff yarns in the 4-ply auxetic yarn remained approximately circular while that of the soft yarns remained slightly elliptical, and those yarns were flattened along the minor diameter direction of the 4-ply auxetic yarn.

Under zero strain (Figure 5-5a), the two soft yarns were laid in the core region and separated the stiff yarns. At strain of 0.02 (Figure 5-5b), the stiff yarns started to migrate towards the yarn center to avoid being strained, while the soft yarns were moved away from the center accordingly. It can be attributed to the great difference in Young's modulus of the constituent yarns, as yarns with higher tensile modulus tend to exhibit an inward movement. Up to 0.11 strain (Figure 5-5g), the two stiff yarns completely migrated to the yarn core and jammed together. Since there was no room for any further movement, the two stiff yarns just closely packed together when tensile strain further increased to 0.15 (Figures 5-5i), and core-indentation phenomenon was observed. The two stiff yarns were embedded into each other and the degree of indentation increased with increasing strain. Concerning that indentation occurred in the minor diameter direction only, maximal thickness of the 4-ply auxetic yarn was

unaffected by the indentation of the stiff yarns.

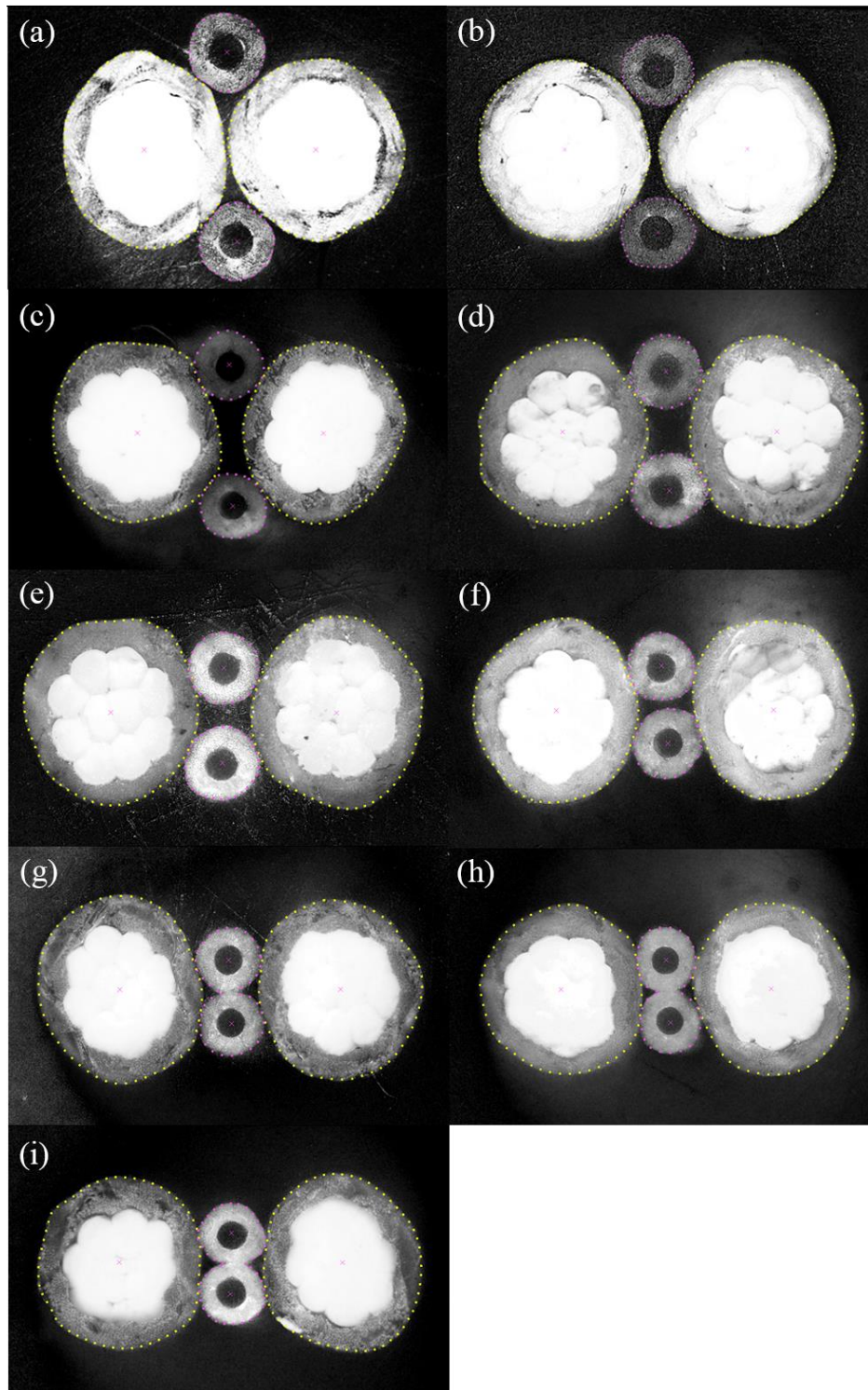


Figure 5-5 Cross-sectional images of sample A-1 (a) at zero strain; (b) at strain of 0.02; (c) at strain of 0.04; (d) at strain of 0.06; (e) at strain of 0.08; (f) at strain of 0.10 (g) at strain of 0.11; (h) at strain of 0.13; (i) at strain of 0.15

Apart from sample A-1, cross-sectional samples of A-4 were also made to evaluate if there are any differences in their internal deformation behavior when the stiff yarn was different. The cross-sectional images of sample A-4 at strain of 0.00, 0.02, 0.04, 0.06, 0.08, 0.10 and 0.11 are shown in Figures 5-6 (a) to (g) respectively.

A similar deformation trend can be observed, in which the two stiff yarns were initially separated by the two soft yarns laid in the core region and they appeared to migrate inwards when the 4-ply auxetic yarn was being stretched. Comparing the two different stiff yarns (yarn 1 and yarn 4) used in sample A-1 and A-4, the stiff yarns used in A-4 have a higher tendency to migrate inward. At strain of 0.08, free space could still be found for the stiff yarns to move further inwards in sample A-1 (Figure 5-6e); in contrast, the two stiff yarns in sample A-4 had already moved to the yarn center and contacted each other (Figure 5-6e). The results revealed that the migration intensity of stiff yarn is significantly affected by the tension variation of the constituent yarns, as discussed earlier. Besides, no indentation is observed after the two stiff yarns contacted with each other (Figures 5-6e-g).

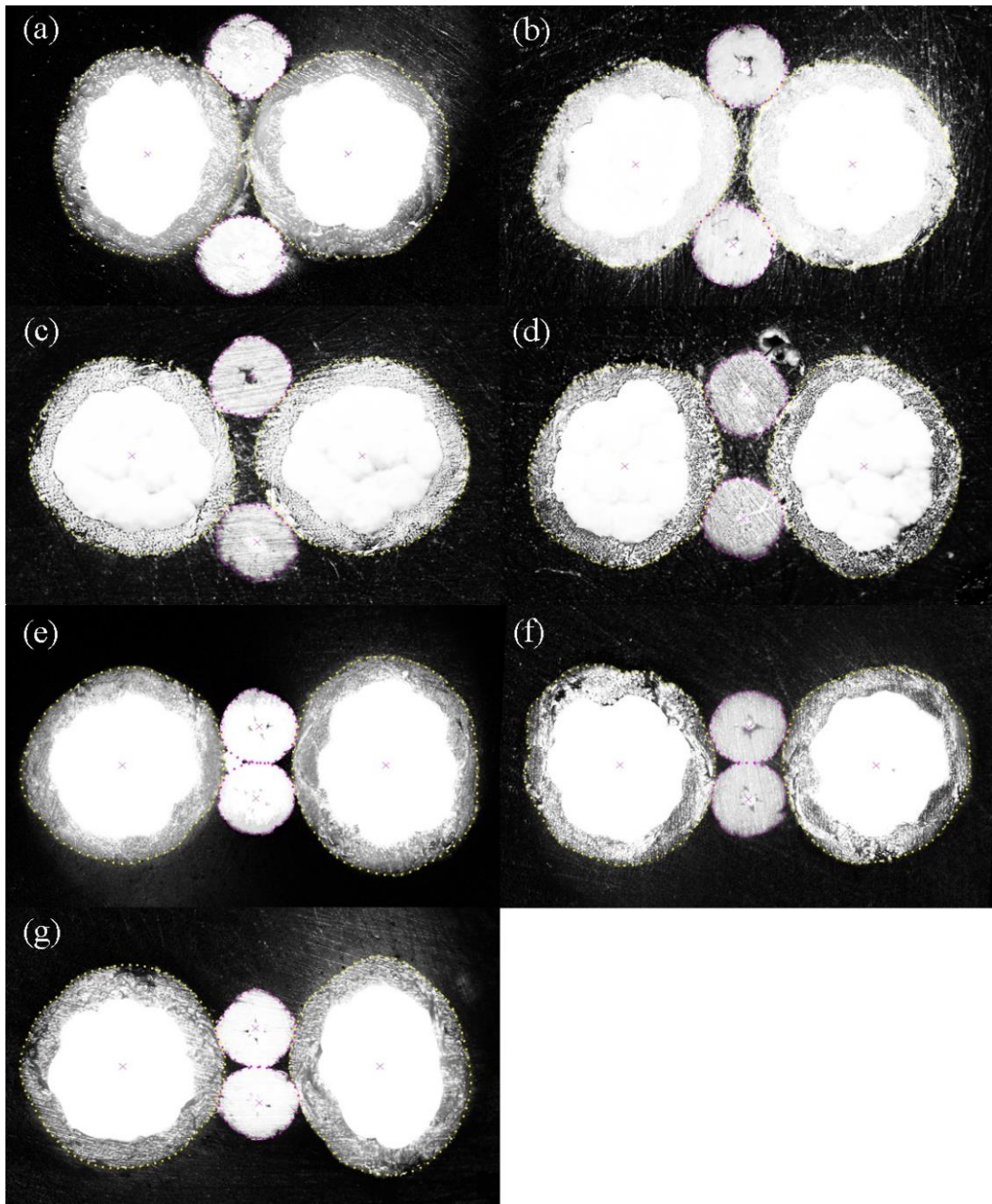


Figure 5-6 Cross-sectional images of yarn A-4: (a) at zero strain; (b) at strain of 0.02; (c) at strain of 0.04; (d) at strain of 0.06; (e) at strain of 0.08; (f) at strain of 0.10; (g) at strain of 0.11

#### 5.4.2 Cross-sectional Deformation Behavior of 6-ply Auxetic Yarn

Cross-sectional samples were made to study the deformation behavior of the 6-ply auxetic yarn sample at various strain levels. Although the cross-sectional samples

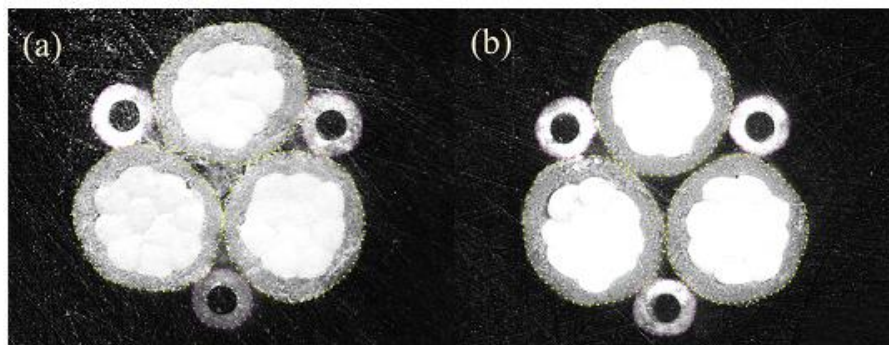
could only be prepared up to a strain of 0.11 due to technical constraints, the cross-sectional images still provided valuable information on how migration was initiated and completed with an idealized configuration.

Cross-sectional images of sample A-1-T at strain of 0.00, 0.02, 0.04, 0.06, 0.08, 0.10 and 0.11 are shown in Figures 5-7 (a) to (g) respectively. Under zero strain (Figure 4-7a), the 6-ply auxetic yarn packed into an arrangement in which three soft yarns formed the core while three stiff yarns were alternatively separated by them; the stiff yarns were preferably aligned as each of them had a more or less equal radial distance from the yarn core.

It is interesting to note that no remarkable difference was found for the first four investigated strain levels (Figures 5-7a to d). The three soft yarns kept occupying the yarn core and no migration was observed. This phenomenon may be attributed to the fact that loading in this strain range is insufficient for minimum initial fiber interaction to take place between neighboring stiff yarn and soft yarn. In the 6-ply auxetic structure, the soft yarns are packing tightly together around the core region. Inward movement of stiff yarn is opposed by inter-fibre frictional forces and by the lateral pressures which are greatest near to the center of the yarn. It prevents the stiff yarns from slipping

over the soft yarns and interchange their positions with each other.

Up to 0.08 strain (Figure 5-7e), migration can be recognized but the three stiff yarns were not moved to the yarn center at the same extent. Two highly tensioned stiff yarns were pressed inward partly, while one was remaining separated apart from the yarn core. It may be due to slight non-uniformity in lateral pressure distribution over the yarn cross-section. Considering that the path a soft yarn or stiff yarn takes in the 6-ply auxetic structure may not be perfectly helical, tensile stresses are not equally distributed so that tendency of migration varies among the constituent yarns. At strain of 0.10 (Figure 5-7f), although the three stiff yarns were moved to the yarn center, two soft yarns were stuck together and caused irregularities in yarn diameter. When tensile strain further increased to 0.11 (Figure 5-7g), a well-balanced structure can be identified finally.





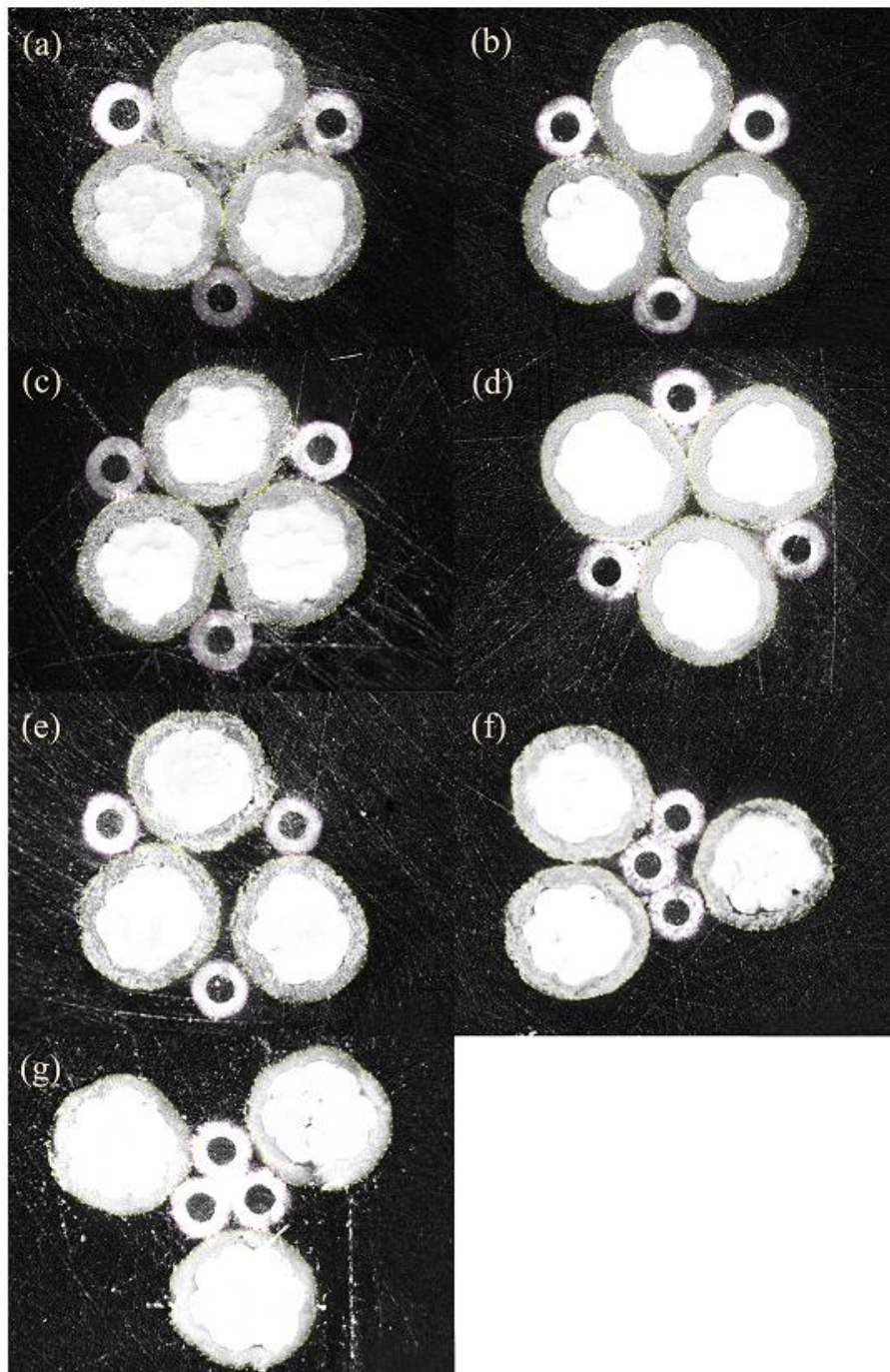


Figure 5-7 Cross-sectional images of yarn A-1-T (a) at zero strain; (b) at strain of 0.02 (c) at strain of 0.04; (d) at strain of 0.06; (e) at strain of 0.08; (f) at strain of 0.10; (g) at strain of 0.11

### 5.4.3 Poisson's Ratio and Cross-sectional Parameters

From the acquired cross-sectional images, average maximal diameters were obtained

and used to calculate the Poisson's ratios and compare with those obtained through tensile test measurements accordingly. As shown in Figures 5-8 (a) to 5-8 (c), Poisson's ratio values of the three samples obtained through the two measurement techniques are similar. Only a relatively larger deviation is observed in sample A-4 at high strains, which may be attributed to a minor shrinkage of the auxetic plied yarn when the specimens were embedded into resin under high loads. It is clearly recognized that migration of stiff yarns during extension initially induced an increase in NPR of the yarn, but further increase in tensile strain eventually led to a decrease in auxetic behavior.

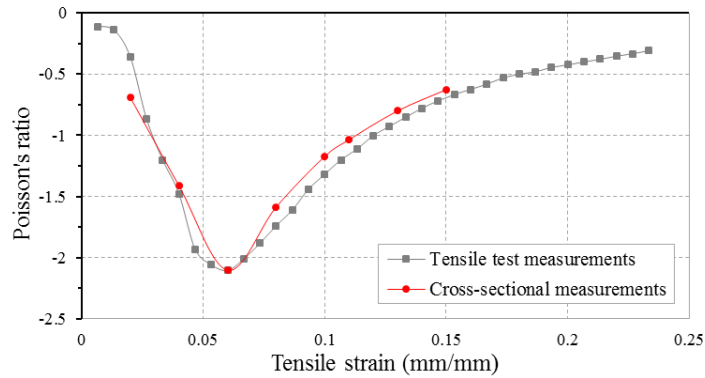


Figure 5-8 (a) Poisson's ratios of sample A-1 obtained with different methods

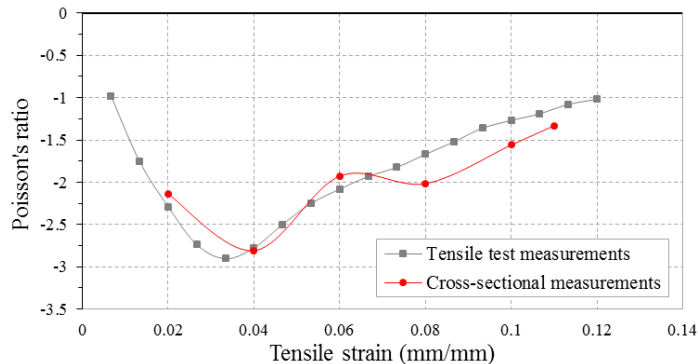


Figure 5-8 (b) Poisson's ratios of sample A-4 obtained with different methods

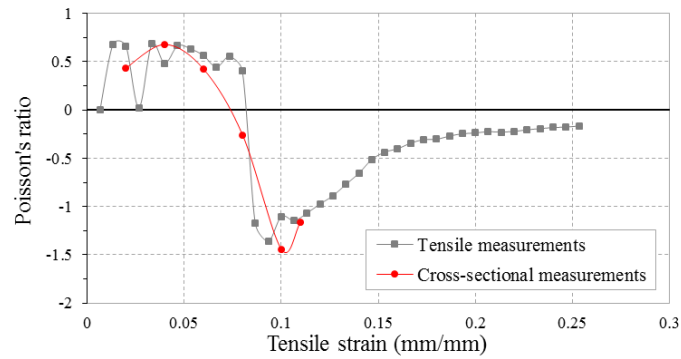


Figure 5-8 (c) Poisson's ratios of sample A-1-T obtained with different methods

Regarding to the cross-sectional parameters obtained, maximum transverse strains of samples A-1, A-4 and A-1-T were obtained at an axial strain of 0.06, 0.08 and 0.10 respectively. Refer to the cross-sectional images in Figures 5-5(d), 5-6(e) and 5-7(f), the maximum transverse strains of samples A-1 and A-1-T were obtained before the stiff yarns completely moved to the yarn core and contacted each other while transverse strain of sample A-4 is maximized when the stiff yarn just moved to the yarn core.

This phenomenon may be explained mostly by the variation in the cross-sectional area of the constituent yarns which was measured and shown in Figure 5-9. At low strain level, helical angle of the auxetic plied yarn continues to decrease slowly. When the decrease in helical angle becomes attenuate, the constituent yarns are straightened and become thinner due to their inherent Poisson's ratios. Therefore, increase in maximal

diameter due to inward movement of the stiff yarns is compensated by the decrease in cross-sectional area of the constituent yarns; NPR of the auxetic plied yarn is maximized before the stiff yarns migrate to the yarn center thoroughly.

For sample A-4, even though cross-sectional area of both of the soft yarns and stiff yarns decreased sharply at strain of 0.08, diameter of the auxetic yarn was maximized at that point. It may be due to the fact that the stiff yarns used in yarn A-4 have a higher migration intensity, so that they could move to the yarn core before the inherent Poisson's ratios of the four constituent yarns impose an opposing effect on the maximal diameter of the auxetic plied yarn. As a result, increase in maximal diameter of the yarn due to stiff yarn migration outweighs the decrease due to contraction of the constituent yarns.

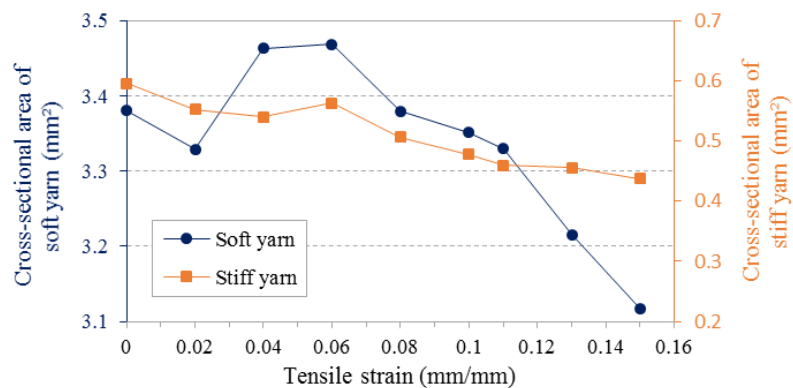


Figure 5-9(a) Cross-sectional area of soft yarns and stiff yarns as a function of axial strain for sample A-1

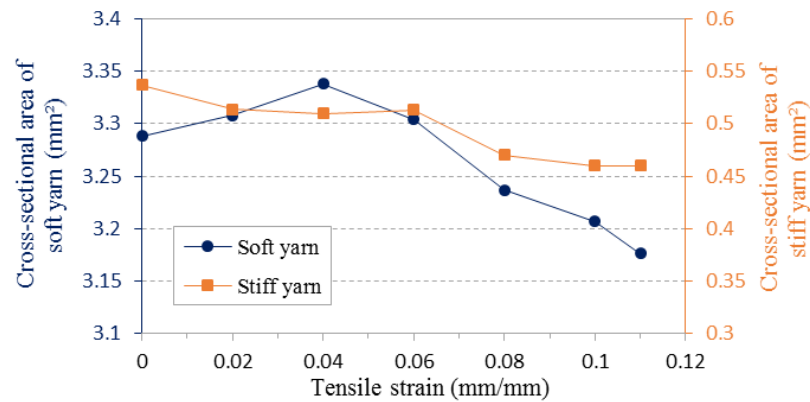


Figure 5-9(b) Cross-sectional area of soft yarns and stiff yarns as a function of axial strain for sample A-4.

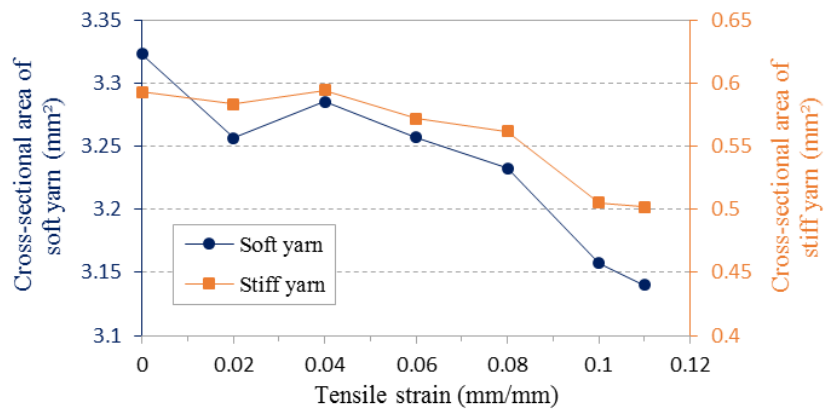


Figure 5-9(c) Cross-sectional area of soft yarns and stiff yarns as a function of axial strain for sample A-1-T.

### 5.5 Conclusion

Two kinds of 4-ply auxetic yarn samples and one kind of 6-ply auxetic yarn sample were selected and made into cross-sectional specimens under different extension levels.

The cross-sectional samples were viewed under microscope, images were captured and relevant parameters were measured. The main conclusions to be drawn from this

chapter are:

- (1) Deformation mechanism of the 4-ply and 6-ply auxetic yarn structures have been verified through microscopic examination, that is, the migration of stiff yarns during extension pushes the soft yarns outward and induces an increase in maximal diameter of the auxetic yarn structure. Stiff yarn of higher tensile modulus clearly demonstrated a higher migration intensity.
- (2) The study of 6-ply auxetic yarn is valuable as an aid to understand what is happening in more complex auxetic plied yarn structure. A belated initiation of migration was observed in the 6-ply auxetic yarn structure, along with an inconsistent movement of the three stiff yarns leading to an imbalanced structure.
- (3) The auxetic plied yarns may not necessarily expand to its greatest extent at the point where the two stiff yarns moved to the yarn center thoroughly, because magnitude of auxetic behavior is affected by the thinning of the constituent yarns due to their inherent Poisson's ratio effect.

## **CHAPTER 6 DEVELOPMENT OF TEXTILE FABRICS MADE OF AUXETIC PLIED YARN**

### **6.1 Introduction**

Poisson's ratio is one of the fundamental properties of fabrics which can be used to determine their applications based on the deformation behavior under tensile loading.

Over the past years, considerable studies have been undertaken to investigate the Poisson's ratio of various kinds of conventional fabrics, and a positive Poisson's ratio behavior was observed. Nowadays, researchers have started to develop fabric textiles with NPR effect to enhance certain mechanical properties over their non-auxetic counterparts. However, fabrication of auxetic textiles has remained largely unexplored.

A variety of DHYs were made into auxetic textiles, suggesting that the resultant fabrics are not only able to obtain auxetic behavior, but also capable to produce an open pore effect upon stretching. Owing to the non-auxetic behavior in conventional fabric structure, pores elongate in the direction of force and contract in the perpendicular direction upon tensile extension. By contrast, auxetic fabrics cause the pores to open in both transverse and longitudinal directions upon stretching.

Since the auxetic effects and open pore property of textiles made of auxetic plied yarns are unknown, experiment is carried out in this chapter in an attempt to fabricate textiles

with auxetic plied yarns to produce NPR behavior, and to evaluate their variations brought by different design parameters. Moreover, investigation is extended to study the open pore properties of these fabrics.

To study the Poisson's ratio of fabric, tensile test can be carried out equipped with image processing analysis. On the other hand, the images captured can be used to study the open pore effect of the fabric samples as well. So far, attempts to investigate the pore morphology encompassed physical and optical methods. The optical method is chosen in this study as it provides a practical indication of the permeability of fabric to light, gases, liquids and solid particles for many different potential applications.

### **6.2 Design Consideration of Fabrics made of Auxetic Plied Yarn**

In an attempt to produce immediate auxetic effect upon stretching, auxetic plied yarns should be arranged as straight as possible in the textile fabric. In accordance with this criterion, knitted fabrics seem to have the least potential to generate auxetic effect as loops in the knitted fabric will give the auxetic plied yarns great crimp, unless they are incorporated into the structure as in-laid yarns. As illustrated in Figure 6-1, conventional yarns can be used to form the weft-knitted jersey fabric, while the auxetic plied yarns can be introduced to the ground fabric on a tuck and miss basis in the



course-wise direction. As a result, the auxetic plied yarns will not form into a knitted loop, but they will be hold straightly in the technical back of the structure.

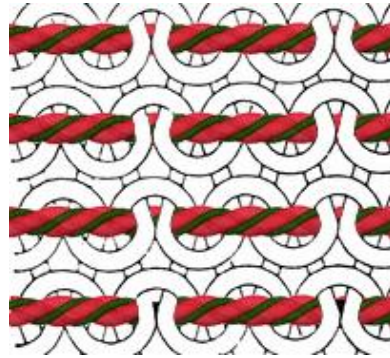


Figure 6-1 Single jersey fabric with the laying-in auxetic plied yarns

To realize NPR effect in such a knitted structure, flat knitting machine with proper gauge is needed. More than that, control of loop length is essential as it determines the spacing of the auxetic plied yarns, given that NPR effect can only be obtained when they are able to contact and push against each other in the wale-wise direction. Due to the lack of technical support, auxetic behavior of such a knitted structure remains questioned.

As knitting has been withdrawn from further consideration, weaving seems to represent the greatest potential for obtaining desirable auxetic effect. Even though it may be practical to align the auxetic plied yarns in a parallel manner and impregnate with resins to produce non-crimp auxetic plied yarn composite, it is expected that

relatively large number of pores will become inaccessible.

To create effective woven fabric structure, 4-ply auxetic yarn can be used for the warp, weft or both to produce auxetic effect in different directions according to the applications. However, since decrease in crimp in one direction of the woven fabric induces crimp in another direction, this anisotropic behavior must be taken into account to design the auxetic woven fabric. Figure 6-2 illustrates the design concept of woven fabric made of auxetic plied yarns. In the case of uniaxial loading, auxetic plied yarns can be arranged vertically for the warp, given that tension on the warp yarn is higher than the weft yarn during weaving process and this characteristic can be utilized to minimize the crimp exerted on the auxetic plied yarns. On the other hand, conventional elastic materials can be used for the weft, as a soft weft compresses more easily thus allowing the auxetic warp yarn to lie straighter and expand in weft-wise direction upon extension.

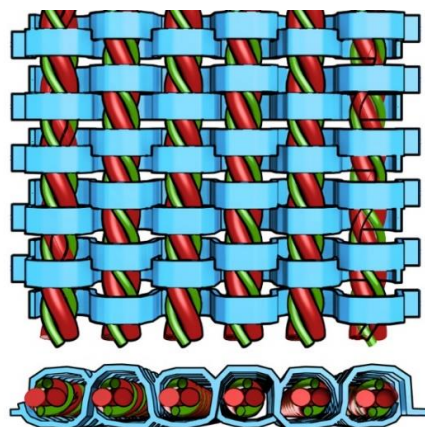


Figure 6-2 Woven fabric design with crimp-free auxetic plied yarns

Apart from weaving, it is also possible to introduce the 4-ply auxetic structure in a net-like knotted fabric, such that high flexibility can be obtained for the fabric to expand in the direction perpendicular to the tensile loading. As shown in Figure 6-3(a), pairs of soft yarn and stiff yarn can be grouped together as one strand whereas a number of parallel strands can be interlinked by exchanging their position between neighboring strands. As a result, the knotting position will form a 4-ply helix structure. The principle to produce such a structure is similar to that of hexagonal mesh nets (Figure 6-3b), which can be made by machines such as bobbinet and tulle. However, due to constraints on technology, the new structure can only be fabricated by hand, serving as a preliminary study to explore the potential areas of investigation.

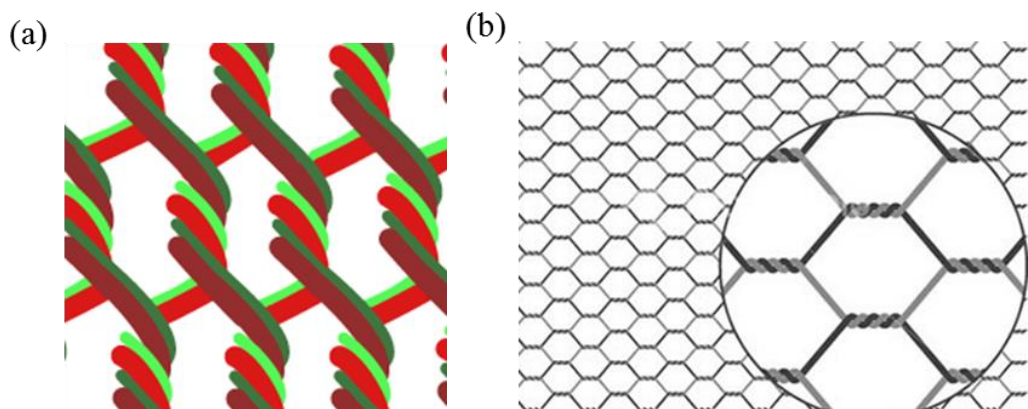


Figure 6-3(a) Hexagonal mesh net with 4-ply auxetic structure; (b) typical hexagonal mesh net pattern

## **6.3 Experimental Details**

### **6.3.1 Experimental Design**

The focus of this study is to investigate the auxeticity and open pore behavior of the woven fabrics made of auxetic plied yarns. It is known that a woven fabric is an extremely complex structure which consists of several structural levels from fiber to yarn and eventually to the fabric construction. Simply knowing the auxetic behavior of the auxetic plied yarn is not enough to predict the properties of the resultant fabric. A systematic study is necessary to evaluate the influence of each parameter on the mechanical properties of the fabric made of auxetic plied yarns, such that correct selection of the parameters can be made for specific areas of applications.

In the yarn level, auxetic plied yarn has its own geometrical and mechanical variables which may control or influence to varying degrees the auxetic behavior and open pore property of woven fabric made thereby. In this study, effect of auxetic plied yarn component was investigated, including diameter of soft yarn and tensile modulus of stiff yarn. In addition, as the HAYs with different helical structures have shown a vastly different auxetic behavior, an attempt was also made to investigate the performance of their resultant woven fabrics.

In the fabric level, weave structure is a typical factor to be considered. The effect of weave structure on the Poisson's ratio of fabric has been studied by many researchers, revealing that various woven fabric structures induce positive Poisson's ratio behavior at different levels. Therefore, it is important to investigate whether this nature would affect the performances of the auxetic woven fabric.

Furthermore, the investigation was extended to evaluate the effect of auxetic plied yarn arrangement as well. A few researchers have suggested that yarn twisted in different direction affects the fabric properties in some aspects. For instance, Whitman has proposed a weaving structure with alternate pairs of warp yarns in S and Z twists and suggested that fabric with such arrangement has substantially no tendency to curl [132].

According to the previous studies, DHYs were arranged alternatively to fabricate auxetic textiles (Figure 6-4), with an assumption that auxeticity and pore size are maximized with this arrangement under ideal conditions; however, no experimental comparison has been made. In this experiment, an attempt was made to investigate how exactly does the arrangement of auxetic plied yarn influence the performances of the resultant fabric made of 4-ply auxetic yarns.

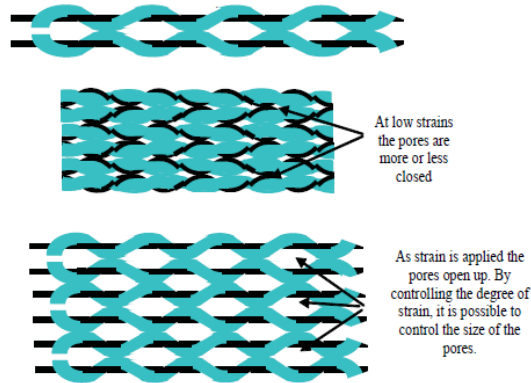


Figure 6-4 Arrangement of DHYs in previous literature [56]

### 6.3.2 Fabric Sample Preparation

Based on the variables identified in the previous section, a total number of 12 woven fabric samples were made on a hand loom. Their constructional characteristics and photographs are presented in Tables 6-1 and 6-2 on pages 102 and 103 respectively.

All samples were manufactured on the basis of two wefts, including a 4mm flat braided polyester elastic band and a 100D polyester-covered spandex yarn with a tensile modulus of 13.16MPa and 2.02MPa respectively. Different kinds of helical auxetic yarns were used as warp, arranging either in the same twist direction (S/S) or in the opposite direction (S/Z) to study the effect of different design parameters.

The woven fabric samples were divided into six groups according to the parameters investigated. Firstly, two different auxetic plied yarn arrangements were selected for the study. In the first case, S and Z twisted 4-ply auxetic yarns were arranged alternatively to fabricate sample F1. In the second case, all auxetic yarns were twisted

in S direction to produce sample F2. Flat braided polyester elastic band was used as weft for easy manipulation. Secondly, same kind of 4-ply auxetic yarn (sample A-1) was used as warp and a 100D polyester-covered spandex yarn was used as weft to produce sample F3 and compare with sample F1 to evaluate the effect of different weft types. A warp-faced plain weave structure was selected to give a high extensibility in weft-wise direction, by spacing out the weft yarn at a distance of 7mm after every two picks. Thirdly, five kinds of 4-ply auxetic yarn samples were selected as warp to interlace with polyester-covered spandex yarn to study the effect either brought by different soft yarn diameter or different tensile modulus of stiff yarn. Fourthly, sample A-1 was used as warp to incorporate with the polyester elastic band in plain weave, 2x1 twill weave, 3x1 twill weave and 5-end Satin weave with the same pick density to evaluate the effect of weave structure. Finally, additional fabric samples were made by means of DHY and 6-ply auxetic yarn samples with the same weft, weave structure and pick density to investigate the effect brought by different helical structures.

Apart from the woven fabric samples, yarn A and yarn 1 were selected to fabricate the hexagonal mesh net sample, namely F13, by hand knot (Figure 6-5). Samples were prepared for narrow strip tensile testing with a dimension of 25x5cm. All specimens were conditioned at  $20 \pm 2^\circ\text{C}$  and  $65 \pm 2\%$  relative humidity for 24 hours prior to testing.

Table 6-1 Constructional characteristics of woven fabrics investigated

Parameter consideration	Fabric code	Material		Fabric density		Fabric structure
		Warp	Weft	Ends/inch	Picks/inch	
Direction of twist	F1	A-1 (S/Z)	4mm flat braided polyester elastic band	6.35	6.46	Plain
	F2	A-1 (S/S)				
Weft type	F1	A-1(S/Z)	4mm flat braided polyester elastic band	6.35	6.46	Plain
	F3		100D polyester-covered spandex yarn		6.10*	
4-ply auxetic yarn properties: diameter of soft yarn	F3	A-1(S/Z)	100D polyester-covered spandex yarn	6.35	6.10*	Plain
	F4	B-1(S/Z)		8.63		
	F5	C-1(S/Z)		9.03		
4-ply auxetic yarn properties: tensile modulus of stiff yarn	F3	A-1(S/Z)	100D polyester-covered spandex yarn	6.35	6.10*	Plain
	F6	A-3(S/Z)		6.35		
	F7	A-4(S/Z)		6.35		
Weave	F1	A-1(S/Z)	4mm flat braided polyester elastic band	6.35	6.46	Plain
	F8			6.35		2x1 Twill
	F9			6.35		3x1 Twill
	F10			6.35		5-end Satin
Helical structure	F11	A-1-D(S/Z)	100D polyester-covered spandex yarn	9.14	6.10*	Plain
	F3	A-1(S/Z)		6.35		
	F12	A-1-T(S/Z)		5.59		

\*Average picks per inch - the weft yarn is spaced out at a distance of 7mm after every two picks



Table 6-2 Photographs of the woven fabric samples



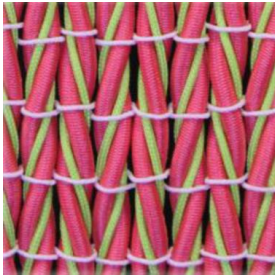
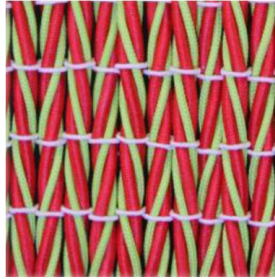
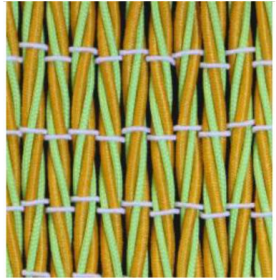
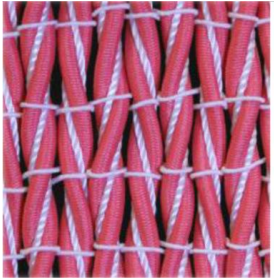
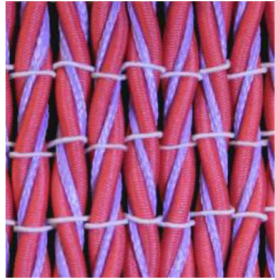





			
F1	F2	F3	F4
			
F5	F6	F7	F8
			
F9	F10	F11	F12



Figure 6-5 Photograph of the hexagonal mesh net sample

### 6.3.3 Testing Method

Fabric samples with above-mentioned constructions were subjected to investigation. For measuring the open area of the fabric samples, four points were marked on each specimen, with a distance of 2cm each prior to testing. The marks were made in the middle of the specimen to avoid necking effect imposed by both ends of the clamps during tensile testing.

Tensile properties were obtained with reference to the standard ASTM D 5035-95 using a strip test method on an INSTRON 4411 mechanical testing machine. Setting of the experiment is shown in Figure 6-6. Tensile test was conducted at a gauge length of 150mm and a crosshead speed of 50mm/min till rupture. Three specimens were tested for each sample in the direction of the helical auxetic yarns. To measure the auxetic behavior and open area of the fabric samples, a high-resolution CMOS camera was placed on the tripod in front of the tensile testing machine to capture consecutive

images of the tested sample at 2-second intervals during the experiments, which corresponded to a 1.1% interval of the tensile strain  $\epsilon_x$ . A diffused white light source is attached to the camera to enhance consistency and accuracy of the image analysis measurements. Contrasting background was arranged so that the yarns in the fabric can be identified clearly.

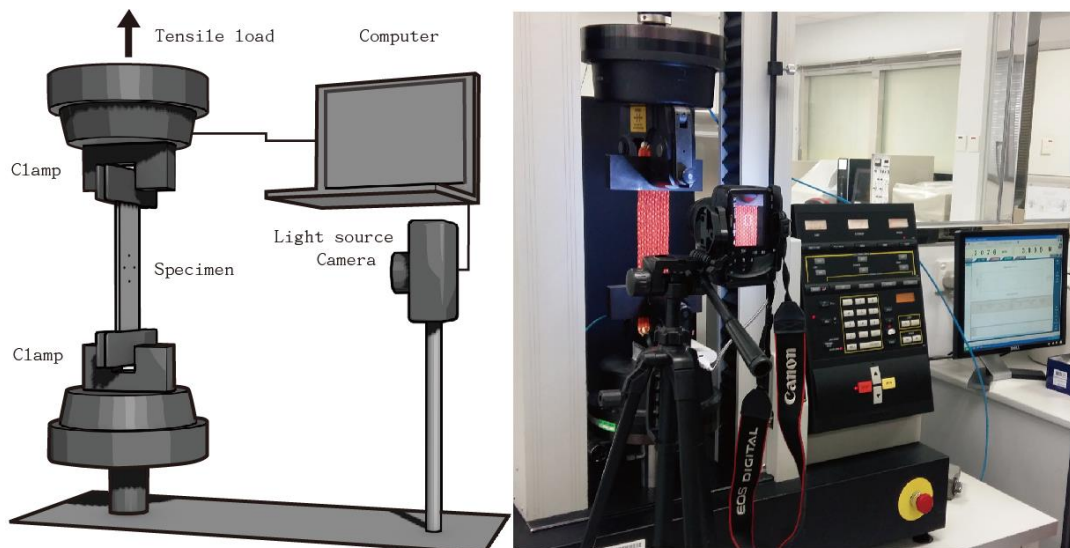


Figure 6-6 Schematic diagram and photograph of the fabric tensile testing system

Color images were exported to computer and duplicated into two sets for evaluation of lateral strain and open area separately with ImageJ public domain image processing software. The first set of duplicates was binarized with a thresholding procedure; the width of each specimen was then measured in three spots in order to ensure higher accuracy of the transverse strain values. Since tensile strain was provided by the tensile testing machine directly, Poisson's ratio of the fabric sample could be calculated

correspondingly. To measure open area of the fabric, another set of duplicates was loaded into ImageJ and cropped according to the markers on the specimen. As shown in Figure 6-7, the cropped images were binarized with the same thresholding procedure. Each image consists of 1420 x 1420 pixels, and each pixel represents an area of 14.08  $\mu\text{m}$  x 14.08  $\mu\text{m}$  on the fabric specimen. Every single image pixel was determined to be either the yarn (black pixels) or void space (white pixels). The area of void space was summed up and the percent open area was calculated as: percent open area = void pixels/ total pixels x 100%.

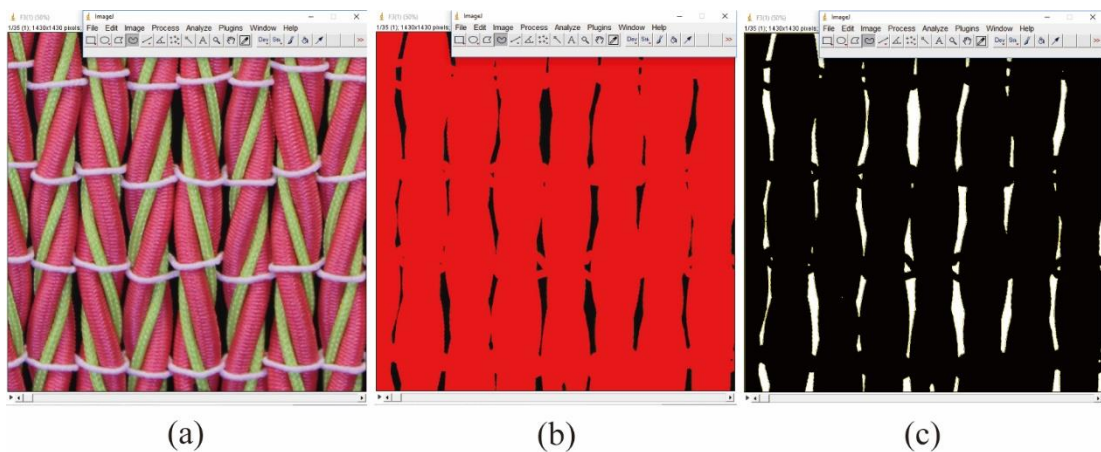


Figure 6-7 Conversion of the cropped image: (a) original image; (b) threshold color; (c) binary image

## 6.4 Results and Discussions

### 6.4.1 Typical Mechanical Properties of the Woven Fabrics made of 4-ply Auxetic Yarn

Understanding the load-strain relationship of a fabric is important and useful to

evaluate its auxetic behavior. Before studying the effect of each design parameter, sample F3 was selected here as an example to discuss the tensile properties of the woven fabric samples. Its load- strain curve, transverse-axial strain curve and Poisson's ratio-tensile strain curve are shown in Figure 6-8a-c, respectively. For the comparison, the same type of curves of 4-ply auxetic yarn are also illustrated in these figures. As shown in Figure 6-8a, three main regions can be identified in the load-strain curve of the fabric, including an initial linear region, followed by a nonlinear region and a second linear region before rupture.

In a typical load-strain curve of woven fabric, the initial linear region is caused by the resistance against friction and bending of the fabric, while the non-linear region of very low slope is caused by decrimping of yarns in the direction of force and subsequent crimp interchange between the warps and wefts. When the crimp is fully extended, further fabric elongation is achieved by yarn extension, leading to a secondary linear region in its load-strain curve. Regarding to the woven fabric made of auxetic plied yarns, its deformation mechanism is different from the typical one. Since the auxetic plied yarns are nearly straight in the warp direction, they have no crimp and no decrimping is expected when the fabric extends. No length-ways extension is possible without extending the yarns themselves. Auxetic plied yarns start

to bear the load and show a relatively small increase in force and high elongation due to migration of stiff yarn. Therefore, a non-linear region is resulted in its load-strain curve.

In order to compare the tensile behavior of the fabric and the auxetic yarn, the load-strain curve per yarn (N per yarn) is also presented in Figure 6-8a. It is the total load carried by the tested fabric sample divided by the total number of the auxetic yarns in the fabric. It can be seen that initial tensile behavior of the fabric is identical to that of a single 4-ply auxetic yarn. This reflects that the effect of yarn-yarn interactions in the fabric is small at the initial stretching stage. In this stage, the low modulus soft yarns of the 4-ply auxetic yarn bear the load and show a relatively small increase in force and high elongation. When the stiff yarns in the 4-ply auxetic structure gradually move to the yarn core, they start to bear a greater load. An increased slope results in both the load-strain curves of the single 4-ply auxetic yarn and load of fabric per yarn. However, the load per yarn of the fabric increases in a lower extent than that of the single 4-ply auxetic yarn. The reason is uneven distribution of the yarn stress in the fabric, which inevitably causes a decrease in the load-bearing capacity of individual 4-ply auxetic yarns in the fabric.

From Figure 6-8(b), it can be seen that the transverse strain of the fabric first increases up to an axial strain of 0.04 and then gradually decreases. Along with the results of single auxetic yarn, it is revealed that the auxetic plied yarns in the fabric are extended at low strains and the increase in their maximal diameters results in an increase of fabric width. However, the fabric reaches the highest transverse strain at a lower tensile strain than that of the yarn. The reason for this may come from the overlapping effect of the auxetic plied yarns in the fabric, which causes an expansion of the fabric in the thickness direction. From Figure 6-8(c), it can be seen that NPR of the fabric first increases, reaches its maximum effect at a strain of about 0.03, and then decreases toward zero. Compared to the auxetic plied yarn which has a maximum NPR value of  $-2.1$ , the auxetic behavior of the fabric is greatly reduced. Other than the overlapping effect, lateral expansion of the auxetic yarns in the fabric is also constrained by the weft yarns. With the diameter increase of each individual auxetic yarn in the fabric during extension, crimp in the weft yarns increases at the same time. Consequently, tension increase of the weft yarns prohibits further lateral expansion of the fabric. Table 6-3 illustrates photographs and the corresponding PR values of the fabric at different extension levels. Fabric expansion can clearly be observed at low strains, accompanying with the increased overlapping effect of auxetic yarns at high axial strains.

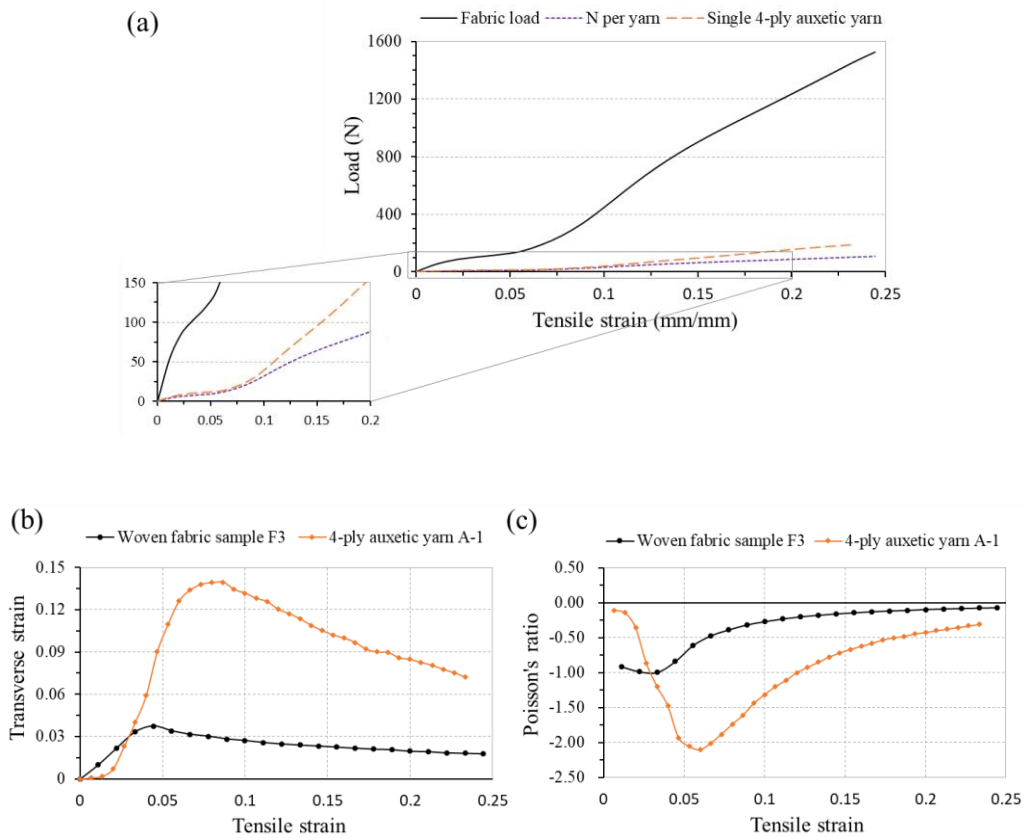


Figure 6-8 Tensile behavior of a typical auxetic woven fabric and its constituent auxetic yarn: (a) load-strain curves (the inset shows the enlargement at small load); (b) transverse-tensile strain curves; (c) PR-tensile strain curves.

Table 6-3 Pictures and Poisson's ratio values of sample F3 at different extension levels

Strain	Raw image	$\nu$	Strain	Raw image	$\nu$
0		n/a	0.13		-0.18
0.03		-1.00	0.21		-0.09
0.07		-0.47	0.29		-0.06
0.1		-0.27	0.38		-0.04

### 6.4.2 Effect of 4-ply Auxetic Yarn Arrangement

Two identical fabrics were made with the auxetic plied yarn A-1 either of the same



twist direction (S/S) or of different twist directions (S/Z) as the warp. Study on the Poisson's ratio-tensile strain curves of these samples in Figure 6-9 revealed that arranging 4-ply auxetic yarns in an alternate twist direction (S/Z) generates a slightly higher NPR of the woven fabric throughout the whole tensile process. As pairs of Z- and S-twisted auxetic plied yarns have a tendency to move to opposite direction upon stretching, the fabric is able to expand to a greater extent. However, difference in auxeticity of the two fabrics is not significant. It may be due to the fact that the 4-ply helix configuration forms a balanced structure with good stability towards tensile loading.

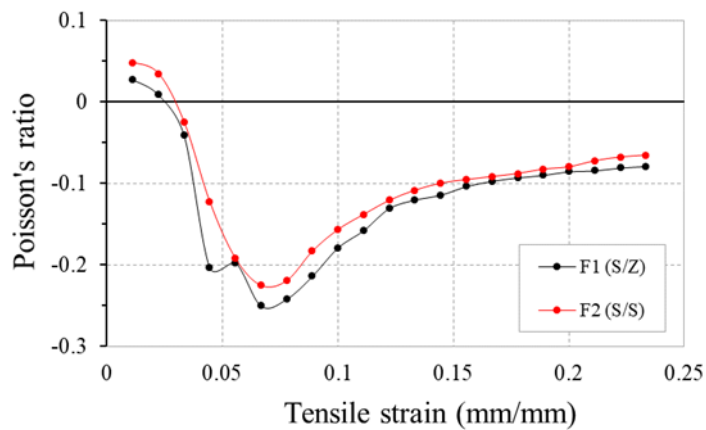


Figure 6-9 Poisson's ratio-tensile strain curves for samples F1 and F2

Another interesting phenomenon observed in this work is that alignment of the 4-ply auxetic yarns in the fabric sample is different from the ideal configuration proposed regardless of the direction of twist (Figure 6-10). Owing to the spiraling cross-section

of the 4-ply helix structure, the auxetic plied yarn consists of major and minor diameters in the same plane. If all the 4-ply auxetic yarns are oriented exactly parallel to each other, at a particular weave unit their respective major diameters in the plane will be parallel to the fabric surface, while the minor diameters in the plane will be oriented in the perpendicular direction and the auxetic behavior of the fabric will be maximized upon stretching. However, orientation of the individual auxetic plied yarn was hardly possible to control and it changed depending on the position of the yarn and its neighbors during sample fabrication. It is likely that the 4-ply auxetic yarns have a tendency to rotate inside the fabric until they are locked into a new position and bedded into each other. As a result, load is uniformly distributed at each and every weave unit, and the auxeticity of fabric is diminished at the same time.



Figure 6-10 Alignment of 4-ply auxetic yarns in the fabric sample

Figure 6-11 compares the percent open area-tensile strain curves of fabrics F1 and F2 under tensile loading. It is noted that the percent open area of both the fabrics is zero

at zero strain, which means the two fabrics are close fabrics. When extension is applied, the fabrics are opened. However, the percent open areas of the two fabrics are different. F1 has a higher percent open area than that of F2, and this difference increases with the increase in tensile strain. It is believed that the percent open area increases due to pore elongation, and the extent of increase is governed by the yarn arrangement in the fabric structure. Pairs of Z- and S-twisted auxetic plied yarn can form larger gaps between the yarns so that pore size is comparatively larger and leads to a higher percent open area.

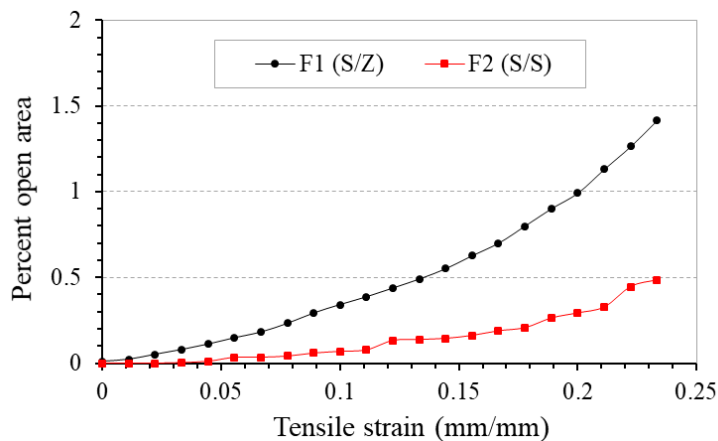


Figure 6-11 Percent open area in relation to tensile strain for samples F1 and F2

### 6.4.3 Effect of Weft Type

Two weft materials were selected to fabricate samples F1 and F3 with the same warp, and their Poisson's ratio-tensile strain curves are shown in Figure 6-12. It can be seen that weft yarn type can cause a large variation in NPR of the fabrics at low strains due to different extents of weft yarn constraint to the expansion of auxetic yarns. Looking

to the tensile stress-strain curves of the two weft yarns in Figure 6-13, it is obvious that the polyester-covered spandex yarn is more elastic than the polyester elastic band. Coupled with a lower weft yarn density, the polyester-covered spandex yarn in F3 has a much lower constraint to the expansion of auxetic yarns than the polyester elastic band. As a result, fabric F3 shows a higher NPR than F1 at low tensile strains. However, with the increase of the tensile strain, the difference in NPR of the two fabrics decreases due to the reduced NPR of the auxetic yarns. At the high extension, the constraint of the weft yarns becomes less important as all the auxetic warp yarns are in close contact.

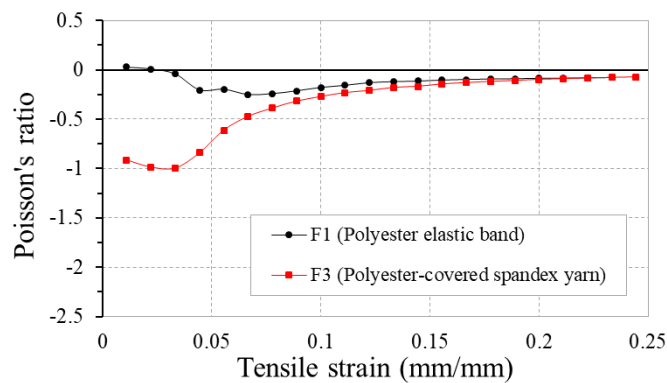


Figure 6-12 Poisson's ratio-tensile strain curves for samples F1 and F3

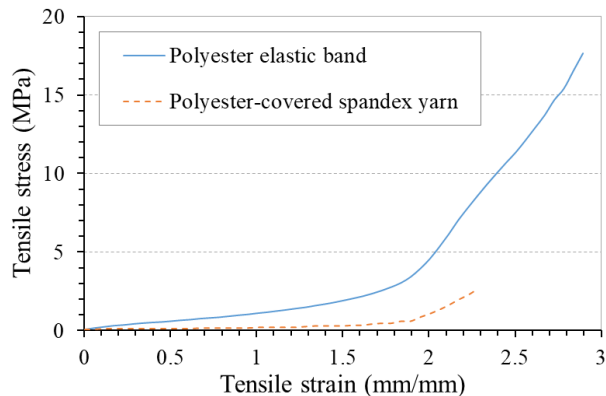


Figure 6-13 Tensile stress-strain curves of the weft yarns used

Figure 6-14 compares the percent open area of the two fabric samples under tensile loading. There is no doubt that the weft cover factor influences the total cover area of the fabrics. Comparing the two types of weft yarn, the polyester-covered spandex yarn used in this experiment is much finer than the polyester elastic band. In addition, it was spaced out at a distance of 7 mm after every two picks during weaving. This decreases the weft cover factor in F3 and results in a higher percent open area at zero strain. In addition, variation in percent open area displays a different trend. There is a region in the initial stage of tensile deformation showing a sharp increase in percent open area. Subsequently, percent open area gradually descends, and then steadily increases again up to the point of rupture.

This trend can be explained by the variation in 4-ply auxetic yarn structure during extension. At the beginning of the tensile test, migration of stiff yarns begins and thus minimal diameter of the auxetic plied yarn decreases and the maximal one increases simultaneously. The reduction in minimal diameter creates a large inter-yarn space between the 4-ply auxetic yarns so that a net increase in percent open area is resulted. When tensile strain increases, reduction in open area caused by increased maximal diameter outweighs the increase in open area caused by reduced minimal diameter. Along with the overlapping effect, a net decrease in percent open area is resulted. After

the stiff yarns thoroughly migrate to the yarn core, maximal diameter stops increasing. Pores elongate in the direction of force and the percent open area increases again. This variation trend can be observed in fabrics F3, F4, F5, F6 and F7, when the same weft yarn material and weft yarn density are used.

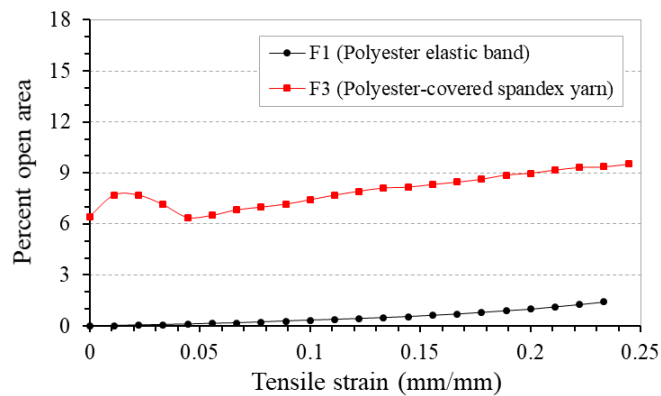


Figure 6-14 Percent open area in relation to tensile strain for samples F1 and F3

#### 6.4.4 Effect of 4-ply Auxetic Yarn Components

Auxetic plied yarns can be fabricated by using soft yarns and stiff yarns with different properties and sizes which may influence the NPR behavior and open pore property of woven fabrics made thereby. In this section, two variables, the diameter of soft yarn and tensile modulus of stiff yarn in the 4-ply auxetic yarn structure are selected for investigation.

Diameter of soft yarn is one of the significant design variables to alter the auxetic performance of the 4-ply auxetic yarn. The Poisson's ratio-tensile strain curves of three

fabrics F3, F4, and F5 fabricated with 4-ply auxetic yarns made of different soft yarn diameters are shown in Figure 6-15. For comparison, the curves of the 4-ply auxetic yarns used (A-1, B-1 and C-1) are also shown in the figure. The previous study showed that the reduction of soft yarn diameter would result in a sharp increase in NPR, and the auxetic effect would be maximized earlier. Accordingly, 4-ply auxetic yarn sample C-1 with a soft yarn diameter of 1.14mm could obtain a higher NPR value at an early deformation stage, followed by samples B-1 and A-1. When these yarns are incorporated into fabric, variation trend of the fabrics can be different.

From Figure 6-15, it can be seen that although fabric F5 behaves most auxetically at strain of around 0.01, its NPR value quickly decreases with a further increase of tensile strain, leading to a lower NPR of F5 if compared with fabrics F3 and F4. This may be due to the fact that in fabric F5, the stiff yarns separated by the finer soft yarns have a shorter path to migrate to the auxetic yarn core. As a result, the NPR effect reaches its maximal point at an early stage. After the maximal point, as the lateral contraction of the soft and stiff yarns become the main deformation mode of auxetic yarns, the NPR behavior of the fabric quickly decreases.

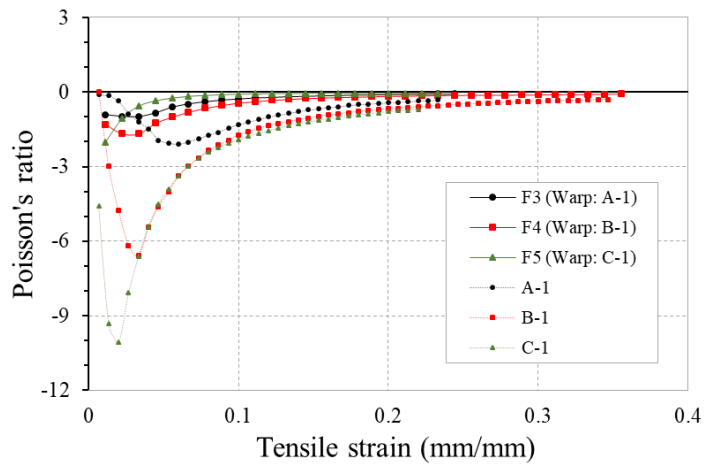


Figure 6-15 PR-tensile strain curves of fabrics F3, F4, F5 and their respective 4-ply auxetic yarns.

Figure 6-16 depicts the percent open area of these samples under tensile loading. Comparing the percent open area of the three samples, it is clear that the one which consisted of a thicker soft yarn in the 4-ply auxetic yarn structure yielded a lower percent open area at all strains. It is because the coarser the auxetic plied yarns, the fewer of them go into the same measured space. Consequently less inter-yarn spacing is resulted and lead to a lower percentage of open area.

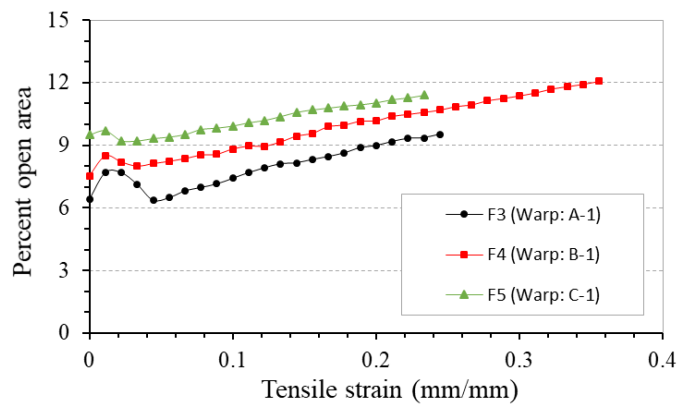


Figure 6-16 Percent open area in relation to tensile strain for samples F3, F4 and F5



In addition to the soft yarn diameter, the tensile modulus of stiff yarn also plays a significant role in the determination of the NPR behavior of 4-ply auxetic yarn. Three fabric samples were produced using 4-ply auxetic yarns with stiff yarns of different tensile modulus. The Poisson's ratio-tensile strain curves of these fabrics are shown in Figure 6-17. For the comparison, the curves of the 4-ply auxetic yarns used (A-1, A-3, and A-4) are also shown in the figure.

Among the three auxetic yarns, auxetic yarn A-4 made of waxed polyester cord as stiff yarn possesses the highest tensile modulus (1307 MPa). It can be seen that fabric F7 produced with it has a higher NPR effect compared to fabrics F3 and F6, given that the NPR of fabric F7 is higher than fabrics F3 and F6 at all strains. The result implies that the migration intensity of stiff yarn still imposes a significant effect on the NPR behavior of the woven fabric made therefrom.

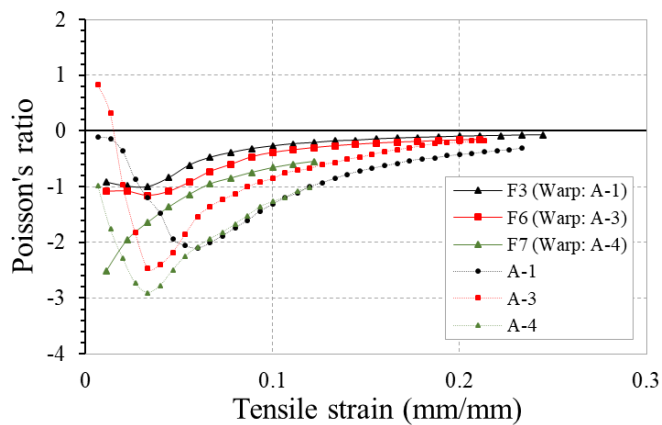


Figure 6-17 Poisson's ratio-tensile strain curves for samples F3, F6 and F7 and their respective 4-ply auxetic yarns

Figure 6-18 shows the percent open area in response to tensile loading of these samples. It is observed that variation in percent open area follows the same trend, in which percent open area first increases, then decreases and then increases again. Among the three fabric samples, the one that possesses a higher stiff yarn modulus has a slightly higher percent open area at small strain range. It may due to the fact that high tensile modulus stiff yarns have a higher migration intensity; once the strain is applied, minimal diameter decreases sharply so that a larger pore is resulted between the 4-ply auxetic yarns and percent open area increases to a greater extent. Under high strains, percent open areas of the three fabric samples are similar, owing to the fact that the three auxetic plied yarns have a more or less similar aspect ratio under jamming condition.

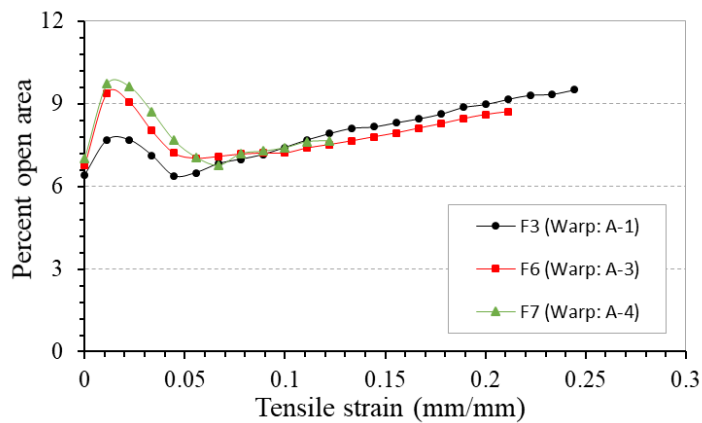


Figure 6-18 Percent open area in relation to tensile strain for samples F3, F6 and F7

#### 6.4.5 Effect of Weave Structure

The effect of weave structure on the auxetic behavior of the woven fabric made of 4-

ply auxetic yarn is illustrated in Figure 6-19. Differences in Poisson's ratio of the four fabric samples are prominent. The plain weave sample (F1) and 2x1 twill weave sample (F8) exhibit a NPR behavior for more than 95% of the total strain, while the 3x1 twill weave sample (F9) and 5-end stain weave sample (F10) exhibit a positive Poisson's ratio over most of the strain range. The results revealed that interaction between the 4-ply auxetic yarns plays an important role in generating the auxetic effect of the fabric. This is mainly due to the fact that weaves with long floats and few intersection points would allow the 4-ply auxetic yarns to move nearer together upon tensile loading. As a result, yarns overlap easily, and it increases the out-of-plane NPR of the fabric.

Even though increasing the number of interlacement can efficiently avoid adjacent auxetic yarns from bedding into each other, it can be seen that the plain weave structure does not necessarily guarantee the best auxetic effect. As plain weave has comparatively more interlacing points than twill and satin weaves, the 4-ply auxetic yarns have to overcome a greater frictional restraint imposed by the weft yarn at crossover regions when the fabric is under tension. Consequently NPR of the fabric is attenuated.

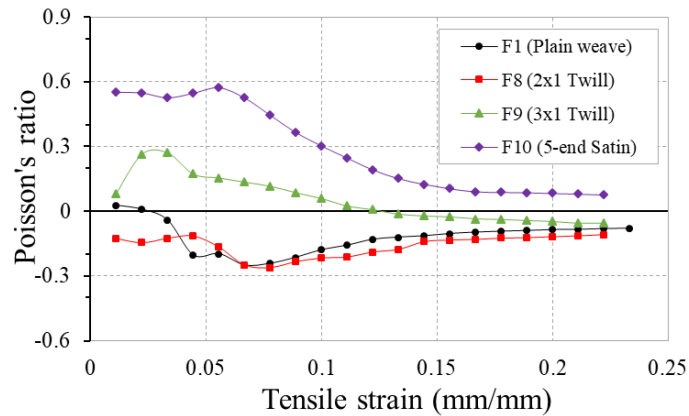


Figure 6-19 Poisson's ratio-tensile strain curves for samples F1, F8, F9 and F10

Figure 6-20 compares the percent open area of the three fabric samples under tensile loading. To identify the influence of weave structure clearly, all these four fabrics were fabricated with the same flat and wider polyester elastic band as weft yarns. Although the performance of the 4-ply auxetic yarns under different weave structures may affect the warp cover, the cover changes of the fabrics are dominated by the weft yarns. Therefore, variation in percent open area of the four fabrics follows the same trend, that is, the percent open area increases with increasing tensile strain due to the pore elongation

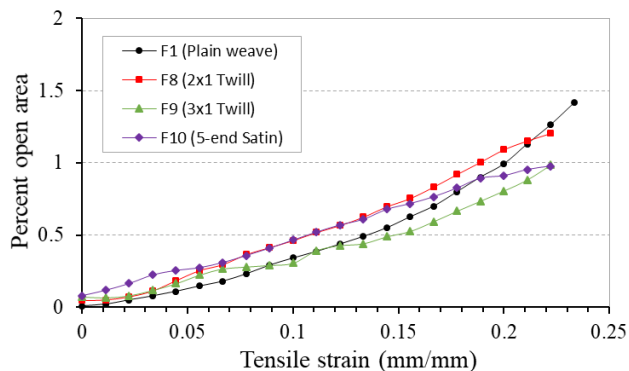


Figure 6-20 Percent open area in relation to tensile strain for samples F1, F8, F9 and F10

#### **6.4.6 Effect of Helical Structure**

Fabric samples made of double helix yarn and two kinds of auxetic plied yarns (4-ply and 6-ply) were tested and the effect of helical structure on the auxetic behavior of the three fabric samples is illustrated in Figure 6-21. Among the three HAYs fabric samples, sample F3 which is made of 4-ply auxetic yarns yielded a highest NPR effect, followed by samples F12 and F11. In the tensile measurement of the single HAYs, the DHY and 6-ply auxetic yarn samples exhibited a positive Poisson's ratio at low strain ranges. It is interesting to note that auxetic behavior is expedited when they are incorporated into fabric, and it is likely to be due to the different testing condition. To avoid yarn slippage in the fabric sample, another grip was used in this experiment and the extendable length reduced greatly. To overcome this limitation in testing, gauge length was reduced from 250mm to 150mm. It is expected that a more localized deformation is resulted, leading to an expedited auxetic behavior in the woven fabric samples. However, the DHY fabric sample still exhibits a positive Poisson's ratio at the beginning of stretch due to its specific deformation mechanism. It is also important to observe that 6-ply auxetic yarns did not overlap in sample F12 upon stretching, and it may be attributed to the increased circularity in the 6-ply auxetic yarn structure. Upon extension, the three soft yarns create a larger contact area. As a consequence, the 6-ply auxetic yarns become more rigid to shear and to overlap with each other. Figure

6-22 shows an inserted image of sample F12 under high strains.

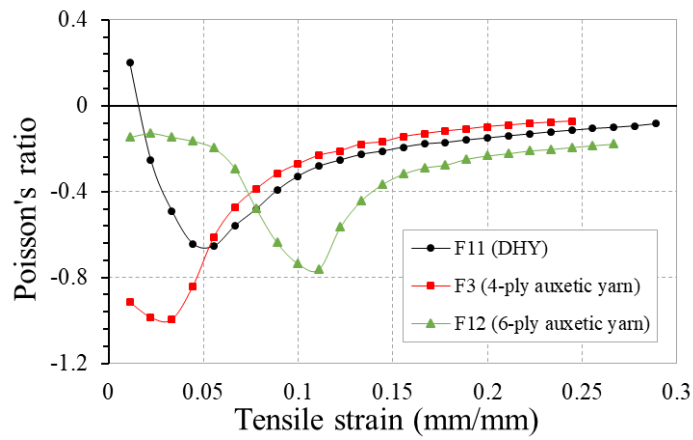


Figure 6-21 Poisson's ratio-tensile strain curves for samples F11, F3 and F12



Figure 6-22 Sample F12 at strain of 0.4

Figure 6-23 compares the percent open area of the three fabric samples under tensile loading. It can be observed that percent open area of fabric made of DHYs is much higher than those made of auxetic plied yarns. Because of the unbalanced double helix structure, large inter-yarn space is created between the DHYs under tensile loading. The result revealed that open pore properties of these three fabric samples are different due to a different helical structure, and it is not correlated to their respective auxetic behavior.

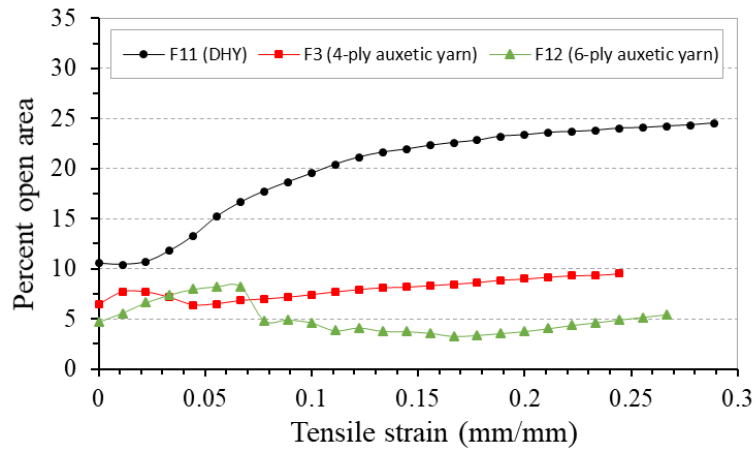


Figure 6-23 Percent open area in relation to tensile strain for samples F11, F3 and F12

#### 6.4.7 The Hexagonal Mesh Net Based on 4-ply Auxetic Structure

Hexagonal mesh sample based on 4-ply auxetic structure was fabricated successfully and the Poisson's ratio-tensile strain curve is shown in Figure 6-24(a). The result revealed that there is potential to apply the 4-ply auxetic yarn structure in hexagonal mesh as NPR effect is obtained at low strain ranges. However, Poisson's ratio increases to a positive value at high strains due to overlapping effect and the inherent non-auxetic properties brought by each constituent yarn. Figure 6-24(b) shows the percent open area of this fabric sample. A long duration of decreasing open area is observed, and it may be attributed to the overlapping effect which draws the neighboring yarns to come closer to each other.

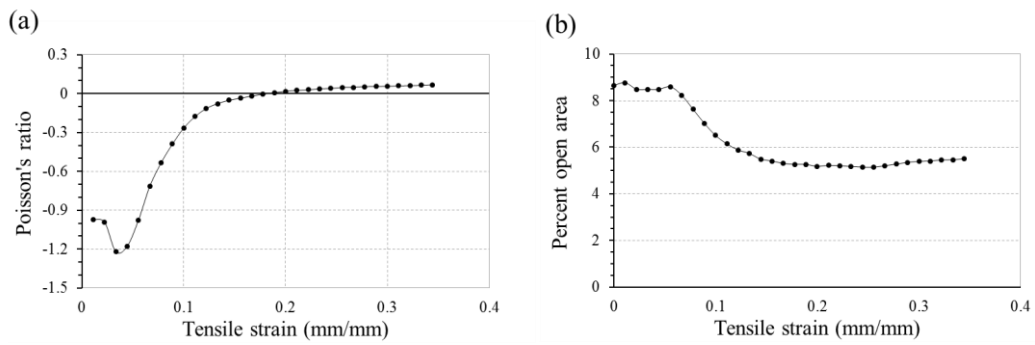


Figure 6-24(a) Poisson's ratio-tensile strain curve for sample F13; (b) Percent open area in relation to tensile strain for sample F13

### 6.5 Conclusions

Different types of auxetic yarns including the 4-ply yarns, 6-ply yarn, and DHY were used to fabricate woven fabrics in this chapter. Fabric samples were tested to measure the auxetic behavior and percent open area of these samples. Effect of various design parameters including auxetic plied yarn arrangement, weft type, 4-ply auxetic yarn properties and weave structure were analyzed. Lastly, hexagonal mesh net was fabricated in 4-ply auxetic structure and the potential to generate auxetic effect in this type of fabric was verified. The main conclusions to be drawn from this study are:

- (1) The in-plane NPR behavior of a woven fabric can be inherited from its constituent auxetic yarns, but with a significant reduction due to a combination of different factors. These factors include the embedding of auxetic plied yarns during weaving, the constraint of weft yarns, and the overlapping effect of auxetic yarns upon extension.



- (2) The alternative arrangement of S- and Z-twisted auxetic yarns in a woven fabric can generate higher NPR and percent open area to the fabric.
- (3) Weft yarns with low modulus and short float over the 4-ply auxetic yarns are favorable for producing high NPR values of the fabric.
- (4) Weave structure has significant effect on the NPR behavior of the woven fabric. More intersections help to prevent the auxetic plied yarns from embedding to each other.
- (5) Stiff yarns with high tensile modulus in a plied auxetic yarn structure result in a higher NPR effect in the fabric. However, a finer soft yarn does not necessarily produce a higher NPR due to the early onset of fabric contraction.
- (6) Weft cover factor plays a significant role in the determination of the open pore properties of the woven fabrics. When the weft cover factor is reduced to certain extent, different variation trends can be identified. Variation in the major diameter and minor diameter of the auxetic plied yarn upon extension induces opposing effects on the percent open area of the auxetic woven fabrics.

## **CHAPTER 7 CONCLUSIONS AND FUTURE WORK**

### **7.1 Conclusions**

A comprehensive experimental study was conducted to characterize the tensile properties and auxetic behavior of the auxetic plied yarn structures in this project. Influence of structural parameters and material properties were discussed. Undoubtedly, auxetic plied yarn is a kind of stress-responsive material which alters the fundamental positive Poisson's ratio property in yarns. The auxetic effect in the auxetic plied yarn structure can be utilized to result in many beneficial effects for various kinds of specific applications. Among the three HAYs with different helical structures, 4-ply auxetic yarn has shown the greatest potential to produce immediate auxetic effect.

Microscopic examination provided a deep insight into the deformation mechanism of 4-ply and 6-ply auxetic yarns to generate auxetic effect. The results revealed that stiff yarn with higher modulus has a higher migration intensity, while the 6-ply auxetic yarn has an unbalanced structure during stiff yarn migration. This experiment provided proper evidence to explain how the NPR effect is generated in the auxetic plied yarn structure.

This study also demonstrated that the auxetic plied yarns are not only suitable to use

exclusively, but also feasible to incorporate into fabric to obtain NPR behavior. Previous literature has shown that auxetic fibers and yarns can be used to generate auxetic effect in textiles. However, application of this approach remains largely unexplored due to limited auxetic fibers and yarns up to now. This study certainly opened up the possibilities for alternatives other than those currently present in the academic community. Additionally, an innovative approach for using the 4-ply auxetic yarn structure to fabricate hexagonal mesh has been developed and the auxetic effect was verified. Although the fabric samples are produced on laboratory scale, the experimental study conducted can definitely serve as a fundamental source of information for continuing research.

With the investigation of the influence of each design parameter, idealized material and structure to obtain desired auxetic performance and open pore properties were identified. Besides, it was found that woven fabric made of 4-ply auxetic yarn still demonstrated the greatest potential to generate immediate auxetic behavior upon extension, while the 6-ply auxetic yarn fabric sample has shown great potential to produce non-overlapping woven fabric during lateral expansion.

## 7.2 Future Work

As the geometrical model developed by Ge et al. [23] is only capable to predict the auxetic behavior of 4-ply auxetic yarn under high strains, mechanical model can be developed based upon the founding obtained in this study to predict and tailor the auxetic behavior of the auxetic yarn for specific application.

Study on the auxetic plied yarn can be extended to evaluate how does the auxetic behavior of the auxetic plied yarn structure affect the other mechanical properties of the yarn, such as the pull-out resistance under tension load.

In addition, technology to incorporate auxetic plied yarns into fabric on larger scale is needed to be developed as the fabric samples produced in this project were on laboratory scale so far. Furthermore, study can be carried out to investigate how to maximize the auxetic behavior in fabric with the combination of auxetic plied yarns and special geometrical configuration.

As the hexagonal mesh sample with 4-ply auxetic yarn structure has shown potential to produce auxetic effect upon extension, further investigation can be made to figure out if it is possible to produce the same structure in the industrial netting machine to generate the NPR behavior.

---

## REFERENCES

1. Love, A.E.H., *A treatise on the mathematical theory of elasticity*. 4th ed. 1944, New York: Dover Publications. xviii, 643.
2. Yeganeh-Haeri, A., D.J. Weidner, and J.B. Parise, *Elasticity of  $\alpha$ -Cristobalite: A silicon dioxide with a negative Poisson's ratio*. *Science*, 1992. **257**(5070): p. 650-652.
3. Gunton, D. and G. Saunders, *The Young's modulus and Poisson's ratio of arsenic, antimony and bismuth*. *Journal of Materials Science*, 1972. **7**(9): p. 1061-1068.
4. Williams, J.L. and J.L. Lewis, *Properties and an anisotropic model of cancellous bone from the proximal tibial epiphysis*. *J Biomech Eng*, 1982. **104**(1): p. 50-6.
5. Veronda, D.R. and R.A. Westmann, *Mechanical characterization of skin—Finite deformations*. *Journal of Biomechanics*, 1970. **3**(1): p. 111-124.
6. Frolich, L.M., M. LaBarbera, and W.P. Stevens, *Poisson's ratio of a crossed fibre sheath: the skin of aquatic salamanders*. *Journal of Zoology*, 1994. **232**(2): p. 231-252.
7. Lakes, R., *Foam structures with a negative Poisson's ratio*. *Science*, 1987. **235**(4792): p. 1038-1040.
8. Alderson, K.L., R.S. Webber, and K.E. Evans, *Novel variations in the microstructure of auxetic ultra-high molecular weight polyethylene. Part 2: Mechanical properties*. *Polymer Engineering & Science*, 2000. **40**(8): p. 1906-1914.

9. Caddock, B.D., *Microporous materials with negative poisson's ratios. i. microstructure and mechanical properties*. Journal of Physics D: Applied Physics, 1989. **22**(12): p. 1877-1882.
10. Masters, I.G. and K.E. Evans, *Models for the elastic deformation of honeycombs*. Composite Structures, 1996. **35**(4): p. 403-422.
11. Mousanezhad, D., et al., *Spiderweb honeycombs*. International Journal of Solids and Structures, 2015. **66**: p. 218-227.
12. Friis, E., R. Lakes, and J. Park, *Negative Poisson's ratio polymeric and metallic foams*. Journal of Materials Science, 1988. **23**(12): p. 4406-4414.
13. Brandel, B. and R.S. Lakes, *Negative Poisson's ratio polyethylene foams*. Journal of Materials Science, 2001. **36**(24): p. 5885-5893.
14. Grima, J.N., et al., *Negative Poisson's ratios in cellular foam materials*. Materials Science and Engineering: A, 2006. **423**(1–2): p. 214-218.
15. Chan, N. and K. Evans, *Fabrication methods for auxetic foams*. Journal of Materials Science, 1997. **32**(22): p. 5945-5953.
16. Ledbetter, H. and M. Lei, *Monocrystal elastic constants of orthotropic Y sub 1 Ba sub 2 Cu sub 3 O sub 7 : An estimate*. Journal of Materials Research, 1991. **6**(11).
17. Topolov, V.Y. and C.R. Bowen, *Characteristics of 1–3-type ferroelectric ceramic/auxetic polymer composites*. Modelling and Simulation in Materials Science and Engineering, 2008. **16**(1): p. 015007.
18. Alderson, K.L., et al., *How to make auxetic fibre reinforced composites*. physica status solidi (b), 2005. **242**(3): p. 509-518.
19. He, C., P. Liu, and A.C. Griffin, *Toward negative Poisson ratio polymers through molecular design*. Macromolecules, 1998. **31**(9): p. 3145-3147.

- 
20. Pour, N., et al., *Auxetics at the molecular level: A negative Poisson's ratio in molecular rods*. *Angewandte Chemie International Edition*, 2006. **45**(36): p. 5981-5983.
  21. Rant, D., T. Rijavec, and A. Pavko-Čuden, *Auxetic textiles*. *Acta chimica Slovenica*, 2013. **60**(4): p. 715.
  22. Hook, P.B., *Auxetic mechanisms, structures & materials*, in *School of Engineering and Computer Science*. 2003, University of Exeter.
  23. Ge, Z.Y., H. Hu, and S.R. Liu, *A novel plied yarn structure with negative Poisson's ratio*. *The Journal of The Textile Institute*, 2016. **107**(5): p. 578-588.
  24. Evans, K.E., et al., *Molecular network design*. *Nature*, 1991. **353**(6340): p. 124.
  25. Bhullar, S.K., J.L. Wegner, and A. Mioduchowski<sup>2</sup>, *Strain energy distribution in an auxetic plate with a crack*. *Journal of Engineering and Technology Research*, 2010. **2**(7): p. 118-125.
  26. Scarpa, F., et al., *Dynamic crushing of auxetic open-cell polyurethane foam*. *Proceedings of the Institution of Mechanical Engineers, Part C: Journal of Mechanical Engineering Science*, 2002. **216**(12): p. 1153-1156.
  27. Chan, N. and K.E. Evans, *The mechanical properties of conventional and auxetic foams. Part II: Shear*. *Journal of Cellular Plastics*, 1999. **35**(2): p. 166-183.
  28. G.Cicala, et al., *Auxetic hexachiral truss core reinforced with twisted hemp yarns: out of plane shear properties*, A.J.M. Ferreira, Editor. 2011, 16th International Conference on Composite Structures (ICCS 16).
  29. Scarpa, F. and P.J. Tomlin, *On the transverse shear modulus of negative Poisson's ratio honeycomb structures*. *Fatigue & Fracture of Engineering Materials & Structures*, 2000. **23**(8): p. 717-720.

- 
30. Evans, K.E. and K.L. Alderson, *Auxetic materials: the positive side of being negative*. Engineering Science and Education Journal, 2000. **9**(4): p. 148-154.
  31. Coenen, V.L. and K.L. Alderson, *Mechanisms of failure in the static indentation resistance of auxetic carbon fibre laminates*. physica status solidi (b), 2011. **248**(1): p. 66-72.
  32. Alderson, A., *A triumph of lateral thought*. Chemistry and Industry, 1999(10): p. 384.
  33. Liu, Q., *Literature review: Materials with negative Poisson's ratios and potential applications to aerospace and defence*. 2006.
  34. Stott, P.J., et al., *A growing industry*. Materials World, 2000. **8**: p. 12-14.
  35. Simkins, V., et al., *Single fibre pullout tests on auxetic polymeric fibres*. Journal of Materials Science, 2005. **40**(16): p. 4355-4364.
  36. Sanami, M., et al., *Auxetic materials for sports applications*. Procedia Engineering, 2014. **72**: p. 453-458.
  37. Lim, T.-C., *Thermal stresses in thin auxetic plates*. Journal of Thermal Stresses, 2013. **36**(11): p. 1131-1140.
  38. Evans, K.E. and A. Alderson, *Auxetic materials: Functional materials and structures from lateral thinking!* Advanced Materials, 2000. **12**(9): p. 617-628.
  39. Underhill, R.S., *Defense applications of auxetic materials*. DSIAC Journal, 2014. **1**(1): p. 7-13.
  40. Howell, B., P. Prendergast, and L. Hansen, *Examination of acoustic behavior of negative poisson's ratio materials*. Applied Acoustics, 1994. **43**(2): p. 141-148.
  41. Scarpa, F., W.A. Bullough, and P. Lumley, *Trends in acoustic properties of iron particle seeded auxetic polyurethane foam*. Proceedings of the Institution



- of Mechanical Engineers, Part C: Journal of Mechanical Engineering Science, 2004. **218**(2): p. 241-244.
42. Alderson, A., et al., *An auxetic filter: A tuneable filter displaying enhanced size selectivity or defouling properties*. Industrial & Engineering Chemistry Research, 2000. **39**(3): p. 654-665.
43. Alderson, A. and K. Alderson, *Expanding materials and applications: exploiting auxetic textiles*. Technical Textiles International : TTI, 2005. **14**(6): p. 29-34.
44. Scarpa, F., et al., *Mechanical performance of auxetic polyurethane foam for antivibration glove applications*. Cellular Polymers, 2005. **24**(5): p. 253-268.
45. Lira, C., F. Scarpa, and R. Rajasekaran, *A gradient cellular core for aeroengine fan blades based on auxetic configurations*. Journal of Intelligent Material Systems and Structures, 2011. **22**(9): p. 907-917.
46. Stavroulakis, G.E., *Auxetic behaviour: appearance and engineering applications*. physica status solidi (b), 2005. **242**(3): p. 710-720.
47. Ugbolue, S., et al., *The formation and performance of auxetic textiles. Part I: theoretical and technical considerations*. Journal of The Textile Institute, 2010. **101**(7): p. 660-667.
48. Choi, J.B. and R.S. Lakes, *Design of a fastener based on negative Poisson's ratio foam*. Cellular Polymers, 1991. **10**(3): p. 205-212.
49. LOWE, A. and R.S. LAKES, *Negative Poisson's ratio foam as seat cushion material*. Vol. 19. 2000: Cellular Polymers.
50. Wang, Y.-C. and R. Lakes, *Analytical parametric analysis of the contact problem of human buttocks and negative Poisson's ratio foam cushions*. International Journal of Solids and Structures, 2002. **39**(18): p. 4825-4838.

- 
51. Rasburn, J., et al., *Auxetic structures for variable permeability systems*. AIChE Journal, 2001. **47**(11): p. 2623-2626.
  52. Alderson, A., et al., *Auxetic polymeric filters display enhanced de-fouling and pressure compensation properties*. Membrane Technology, 2001. **2001**(137): p. 6-8.
  53. Friis, E.A., *Surgical implants incorporating re-entrant material*. 1991, Google Patents.
  54. Moyers, R.E., *Dilator for opening the lumen of a tubular organ*. 1992, Google Patents.
  55. Walter, P., *Spinning a blast-proof yarn*. Chemistry and Industry, 2010(13): p. 10.
  56. *Safe at work.(Bomb blast curtains)*. Professional Engineering Magazine, 2010. **23**(10): p. 38.
  57. *Expanding blast-proof curtain will reduce impact of bomb explosions*. 2010. p. 1150.
  58. Glazzard, M. and P. Breedon, *Weft-knitted auxetic textile design*. physica status solidi b - basic solid state physics, 2014. **251**(2): p. 267.
  59. Wang, Z. and H. Hu, *Auxetic materials and their potential applications in textiles*. Textile Research Journal, 2014. **84**(15): p. 1600-1611.
  60. Toronjo, A., *Articles of apparel including auxetic materials*. 2014, Google Patents.
  61. Scarpa, F., *Dynamic properties of high structural integrity auxetic open cell foam*. Smart Materials and Structures, 2004. **13**(1): p. 49-56.
  62. Alderson, K.L., et al., *An experimental study of ultrasonic attenuation in microporous polyethylene*. Applied Acoustics, 1997. **50**(1): p. 23-33.

- 
63. Hook, P., *Uses of auxetic fibres*. 2011, Google Patents.
  64. Caddock, B.D. and K.E. Evans, *Microporous materials with negative Poisson's ratios. I. Microstructure and mechanical properties*. Journal of Physics D: Applied Physics, 1989. **22**(12): p. 1877.
  65. Evans, K.E., *Microporous materials with negative poisson's ratios. ii. mechanisms and interpretation*. Journal of Physics D: Applied Physics, 1989. **22**(12): p. 1883-1887.
  66. Alderson, K.L. and K.E. Evans, *The fabrication of microporous polyethylene having a negative Poisson's ratio*. Polymer, 1992. **33**(20): p. 4435-4438.
  67. Pickles, A.P., K.L. Alderson, and K.E. Evans, *The effects of powder morphology on the processing of auxetic polypropylene (PP of negative poisson's ratio)*. Polymer Engineering & Science, 1996. **36**(5): p. 636-642.
  68. Alderson, K., et al., *Evidence for Uniaxial Drawing in the Fibrillated Microstructure of Auxetic Microporous Polymers*. Journal of Materials Science Letters, 1998. **17**(16): p. 1415-1419.
  69. Alderson, K.L., et al., *Auxetic polypropylene fibres : Part 1 - Manufacture and characterisation*. Plastics, Rubber and Composites, 2002. **31**(8): p. 344-349.
  70. Ravirala, N., et al., *Expanding the range of auxetic polymeric products using a novel melt-spinning route*. physica status solidi (b), 2005. **242**(3): p. 653-664.
  71. Ravirala, N., et al., *Negative Poisson's ratio polyester fibers*. Textile Research Journal, 2006. **76**(7): p. 540.
  72. Zhang, G.H., O. Ghita, and K.E. Evans, *The fabrication and mechanical properties of a novel 3-component auxetic structure for composites*. Composites Science and Technology, 2015.

- 
73. Lim, T.-C., *Semi-auxetic yarns*. *physica status solidi b - basic solid state physics*, 2014. **251**(2): p. 273.
74. Shahabi, N.E., et al., *Crimp analysis of worsted fabrics in the terms of fabric extension behaviour*. *Fibers and Polymers*, 2014. **15**(6): p. 1211-1220.
75. Hu, J., *Structure and mechanics of woven fabrics*. 2004, Boca Raton, Fla. : Cambridge: Boca Raton, Fla. : CRC Press ; Cambridge : Woodhead Pub.
76. Saeed Ajeli, A.A.A.J., *Geometrically Poisson's Ratio of the Polyester Double-bar Warp-Knitted Structures on the Jamming Point*. *JOURNAL OF TEXTILES AND POLYMERS*, 2014. **2**(1): p. 24-28.
77. Wang, Z., H. Hu, and X. Xiao, *Deformation behaviors of three-dimensional auxetic spacer fabrics*. *Textile Research Journal*, 2014. **84**(13): p. 1361-1372.
78. Liu, Y.P., et al., *Negative Poisson's ratio weft-knitted fabrics*. 2010. p. 856-863.
79. Hu, H., Z.Y. Wang, and S. Liu, *Development of auxetic fabrics using flat knitting technology*. *Textile Research Journal*, 2011. **81**(14): p. 1493-1502.
80. Starbuck, M., et al., *Fabrics having knit structures exhibiting auxetic properties and garments formed thereby*. 2008, Google Patents.
81. Ugbolue, S.C., et al., *The formation and performance of auxetic textiles*, in *National Textile Center Annual Report*. 2009, University of Massachusetts Kyiv National University of Technologies and Design.
82. Ugbolue, S., et al., *The formation and performance of auxetic textiles. Part II: geometry and structural properties*. *Journal of The Textile Institute*, 2011. **102**(5): p. 424-433.
83. Ugbolue, S.C., et al., *Auxetic fabric structures and related fabrication methods*. 2011, Google Patents.

- 
84. Alderson, K., et al., *Auxetic warp knit textile structures*. *physica status solidi (b)*, 2012. **249**(7): p. 1322-1329.
  85. Wang, Z. and H. Hu, *3D auxetic warp-knitted spacer fabrics*. *physica status solidi b - basic solid state physics*, 2014. **251**(2): p. 281.
  86. Wright, J.R., et al., *On the design and characterisation of low-stiffness auxetic yarns and fabrics*. *Textile Research Journal*, 2012. **82**(7): p. 645-654.
  87. Vysanskav, M. and P. Vintrova, *Auxetic woven fabrics - Pores' parameters observation*. *Journal of Donghua University*, 2013. **30**(5): p. 416-420.
  88. Miller, W., et al., *A negative Poisson's ratio carbon fibre composite using a negative Poisson's ratio yarn reinforcement*. *Composites Science and Technology*, 2012. **72**(7): p. 761-766.
  89. He, G., et al., *Anovel mechanism for auxetic behavior in entangled materials with a spiral wire structure*. *Smart Materials and Structures*, 2014. **23**(9): p. 095011.
  90. Quadrini, F., et al., *Auxetic epoxy foams produced by solid state foaming*. *Journal of Cellular Plastics*, 2015: p. 0021955X15579456.
  91. Verma, P., et al., *Inducing out-of-plane auxetic behavior in needle-punched nonwovens*. *physica status solidi (b)*, 2015. **252**(7): p. 1455-1464.
  92. Ge, Z. and H. Hu, *Innovative three-dimensional fabric structure with negative Poisson's ratio for composite reinforcement*. *Textile Research Journal*, 2013. **83**(5): p. 543-550.
  93. Jiang, L., B. Gu, and H. Hu, *Auxetic composite made with multilayer orthogonal structural reinforcement*. *Composite Structures*, 2016. **135**: p. 23.

- 
94. Dolla, W.J.S., B.A. Fricke, and B.R. Becker, *Structural and drug diffusion models of conventional and auxetic drug-eluting stents*. Journal of Medical Devices, 2007. **1**(1): p. 47.
95. Hook, P. and K. Evans. *How do auxetic materials work?* 2006; Available from: <http://www.auxetix.com/science.html>.
96. Alderson, A., et al., *Modelling of the mechanical and mass transport properties of auxetic molecular sieves: an idealised organic (polymeric honeycomb) host-guest system*. Molecular Simulation, 2005. **31**(13): p. 897-905.
97. Alderson, A. *Smart solutions from auxetic materials*. 2011; Available from: <http://www.med-techinnovation.com/articles/articles/article/20>.
98. Coxworth, B. *New blast-proof curtain gets thicker when stretched*. 2010; Available from: <http://www.gizmag.com/new-blast-proof-curtain-gets-thicker-when-stretched/15531/>.
99. Wright, J.R., M.R. Sloan, and K.E. Evans, *Tensile properties of helical auxetic structures: A numerical study*. Journal of Applied Physics, 2010. **108**: p. 044905.
100. Sloan, M.R., J.R. Wright, and K.E. Evans, *The helical auxetic yarn – A novel structure for composites and textiles geometry, manufacture and mechanical properties*. Mechanics of Materials, 2011. **43**(9): p. 476-486.
101. Du, Z., et al., *Study on negative Poisson's ratio of auxetic yarn under tension: Part 1 – Theoretical analysis*. Textile Research Journal, 2015. **85**(5): p. 487-498.
102. Du, Z., et al., *Study on negative Poisson's ratio of auxetic yarn under tension: Part 2 – Experimental verification*. Textile Research Journal, 2015. **85**(7): p. 768-774.

- 
103. Sibal, A. and A. Rawal, *Design strategy for auxetic dual helix yarn systems*. Materials Letters, 2015. **161**: p. 740.
  104. Bhattacharya, S., et al., *The variation in Poisson's ratio caused by interactions between core and wrap in helical composite auxetic yarns*. Composites Science and Technology, 2014. **102**: p. 87-93.
  105. Lee, W.D., et al., *Moisture sensitive auxetic material*. 2010, Google Patents.
  106. Miller, W., et al., *The manufacture and characterisation of a novel, low modulus, negative Poisson's ratio composite*. Composites Science and Technology, 2009. **69**(5): p. 651-655.
  107. Cybulska, M., *Assessing Yarn Structure with Image Analysis Methods I*. Textile Research Journal, 1999. **69**(5): p. 369-373.
  108. Watanabe, A., et al., *Analysis of Blend Irregularity in Yarns Using Image Processing: Part I: Fundamental Investigation of Model Yarns*. Textile Research Journal, 1992. **62**(11): p. 690-696.
  109. Watanabe, A., et al., *Analysis of Blend Irregularity in Yarns Using Image Processing: Part III: Evaluation of Blend Irregularity by Line Sense and Its Application to Actual Blended Yarns*. Textile Research Journal, 1995. **65**(7): p. 392-399.
  110. Behtaj, S., H. Tavanai, and S. Sadri, *Characterisation of air-jet textured yarn structure through image analysis*. The Imaging Science Journal, 2015. **63**(1): p. 1-6.
  111. Tsai, I.S. and W.C. Chu, *A New Photoelectric Device for the Measurement of Yarn Diameter and Yarn Evenness. Part I: Improvement of the Variance of Radiant Intensity by Using the Area-compensation Method (ACM)*. Journal of The Textile Institute, 1996. **87**(3): p. 484-495.

- 
112. Miao, M., *Characteristics of carbon nanotube yarn structure unveiled by acoustic wave propagation*. Carbon, 2015. **91**: p. 163.
113. Miao, M., et al., *Poisson's ratio and porosity of carbon nanotube dry-spun yarns*. Carbon, 2010. **48**(10): p. 2802-2811.
114. Huh, Y., et al., *Characterizing the thickness variations in ring spun yarns*. Journal of The Textile Institute, 2005. **96**(6): p. 413-422.
115. Sugimoto, Y., et al., *Structure changes during tensile deformation and mechanical properties of a twisted carbon nanotube yarn*. Carbon, 2013. **60**: p. 193-201.
116. Tsai, I.S. and W.C. Chu, *A New Photoelectric Device for the Measurement of Yarn Diameter and Yarn Evenness. Part II: The Measurement of Yarn Diameter and the Effect of Shape-error Factor (SEF) on the Measurement of Yarn Evenness*. Journal of The Textile Institute, 1996. **87**(3): p. 496-508.
117. Feng, J., B. Xu, and X. Tao, *Structural analysis of finer cotton yarns produced by conventional and modified ring spinning system*. Fibers and Polymers, 2014. **15**(2): p. 396-404.
118. Kumar, A., S. Ishtiaque, and A. Das, *Impact of yarn extension on packing density of ring spun yarn*. Fibers and Polymers, 2012. **13**(8): p. 1071-1078.
119. Ishtiaque, S.M., et al., *Development of image processing based system to study yarn structure during extension*. Journal of The Textile Institute, 2010. **101**(8): p. 687-698.
120. Salehi, M. and M.S. Johari, *Study of fiber packing density of lyocell ring-spun yarns*. Journal of The Textile Institute, 2011. **102**(5): p. 389-394.



- 
121. Zhong Cenran, J.I.N.C., *混纺纱线横截面结构参数分析 - Analysis on cross section structural parameter of blended yarn*. *纺织学报*, 2010(1): p. 40-43.
122. Zheng, S., et al., *A study of the fiber distribution in yarn cross section for vortex-spun yarn*. *Textile Research Journal*, 2012. **82**(15): p. 1579-1586.
123. Najar, S.S., M. Amani, and H. Hasani, *Analysis of Blend Irregularities and Fiber Migration Index of Wool/Acrylic Blended Worsted Yarns by Using an Image-analysis Technique*. *Journal of The Textile Institute*, 2003. **94**(3-4): p. 177-185.
124. Ishtiaque, S.M., K. Sen, and A. Kumar, *Study of engineered carpet yarns structure Part B: By cross-sectional microtomy*. *Journal of Industrial Textiles*, 2015. **44**(4): p. 625-638.
125. Shih-Hsuan, C. and L. Jiun-Jian, *Fiber recognition of PET/rayon composite yarn cross-sections using voting techniques.(new image processing method)*. *Textile Research Journal*, 2005. **75**(5): p. 442.
126. Herath, C.N., et al., *Microscopic Evaluation and Analysis on the Tensile Strength of Hybridized Reinforcement Filament Yarns by the Commingling Process*. *Advanced Composite Materials*, 2008. **17**(3): p. 225-233.
127. Stock, S.R., *X-ray microtomography of materials*. *International Materials Reviews*, 1999. **44**(4): p. 141-164.
128. Pazmino, J., V. Carvelli, and S.V. Lomov, *Micro-CT analysis of the internal deformed geometry of a non-crimp 3D orthogonal weave E-glass composite reinforcement*. *Composites Part B*, 2014. **65**: p. 147-157.
129. Barella, A., *Law of Critical Yarn Diameter and Twist Influence on Yarn Characteristics*. *Textile Research Journal*, 1950. **20**(4): p. 249-258.

130. Onions, W.J., E. Oxtoby, and P.P. Townend, 22—*FACTORS AFFECTING THE THICKNESS AND COMPRESSIBILITY OF WORSTED-SPUN YARNS*. *Journal of The Textile Institute*, 1967. **58**(7): p. 293-315.
131. Hearle, J.W.S. and V.B. Merchant, *Relations between Specific Volume, Count, and Twist of Spun Nylon Yarns*. *Textile Research Journal*, 1963. **33**(6): p. 417-424.
132. Whitman, R.C., *Opposite-twist woven fabric and method*. 1946, Google Patents.